8-30-2011

Resource allocation in realistic wireless cognitive radios networks

Mahmoud Alayesh

Mahmoud A. Alayesh
Candidate

Electrical and Computer Engineering Department
Department

This dissertation is approved, and it is acceptable in quality and form for publication:

Approved by the Dissertation Committee:

Prof. Nasir Ghani Nasir Ghani, Chairperson

Prof. Christos Christodoulou Christos Christodoulou

Prof. Majeed Hayat Majeed Hayat

Prof. Patrick Bridges Patrick Bridges

Resource Allocation in Realistic Wireless Cognitive Radios Networks

by

Mahmoud A. Alayesh

B.S, Electrical Engineering, Mutah University, 2003
M.S., Electrical Engineering, University of New Mexico, 2007

DISSERTATION

Submitted in Partial Fulfillment of the
Requirements for the Degree of

Doctor of Philosophy
Engineering

The University of New Mexico

Albuquerque, New Mexico

July, 2011

Dedication

To my dear parents Ayesh and Seham Khodeir for their continuous support and sincere supplications. To my charming wife Heba for her patience and support during all the busy and long days that I needed to complete my degree. To my beloved sons Basel and Bahaa whom have filled my life with joy, and to all my sisters and brothers.

Acknowledgments

First and foremost, I would like to express my thanks and extend my sincere appreciation and gratitude to my academic advisor, Prof. Nasir Ghani, for having motivated, encouraged and challenged me throughout my research. His patience, guidance and insight were invaluable. I really could not have imagined having a better advisor. I am extremely grateful for his support, advice, and encouragement in this endeavor.

I would also like to express my sincere thanks and gratitude to my respected committee members; Prof. Christos Christodoulou, Prof. Majeed Hayat, and Prof. Patrick Bridges, for their time, assistance, recommendations, comments, and suggestions. Indeed, their feedback was vital for improving the overall quality and presentation of this work.

Last but not least, I am greatly indebted to *Jordan University of Science and Technology* (JUST) for granting me an academic scholarship and for their generous support throughout my studies toward my doctoral degree.

Resource Allocation in Realistic Wireless Cognitive Radios Networks

by

Mahmoud A. Alayesh

ABSTRACT OF DISSERTATION

Submitted in Partial Fulfillment of the
Requirements for the Degree of

Doctor of Philosophy
Engineering

The University of New Mexico

Albuquerque, New Mexico

July, 2011

Resource Allocation in Realistic Wireless Cognitive Radios Networks

by

Mahmoud A. Alayesh

B.S, Electrical Engineering, Mutah University, 2003
M.S., Electrical Engineering, University of New Mexico, 2007

Ph.D., Electrical Engineering, University of New Mexico, 2011

Abstract

Cognitive radio networks provide an effective solution for improving spectrum usage for wireless users. In particular, secondary users can now compete with each other to access idle, unused spectrum from licensed primary users in an opportunistic fashion. This is typically done by using cognitive radios to sense the presence of primary users and tuning to unused spectrum bands to boost efficiency. Expectedly, resource allocation is a very crucial concern in such settings, i.e., power and rate control, and various studies have looked at this problem area. However, the existing body of work has mostly considered the interactions between secondary users and has ignored the impact of primary user behaviors.

Along these lines, this dissertation addresses this crucial concern and proposes a novel primary-secondary game-theoretic solution which rewards primary users for

sharing their spectrum with secondary users. In particular, a key focus is on precisely modeling the performance of realistic channel models with fading. This is of key importance as simple additive white Gaussian noise channels are generally not very realistic and tend to yield overly optimistic results.

Hence the proposed solution develops a realistic non-cooperative power control game to optimize transmit power in wireless cognitive radios networks running code division multiple access up-links. This model is then analyzed for fast and slow flat fading channels. Namely, the fading coefficients are modeled using Rayleigh and Rician distributions, and closed-form expressions are derived for the average utility functions. Furthermore, it is also shown that the strategy spaces of the users under realistic conditions must be modified to guarantee the existence of a unique Nash Equilibrium point. Finally, linear pricing is introduced into the average utility functions for both Rayleigh and Rician fast-flat fading channels, i.e., to further improve the proposed models and minimize transmission power for all users. Detailed simulations are then presented to verify the performance of the schemes under the proposed realistic channel models. The results are also compared to those with more basic additive white Gaussian noise channels.

Contents

List of Figures

Glossary

AP	Access point
AWGN	Additive white Gaussian noise
BER	Bit error rate
BFSK	Binary frequency shift keying
BS	Base station
CDMA	Code division multiple access
CR	Cognitive radio
DSA	Dynamic spectrum access
DSS	Dynamic spectrum sharing
i.i.d.	Independent and identically distributed
LMMSE	Linear minimum mean squared error
LOS	Line of sight
MF	Matched filter
NE	Nash equilibrium

pdf	Probability density function
PU	Primary user
QoS	Quality of service
RMS	Root mean square
SDR	Software defined radio
SINR	Signal to interference plus noise ratio
SU	Secondary user

Chapter 1

Introduction

1.1 Background

Wireless networks use *electromagnetic waves*, e.g., such as radio transmissions, to carry information. Unlike wired infrastructures, these setups enable *tetherless* communication and provide unprecedented freedom of mobility for users. Now over the years, wireless networking technologies have seen tremendous levels of innovation, evolving from basic voice-only capabilities to full-fledged multimedia paradigms, i.e., voice, video, and data. As a result, wireless communications has become an entrenched facet of modern society, and users are continuing to demand faster and more reliable wireless connectivity. This push, in part, is being driven by the massive commoditization (price reduction) of high-speed and power-efficient computing technologies.

Now in general, there are several key resources in wireless networking environments. A foremost resource is the available spectrum to carry user transmissions, i.e., bandwidth. For the most part, access to this spectrum is tightly regulated by governmental (and also international) agencies, i.e., as defined by licensed bands for 2G, 3G and 4G wireless technologies. For example in the United States, all commercial spectrum allocation is done by the *Federal Communication Commission* (FCC). In addition, another key resource in wireless networks is user power. This contrasts with wired networks as most mobile terminals handset devices are battery-powered. Finally, computing power (on a mobile devices) is also another key resource and can impact the the type of processing/transmission that can be done.

Overall, given the highly-controlled nature of spectrum allocation and limited power resources on most mobile platforms, commensurate resource allocation issues are of paramount importance [1]. These challenges are further compounded by the myriad of transmission concerns in wireless settings, e.g., propagation losses, fading, multi-path, etc. As a result, a full range of schemes have been studied over the years, e.g., modulation, power/rate control, and coding [1], [8].

Nevertheless, many studies have shown that sizable portions of the allocated spectrum are not utilized in many cases. For example, a recent FCC study revealed that almost 90-95% of frequency bands are either unoccupied most of the time or only partially occupied [2]. Indeed this inefficient usage of allocated spectrum is major cause for concern, as in general, increased user demands are mandating increased bandwidth resources. Hence in order to resolve this concern, *dynamic spectrum access* (DSA) strategies have been proposed. Namely, the overall goal here is to allow users to share unused spectrum from designated (but idle) users. Specifically, wireless network users are segmented into two groups, *primary users* (PUs) and *secondary users* (SUs). Here, the PUs own the allocated spectrum but allow SUs to share it, essentially letting them act as a source of interference. Hence *hierarchical access models* have been introduced to perform efficient power control in order to reduce the amount of interference, i.e., by reducing the power consumed at PU and SUs terminals, see [3] and [4].

Now the *cognitive radio* (CR) concept leverages DSA strategies to help improve spectrum utilization efficiency. Here the SUs are allowed to sense and tune to (access) unused parts of the licensed spectrum, i.e., by learning, observing, and reconfiguring their radio systems to capitalize on unused spectral bands [5]. A key goal in CR networks is to ensure that associated interference levels are kept in line with the *quality of service* (QoS) requirements of all users, particularly PUs. In addition, when the PU of a given channel (band) returns, the SUs must vacate the channel, i.e., termed as *forced termination*. Here the SUs may shift to other available channel bands and recover from the forced termination state, i.e., termed as *spectrum hand-off*. In this setup the SUs are serviced when the channels are free, resulting in higher spectrum utilization. Furthermore, since the availability of the spectrum depends upon the PUs' traffic, the number of SUs serviced also varies with the PU's traffic usage. Hence the amount of service that can be squeezed out of the free spectral bands is called the capacity of the SUs.

Overall the field of CR networking has seen much growth in recent years, especially with the advent of *software defined radio* (SDR) devices. In general, the operation of CR is summarized in five steps [6]: observe, orient, decide, act, and learn. Here DSA systems can sense the operating environment, return a value for the sensing result, vary the operating parameters, learn from the past experience and current states, and also use predictive capabilities to help further improve transmission behaviors (at the PUs and SUs). Along these lines, various game-theoretic models have recently been developed for PU/SU transmission behaviors and used to analyze decision making processes in CR networks [5], [6].

1.2 Motivation

In general, most the game-theoretic studies in CR have looked at power control performance under *additive white Gaussian noise* (AWGN) channels model [7]. Albeit insightful, these models do not adequately account for the impact of a range of real-world wireless channel impairments, e.g., such as fading, frequency selectivity, interference, nonlinearity, or dispersion of channels upon the total performance of power control algorithms. Moreover, AWGN channels are generally not considered as good models for most terrestrial wireless links because of added effects such as multi-path, terrain blocking, interference, etc. As such, they tend to give overly-optimistic results which generally may not reflect real-world conditions. Nevertheless, these models do provide simple *baseline* mathematical frameworks which give some insights into the underlying behavior of certain systems (before these other more complex phenomena are considered).

In addition, many game-theoretic studies have tended to focus on broader aspects of the CR problem by modeling multiple PUs. As such, there is a critical need to focus on more challenging channel types, and address power control issues under more focused, realistic conditions. Indeed, the application of game theory in this context is a largely unaddressed and open issue. In particular, it is very plausible that space diversity techniques may be able to take advantage of random fading channels here, i.e., multiple antennas. Namely, the likelihood that all channels are in deep fading is less than that for a single channel, i.e., information may still be conveyed through other channels. This forms the key motivation for this effort.

1.3 Proposed Work

Based upon the above, this dissertation extends the game-theoretic modeling of CR networks by focusing on a host of realistic concerns. First of all, power allocation is considered for fast-flat fading channels models, including Rayleigh and Rician channels. Next, slow-flat fading channels models are also studied for both Rayleigh and Rician channels. In both cases, these models are further verified using numerical simulations to gauge the impact on average utility functions. Further comparisons are also done with results for more basic AWGN channel models. Finally, linear pricing is also added to the utility functions to further improve performance in CR networks. The results of this approach are then compared to the case of utility function without pricing. This completes the study of power allocation for realistic CR networks.

1.4 Dissertation Outline

Overall, this dissertation is organized as follows. First, Chapter 2 presents a broad survey of related areas. Namely, several key wireless communication channel models are introduced. Cognitive radios, spectrum sharing, and game theory are then briefly presented. Finally, a general literature review is presented for related topic areas and a realistic system model is outlined for further development.

Next, Chapter 3 proposes realistic game-theoretic formulations for CR networks under fast-flat fading channels models, i.e., both Rayleigh and Rician distributions. Here, modified game schemes are presented and their utility functions are derived. The existence and uniqueness of the associated *Nash Equilibrium* (NE) for these games are also proved to guarantee that the models are convergent under the best-response adaptation. The findings are further augmented with numerical analysis results for the spectrum sharing model under both types of fading channels behaviors.

Chapter 4 then addresses realistic games under slow-flat fading channels models, again for both Rayleigh and Rician distributions. The existence and uniqueness of the NE for both of these cases is also shown and numerical analysis presented.

Finally, Chapter 5 introduces the concept of pricing and studies realistic games under Rayleigh and Rician fast-flat fading channels models. Specifically, linear pricing is studied and its superiority over games without pricing is shown. Conclusions and directions for future work are then presented in Chapter 6 to conclude the effort.

Chapter 2

Background Survey

This chapter presents a background review of topics and areas relating to the game-theoretic modeling of CR wireless networks. In particular, some of the key wireless channel models are reviewed first, including fading types. Next, CR networking concepts are highlighted, with a focus on hierarchical access models. The overall area of game theory is then briefed, including the concepts of NE and utility pricing. Finally, a detailed survey is presented on the latest work in game theoretic modeling of CR networks. This background is then used to motivate a realistic model for fading channels, which is further revisited and developed in the subsequent chapters of this dissertation.

2.1 Wireless Channel Models

In general, the term *wireless networking* is quite generic and many different types have been developed. For example, many commercial wireless networks, i.e., cellular, make extensive use of wired networking technologies to interconnect wireless *access point* (AP) and/or *base station* (BS) nodes. In such settings, only the first and last-hop transmissions occur over the wireless medium, i.e., user handsets sending/receiving to/form AP nodes. By contrast other types of wireless networks, such as mobile ad-hoc networks or sensor networks, can be *fully wireless* and may not support any wired links/transmissions whatsoever.

Regardless of the settings, however, wireless links (or channels) are generally where the most transmission degradation tends to occur. As such, these segments determine the capacity and general performance of the end-to-end network. This is due to the fact that wireless channels represent natural mediums which are not necessarily optimized for data transmissions, e.g., versus more predictable man-made media such as copper, coaxial, or fiber optic cable. Therefore, random fluctuations in wireless channels can severely degrade the overall performance of wireless networks. As a result, much effort has been devoted towards building realistic, probabilistic models for wireless transmission channels, and then using these models to study data network transmission behaviors. Nevertheless, these channels models also make wireless network design much more complicated, i.e., with regards to resource allocation (power and rate control) [1]. Further consider the details here.

Wireless signals typically travel from a transmitter to a receiver over multiple reflective paths. This phenomenon, called *multi-path fading*, can cause fluctuations in the received signal's amplitude, phase, and angle of arrival. As such, wireless channel models (i.e., for mobile radio) can be classified into two main categories contingent to the wavelength, λ, of the carrier radio wave, i.e., *large-scale fading* and *small-scale fading* models. The former models slow variations in the signal power over time, and commonly uses log-normal signal representations, i.e., which depend upon the position of the user and the presence of obstacles in the signal path. Meanwhile, the latter models the amplitude of the faded channel using Rician or Rayleigh random distributions [46] in order to capture the effects of a large number of multiple reflective paths, i.e., with or without dominant *line of sight*

(LOS) propagation path. These two models are now discussed further.

2.1.1 Large-Scale Models

In general, large-scale models predict average channel behaviors over distances much greater than the operating wavelength. As a result, these models are generally considered as *frequency-independent* and are functions of distance and other environmental features [1]. Now some specific theoretical large-scale models include the free-space model, reflection model, diffraction model, and scattering model. Various experimental models have also been developed, including log-normal shadowing, outdoor propagation, and indoor propagation. For more details, please refer to [1] and [8].

However, the study in this dissertation does not consider the effects of large-scale fading channels. The key reason here is that these models are more relevant for longer-term issues such as cell site planning, and less for communication system design [9]. As a result the focus here is instead upon addressing much more temporal concerns/challenges caused by more rapidly changing channels. These models are discussed next.

2.1.2 Small-Scale Models

Small-scale fading models capture signal variations on a scale of the carrier wavelength itself. Here Doppler frequency shift and *multi-path* fading effects are the main causes of fading, i.e., defined as the rapid change in a signal's strength over a short distance or short length of time. Hence fading is a time-variant and frequency-dependent phenomenon. Now Doppler's frequency shift can occur due to a wireless user's movement. Namely, this frequency shift can be positive when a mobile user moves toward the base station and negative if the mobile user moves away from the base station. Meanwhile, the frequency shift for each ray in a multi-path environment may be different as well. In turn, this leads to a *spread* in frequencies at the receiver. Hence the maximum Doppler shift, termed as the *Doppler spread* (B_d), is given by:

$$B_d = \frac{v}{\lambda} \tag{2.1}$$

where v is the speed of the the mobile user.

Now the time duration over which the wireless channel's impulse response is considered to be invariant is defined as the *coherence time* (T_c) and is given by:

$$T_c = \frac{c}{B_d} \tag{2.2}$$

where c is constant. Thus if two signals arrive at the receiver with a time separation greater than T_c, then the channel will affect both signals separately. Therefore a baseband signal of *symbol period* (T_s) greater than T_c will be distorted because the channel will vary during the transmission of this signal. Moreover, the interference between two or more versions of the transmitted signal (which arrive at slightly different times) is also termed as multi-path fading. Thus rapid changes to the signal strength can occur over a relatively short time interval or small distance. Moreover, random frequency modulation can also occur due to time dispersion caused by multi-path propagation delays and varying Doppler frequency shifts (in different multi-path signals).

Now generally, two key parameters are used to measure the time dispersion of multi-path components; the *power-delay profile* and *root mean square* (RMS). Namely, the power delay profile (or multi-path intensity profile) is defined as the average power associated with a given multi-path delay [8]. In general, the power-delay profile is represented as a plot of relative received power as a function of excess delay with respect to a fixed time-delay reference. Using this, the *mean excess delay* is defined as the first moment of the power-delay profile as follows [1]:

$$\bar{\tau} = \frac{\sum_n a_n^2 \tau_n}{\sum_n a_n^2} \tag{2.3}$$

where a_n is the amplitude of the n-th multi-path component and τ_n is its corresponding delay. Meanwhile, the RMS is given by the square root of the second control moment of the power-delay profile and is given as follows:

$$\sigma_\tau = \sqrt{\bar{\tau}^2 - (\bar{\tau})^2} \tag{2.4}$$

where

$$\bar{\tau}^2 = \frac{\sum_n a_n^2 {\tau_k}^2}{\sum_n a_n^2} \tag{2.5}$$

It is important to note that the values of *RMS delay spread* (σ_τ) can range from microseconds in outdoor mobile radio channels to nanoseconds in indoor mobile radio channels.

Furthermore, to better characterize the channel in the frequency domain, a *coherence bandwidth* (B_c) parameter is also defined as an analog to the delay spread parameter in the time domain. Namely, the coherence bandwidth is defined as the range of frequencies over which the channel is assumed to be flat. Therefore the frequency components can have strong amplitude correlation, and if the correlation between two multi-path components is above 0.9, then the coherence bandwidth is given by:

$$B_c = \frac{1}{50\sigma_\tau} \tag{2.6}$$

However, if the correlation is greater than 0.5, the above equation can be resolved to:

$$B_c = \frac{1}{5\sigma_\tau} \tag{2.7}$$

To summarize, the coherence bandwidth and delay spread describe the time dispersive nature of the channel in a local area. By contrast, the Doppler spread and coherence time describe the time-varying nature of the channel caused by relative motion of transmitter and receiver in a small-scale region. Moreover, B_c and T_s are termed as signal parameters, while σ_τ and B_d are termed as channel parameters.

Furthermore, small-scale fading channels can further be classified into two groups; *frequency selective fading* and *flat fading* channels. Hence a band-limited transmit signal either sees a frequency-selective channel or a flat frequency channel (non-selective). In particular, this depends upon the transmitted signal bandwidth and symbol period as compared to coherence bandwidth and RMS delay spread, respectively. Namely, if the signal bandwidth is much less than the coherence bandwidth (i.e., narrow-band channel) and the RMS delay spread is much less than symbol period, then the channel is said to be flat fading frequency channel. Otherwise it called a frequency-selective channel, which is much more difficult to model as compared to flat fading channels. Moreover, based upon coherence time (which results from Doppler spread), small-scale fading can be sorted into two main groups; *fast-flat fading* and *slow-flat fading*. Consider these in more details.

Fast-flat fading channels incorporate higher Doppler spread, and here the symbol period is generally greater than the coherence time, i.e., $B_s < B_d$. Therefore the channel impulse response variations are much faster than the baseband signal variations. On the other hand, the Doppler spread for slow fading channel is low and the coherence time is greater than the symbol period. Thus channel variations are considered to be lower than baseband signal variations. In other words the channel does not change during each signal symbol. Hence the velocity of the a wireless user (i.e., mobile user) and/or the velocity of the objects in the channel and the baseband signal determine whether a signal undergoes fast or slow fading.

In general, wireless channels can take advantage of multi-path and Doppler effects to characterize their time and frequency characteristics. However, this is not sufficient and further analysis is usually necessary to capture the statistical characteristics of randomly-varying amplitudes. Therefore several popular channel models have been developed to describe small-scale fading channels for mobile users in wireless *code division multiple access* (CDMA) networks. These include Rayleigh fading channels and Rician fading channels [10, 11]. Namely, Rayleigh models describe the envelope distribution of the received signal for channels that contains no LOS components. Conversely, if one of the multi-path components of the channels has a LOS component, Rician distributions are used instead to describe the envelope of the received signal. Note that Nakagami distributions, which have more degrees of freedom, can also give more accurate models, i.e., control over fading for more dense scatters. Consider Rayleigh and Rician models further [10, 11].

Rayleigh Fading Channels: Here the BS is assumed to be far away from scatterers and the users are surrounded by infinitely many scatterers, e.g., such as indoor environments where there can be many furniture items or walls. Furthermore, given N users within a cell, the fading coefficient α_i is defined by a Rayleigh *probability density function* (pdf) given by:

$$p(\alpha_i) = \frac{\alpha_i}{\sigma^2} e^{-\frac{\alpha_i^2}{2\sigma^2}} \quad i = 1, \ldots, N \tag{2.8}$$

for $\alpha_i \geq 0$ and zero otherwise. In particular, σ is the RMS value of the received voltage signal before envelope detection, and σ^2 is the time-average power of the received signal before envelope detection. In other words, $\sigma^2 = E[0.5(\alpha_i^2)]$ is the measure of the spread of the distribution. Therefore σ is the only parameter that the Rayleigh pdf uses to characterize the channel, i.e., one degree of freedom only. However, other channels, such as the Nakagami model, represent two degrees of freedom [11]. In general, the Rayleigh distribution is used to describe the statistical time varying nature of the received envelope of an individual multi-path component generated mainly from scatterers.

Rician fading channels: In this model, the main contribution of the received signal is due to a direct path, i.e., LOS between the BS and the users. Namely, the fading coefficient α_i has a Rician pdf given by:

$$p(\alpha_i) = \frac{\alpha_i}{\sigma^2} e^{-(\frac{\alpha_i^2+s^2}{2\sigma^2})} I_0(\frac{\alpha_i s}{\sigma^2}) \quad i = 1, \ldots, N \tag{2.9}$$

for $\alpha_i \geq 0$ and zero otherwise. In particular, s^2 represents the power in the non-fading signal components or LOS (dominant) component, which is also known as the *non-centrality parameter* of the pdf. Meanwhile, $I_0(.)$ is the zero-order modified first-kind Bessel function. Overall, $(\alpha_i/\sigma)^2$ has a non-central chi-square distribution with two degrees of freedom (i.e., s and σ) and non-centrality parameter $(s/\sigma)^2$. Furthermore, the Rician distribution is also defined in terms of a K-factor, also termed as Rician factor, i.e., $K = 0.5(s/\sigma)^2$. In particular, this factor is defined as the ratio of signal power in the dominant component (the deterministic signal power) over the (local-mean) scattered power or the variance of the multi-path. Note the Rician density function degenerates to a Rayleigh distribution when the dominant component fades away.

2.2 Cognitive Radio (CR) Networks

The CR concept was first introduced in 1998 by Joseph Mitola and subsequently published in 1999 [6]. In essence, CR embodies a fully-reconfigurable wireless setup, in which a transmission device's communication parameters can be changed automatically to adapt to varying user or operator needs [12]. Overall, CR is a very promising paradigm for wireless telecommunications networks as mobile users can change their transmission and reception parameters (i.e., power or rate) to communicate in a more efficient manner and avoid interference with licensed PUs and unlicensed SUs. This can be achieved by monitoring several parameters in the radio environment, such as wireless network state, mobile user's behavior, and radio frequency spectrum. Now the FCC has found that even though many cellular bands are overloaded, other frequency bands are not, e.g., such as those assigned for paging and military frequencies. Hence, CR techniques are very attractive here as they allows users to circumvent the limitations of basic *fixed spectrum* allocation schemes, i.e., where unlicensed users are not allowed to use idle frequencies assigned to other users or services.

Overall, two types of CR spectrum allocations are possible, *licensed band* and *unlicensed band*. In particular, the former allows CR users to access bands assigned to licensed users which are different from unlicensed bands. Meanwhile the latter allows users to only use unlicensed bands. As a result, CR can be very promising in DSA environments, as PUs and SUs can change their transmission/reception parameters to improve spectrum efficiency and also minimize interference, i.e., power, rate. This can be done by monitoring several radio parameters, i.e., such as network state, mobile user behaviors, RF spectrum usages, etc. Along these lines, the key functions in CR networks generally include the following [12]:

Spectrum Sensing: This function allows SUs in CR to detect idle spectrum bands. The goal here is to *sense* the presence of PU transmissions and find gaps in spectrum usage. In particular, transmitter detection is one of the many techniques used in spectrum sensing, i.e., to determine if a PU signal is present within a certain spectrum band [12].

Spectrum Management: This function determines the best available spectrum band for SU transmission. The objective here is to ensure proper selection so as to meet the QoS requirements of both PUs and SUs, without introducing excessive levels of interference.

Spectrum Mobility: This function handless frequency exchange between SUs. The aim here is to allow dynamic spectral usage for users to operate in the best frequency band.

It is also important to note how SUs actually make use of idle spectral resources. In particular, two DSA approaches have been proposed, *spectrum overlay* and *spectrum underlay*.The former scheme only allows SUs to utilize idle band gaps in the usable spectrum, i.e., called *white spaces*. Now since the SUs have to search for these bands, collisions can occur if there are errors in the sensing and detection processes. Meanwhile, spectrum underlay techniques allow SUs to use the whole usable spectrum, as long as they control their transmission behaviors to limit the total interference levels i.e., QoS degradation for PU. The proposed effort herein makes use of this approach, although it can also be adapted for spectrum overlay operation. Note that other more specialized DSA approaches are also possible, i.e., such as open sharing models [13, 14] and dynamic exclusive models [15–18] etc.

Finally, it is noted that power control is also a crucial aspect in CR networks (and wireless networks in general). Specifically, since wireless users communicate via an air interface over a common shared medium, power control is a problem that affects all users (PU and SUs). In general, each user's transmission power can be considered as source of interference for all the other users, as it can deteriorate their *signal to interference plus noise ratio* (SINR). In addition, power control is also required since data transmission consumes valuable (limited) battery life.

Now typically the goal for most users is to achieve a high SINR while expending the smallest amount of energy. Hence there is a clear trade-off between achieving high SINR levels and lowering energy consumption in CR networks. As a result, the key focus of power control algorithms is to find a good balance between these two objectives. Namely, it is considered to be an effective resource-allocation scenario to compact co-channel interference and fading channel. Here, power control algorithms must also adjust the transmission power according to channel conditions in order to maintain acceptable QoS, i.e., received signal power. Furthermore, the QoS levels can also vary based upon user service type. For example basic voice services can suffice with minimum acceptable SINR support. However, higher-bandwidth data services will mandate larger SINR values to support error-free communication. This is because of the direct dependence on data transmission error probabilities.

2.3 Game Theory Overview

Game theory is a mathematical tool that is used to study the interactions between rational and intelligent *players* in a game. Here a rational player is defined as one whose behavior is consistent with maximizing its own expected utility [1]. In addition an intelligent player is also one who knows everything about the structure of the game, i.e., including the fact that the other players are rational and intelligent. Overall, game theory has been widely used to study problems in diverse fields such as biology, economics, defense, politics, and even resource allocation in CR/wireless networks. Consider some further details.

In general, a strategic game G is defined using the following three key elements:

1) Finite set (i.e., group) of rational players, denoted as $\mathcal{N} = \{1, \ldots, N\}$.

2) An action space or strategy space, $\mathcal{A} = (\mathcal{A}_1 \times \mathcal{A}_2 \times \ldots \times \mathcal{A}_N)$, from which players chooses their actions (i.e., the Cartesian product of each player's action set).

3) A set of utility functions that describes the players' preferences over all possible game outcomes. A real number is assigned to every possible game outcome with property that a higher (or lower) number implies that the outcome of the game is more desirable. Therefore, the utility is a direct function of the game outcome.

Now in general, a strategic game can be defined as being *static* or *dynamic*. In static games, the interaction between users only occurs once. Conversely, in dynamic games multiple user interactions can occur in the action space. Overall, game-theoretic models offer some notable advantages [1]:

• Since players observe outcomes and respond to optimize their own gains, there is no need to collect *global* information and perform constrained optimization. Instead local information is sufficient here.

• Since local information (at the players) is always accurate, the outcome of the distributed game is always robust. This contrasts with other optimization models that can yield *sub-optimal* results with inaccurate global information.

• Game theory is better suited for handling combinatorial problems as compared to traditional optimization techniques. Namely, it formulates and handles the problem in a discretized manner, i.e., such as the strategic form.

The above-said, however, game theory also has some disadvantages:

• It is generally harder to formulate a reasonable utility function in all cases, i.e., since this function must have a physical meaning and the outcome of the game may be non-trivial.

• Players may have multiple objectives, and the strategic influences of all users must be incorporated (otherwise there will be no conflicts).

• Game theory can give lower efficiency outcomes as compared to centralized optimization strategies. Specifically, since players tend to optimize their own gains in a greedy manner, this can yield higher resource usage. Hence cooperative incentive-based techniques have been developed to improve outcome efficiency, i.e., repeated games, pricing, etc. Namely, incentives are given for distributed users to cooperate to arrive at more efficient solution.

Now as noted earlier in Chapter 1, game theory has been used to model wireless CR networks settings as well. In particular, the actual users (PUs, SUs) now can take the role of players trying to maximize their utilities. In turn, the utilities here are defined as a function of transmission power, transmission rate, energy or any combination of these.

2.3.1 Nash Equilibrium (NE)

A key concept in game theory is that of the NE. Specifically, the NE is defined as a steady-state concept where all players in a game have no further incentive to change their actions. Namely, consider a game with N players and an action (strategy) strategy vector $\mathbf{b} = [b_1....b_N]$, where b_i is the i-th player's strategy. In addition, the strategy vector of the i-th player's opponents is given by $\mathbf{b_{-i}} = [b_1...b_{i-1}b_{i+1}...b_N]$ and the i-th player's utility is given by u_i. Using this the NE point $\mathbf{b}$ is defined as [1]:

$$u_i(b_i, \mathbf{b_{-i}}) \geq u_i(b_i^*, \mathbf{b_{-i}}), \quad i = 1, \ldots, N \tag{2.10}$$

In general, a game is said to have a solution if there exists at least one NE for it. As a result no player can further increase its utility alone by changing its strategy, i.e., no further incentive to action. Therefore if any user tries to change its strategy, this will lead to reduced utility for that user (as compared to maintaining its current strategy).

2.3.2 Utility with Pricing

As mentioned above, utility pricing concepts have also been used to improve game theory formulations. The goal here is to introduce appropriate pricing (or taxation) policies in order to incentivize players to cooperate with each other and improve game outcomes. As such, this entices players to cooperate in the game to get an optimal solution for resource usage.

Now generally speaking, each individual player would like to maximize its utility, concurrent with paying the smallest price for using a resource. Hence each user would like to maximize the difference between its utility and the pricing function [1]. However, this may yield multiple NE points, and hence a key goal in pricing-based games is to change the rules to prevent multiple players from falling into less-efficient NE points. For the case of CR networks, pricing will cause the NE point to shift transmission powers to lower values as compared to games without pricing. This will help to increase the utility values obtained, and hence more SUs can be supported in the network. It is also worthwhile to mention that that increased transmission power has nothing to do to lower error rates, and in fact will only results in increased energy usage (wastage) [1].

2.4 Literature Review in Game-Theoretic Approaches for Cognitive Radios

Various studies have looked at improving the bandwidth (i.e., spectrum utilization) efficiency of static spectrum allocation schemes in wireless CR networks, i.e., to allow SUs to compete and access white spaces in licensed spectrum bands already allocated to PUs. Expectedly, power control is critical concern in such settings, as SUs must ensure that they do not introduce excessive levels of interference so as to degrade the QoS of the PUs and also the other SUs. Along these lines, various power control schemes have been proposed, see [24], many of which have used game-theoretic techniques to model the interactions between users in CR networks, i.e., by treating them as rational decision makers.

The first game-theoretic model for power control in wireless data networks was presented in [25]. In particular, a framework was developed for distributed power control based upon economic concepts of utility and pricing, with the goal of maximizing the utility of each user. Meanwhile an alternate approach was outlined in [26] using energy efficient utility functions to derive unique NE points. In particular, this work modeled power control in wireless data network as a non-cooperative power control game and defined the user's utility function as the ratio of throughput to transmit power. Building upon this, the concept of *Pareto efficiency* was introduced in [27] to further handle non-optimal NE cases. Specifically, a linear pricing function (in transmit power) was used to improve the distributed power control game and gain better overall performance. In [27, 28], the authors also used pricing functions to obtain a more efficient solution for the power control game. Next, the work in [29] outlined a more specialized game-theoretic model for handling *linear minimum mean squared error* (LMMSE) receivers, and results showed convergence to a unique NE owing to the *quasi-concavity* property of the utility function. Further QoS-related constraints were also introduced into a game-theoretic formulation in [30] in which users were allow to choose their transmit powers as well as constellation sizes to maximize utility.

Furthermore, some motivation for using game theory in communication system were also provided by the authors in [32], especially in power control problem. The authors in [33] also defined the utility function as S-shaped (sigmoid) function of the user's SINR. Note that earlier resource allocation algorithms for wireless networks have also used non-game theory approaches, where each user allocates their own resources (i.e., power and data rate) iteratively based upon local measurements to meet SINR constraints. See also other studies [34–37]. However, using a game theoretic approach allows each user to choose their own transmit power level or data rate efficiently in such a way as to optimize the total interference introduced to other users.

Now the authors in [31] considered both power and rate control using a game theoretical approach, where the SUs are only considered as active players in the game. Furthermore, an opportunistic power adaptive method for SUs was proposed in [38]. In this method authors made key relaxation in terms of synchronization and perfect channel state information requirements, which are very useful for fading channels. Next, a joint power control and beam-forming scheme using either weighted least squares or admission control was proposed in [39]. In [6] it was shown that CR is good candidate for realizing *dynamic spectrum sharing* (DSS) due to its ability to observe, learn from, and orient to the observed radio frequency environment. Moreover, [40] also presented a game theoretical overview for DSS techniques.

Furthermore, since managing the interference level is the responsibility of the secondary system, either by spectrum overlay or by spectrum underlay DSA, the authors in [15] conducted research in DSA networks to analyze the network users' behaviors, optimality, and fairness among the SUs. Finally, a game-theoretic scheme was also proposed in [41] to achieve power control amongst SUs, where potential games and S-modular games were applied to perform resource allocation in CR networks. Namely, a target SINR game model was introduced to provide each SU with an acceptable SINR while maintaining the SUs' transmission power limited. However, in this formulation the PUs were not considered as decision makers in the overall spectrum sharing process. Hence, these schemes are essentially similar to the power control schemes in traditional wireless networks. For more details on game-theoretic approaches in wireless networks for energy efficient resource allocations schemes, please refer to [42] and [43].

Note that power control in CR networks has also been investigated based upon other methods rather than game theory, see [44], [45]. In particular, a more efficient branch and bound algorithm was proposed in [44] for optimal power control in a CR network, while [45] introduced an adherence to hierarchies between primary and secondary users in a peer-to-peer CR network through distributed power control.

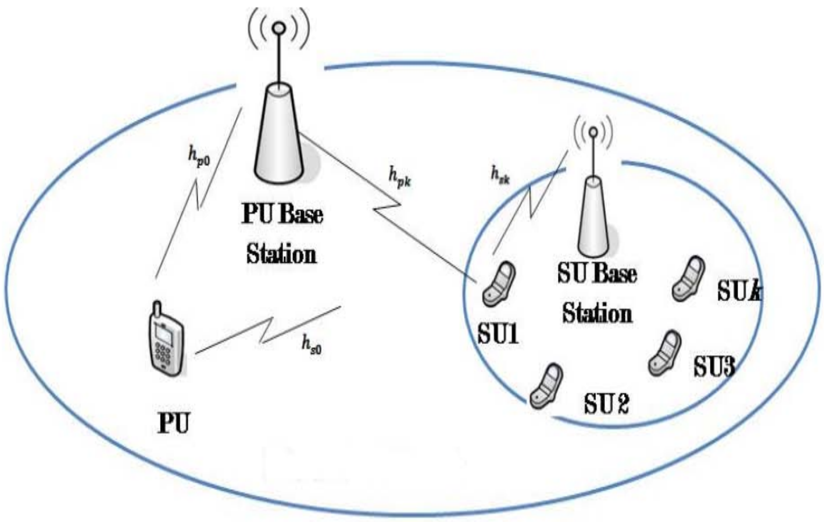

Figure 2.1: The primary-secondary user communications system model [10]

Although the above studies represent a good set of contributions in the CR field, these game-theoretic strategies have only considered interactions between the SUs.

As a result, it is crucial to further incorporate the behavior of the PUs in the power control formulations as well in order to further improve the transmission performance of SUs and also avoid deleterious impacts on QoS. Along these lines, a novel power control scheme was proposed in [7], in which PUs were also treated as decision makers (see Figure 2.1). Namely, PUs were rewarded (i.e., monetarily) to leave a reasonable portion of their spectrum to share amongst the SUs, i.e., assuming that they can first meet their own minimum required QoS requirements, measured as SINR. Concurrently, the SUs were required to achieve energy-efficient transmission without causing excessive levels of interference to the PUs.

In particular, the above objectives were achieved by setting a reasonable *interference cap* (Q_0) for SU transmissions and severely penalizing PUs if their transmissions did not achieve a minimum QoS level. However the work in [7] did not consider the impact of channel fading, and instead focused on simpler AWGN channels which are generally considered as poor models. Along these lines, this dissertation extends upon this primary-secondary formulation to model the performance of the scheme under realistic channel conditions. Specifically, operation is considered for *direct sequence-code division multiple access* (DS-CDMA) CR wireless network settings in which there is a single PU and multiple SUs.

2.5 Proposed Realistic System Model

Based upon the above review, a realistic system framework and notation for CR networks is now proposed. This baseline is then developed and expanded in subsequent chapters of this dissertation. Overall, the main focus here is on capturing the impact of fading channel behaviors. Hence in order to better focus on this concern, only the single PU case is treated, i.e., one PU and multiple SUs sharing a cell. Consider the notation here.

Here the model is formulated as a game with N users (players). Next, the cross correlation coefficients between the signaling waveforms of the i-th SU and that of a PU is denoted by ρ_{ip}, between a PU and the i-th SU is by ρ_{pi}, and between the i-th and the j-th SUs by ρ_{ji}, for all i , $j \in \{1, \ldots, N\}$. Without loss of generality, it is also assumed that $\rho_{ip} = \rho_{pi} = \rho_{ji}$. Meanwhile, the channel gain between the i-th SU and the common secondary receiver is given by h_{si}, between the i-th SU and the primary receiver by h_{pi}, between the PU and the primary receiver by h_{p0}, and between the PU and the common secondary receiver by h_{s0}. Further more, assuming a *matched filter* (MF) detector is used at the primary receiver, the target SINR of the PU is determined by its transmission quality as [7]:

$$\bar{\gamma_0} = \frac{h_{p0}^2 P_0 \alpha_0^2}{Q_0 + \sigma_n^2} \tag{2.11}$$

where α_0 represents the path fading coefficient between the PU and the primary receiver, σ_n^2 the variance of the AWGN at the primary receiver, and P_0 the PU's transmission power. Since Q_0 is the maximum possible interference from all SUs that the PU is willing to tolerate, $\bar{\gamma_0}$ represents the least acceptable transmission quality of the PU. Hence the PU's actual SINR is given by:

$$\gamma_0{}^{(P)} = \frac{h_{p0}^2 P_0 \alpha_0^2}{\sum_{i=1}^{N} h_{pi}^2 \rho_{sp}^2 p_i \alpha_i^2 + \sigma_n^2} = \frac{h_{p0}^2 P_0 \alpha_0^2}{I_0 + \sigma_n^2} \tag{2.12}$$

where $I_0 = \sum_{i=1}^{N} h_{pi}^2 \rho_{sp}^2 p_i \alpha_i^2$ is the *total interference* from all SUs to PU and p_i is the i-th SU's transmit power. Hence by using Eq.(2.11) one gets:

$$\gamma_0{}^{(P)} = \frac{\bar{\gamma_0} Q_0}{\sum_{i=1}^{N} h_{pi}^2 \rho_{sp}^2 p_i \alpha_i^2 + \sigma_n^2} + \frac{\bar{\gamma_0} \sigma_n^2}{\sum_{i=1}^{N} h_{pi}^2 \rho_{sp}^2 p_i \alpha_i^2 + \sigma_n^2} \tag{2.13}$$

Similarly, the i-th SU's received SINR at the common secondary receiver is given by:

$$\gamma_i{}^{(s)} = \frac{h_{si}^2 p_i \alpha_i^2}{\sum_{\substack{j=1\\ j\neq i}}^{N} h_{sj}^2 \rho_{ji}^2 p_j \alpha_j^2 + h_{s0}^2 \rho_{ps}^2 P_0 \alpha_0^2 + \sigma_n^2} \tag{2.14}$$

For simplicity's sake, I_i is also defined to be the total interference introduced to the i-th user from the PU and all other SUs, i.e.,

$$I_i = \sum_{\substack{j=1\\ j\neq i}}^{N} h_{sj}^2 \rho_{ji}^2 p_j \alpha_j^2 + h_{s0}^2 \rho_{ps}^2 P_0 \alpha_0^2 \tag{2.15}$$

Hence by using Eq.(2.15), one can rewrite Eq. (2.14) as follows:

$$\gamma_i{}^{(s)} = \frac{h_{si}^2 p_i \alpha_i^2}{I_i + \sigma_n^2} = A_i \alpha_i^2, \quad \forall i = 1, 2, \ldots, N \tag{2.16}$$

Finally, assuming non-coherent *binary frequency shift keying* (BFSK) transmission, the *bit error rate* (BER) given $\gamma_i^{(s)}$ and I_i for the i-th user is given by [46];

$$\tilde{P}_b(e) = \frac{1}{2} e^{-\frac{\gamma_i^{(s)}}{2}} \tag{2.17}$$

The conditional bit error rate given $\gamma_i^{(s)}$ and I_i which is derived above will be used extensively in this dissertation.

In general, for fast-flat fading channels, the path fading coefficient is not constant over the packet duration. However, it is generally assumed that fading levels are still constant over single bit durations. Hence, for the m-th bit in the packet, one can rewrite Eq. (2.16) as follows [3], [47]:

$$\gamma_i{}^{(s)}(m) = \frac{h_{si}^2 p_i \alpha_i^2(m)}{I_i(m) + \sigma_n^2}, \quad \forall i = 1, 2, \ldots, N \tag{2.18}$$

where

$$I_i(m) = \sum_{\substack{j=1 \\ j \neq i}}^{N} h_{sj}^2 \rho_{ji}^2 p_j \alpha_j^2(m) + h_{s0}^2 \rho_{ps}^2 P_0 \alpha_0^2(m) \tag{2.19}$$

Now consider the derivation of the *average bit error rate*, denoted by P_e, for each bit in the packet and the average utility functions are evaluated for both Rayleigh (and Rician) fast-flat fading channels. In order to find P_e, it is assumed that both $\alpha_i^2(m)$ and $I_i(m)$, are *independent and identically distributed* (i.i.d.) random variables, and $\alpha_i^2(m)$ and $I_i(m)$ are independent random variables for $m = 1, 2, \ldots, M$, where M is the number of bits in one packet.

Chapter 3

Fast-Flat Fading Channels Model

Fading is a major concern in wireless transmission networks. This natural phenomenon occurs due to changes in the attenuation levels of a transmitted signal. In general, fading is a time-varying process and can be affected by the transmission frequency, geographic location, atmospheric conditions, etc. In wireless settings multi-path propagation effects also tend to have a sizable impact on channel fading.

Now generally, there are two key types of fading studied in wireless networks, i.e., fast and slow fading. Specifically, these delineations are made based upon the rate at which the fading effects occur, i.e., changes in amplitude and/or phase of transmitted signal. Here fast fading involves amplitude and phase changes on timescales below the delay constraint, i.e., of the channel. In addition there are also two further types of fast fading, flat fading and frequency-selective fading. In the former, all frequency components of a signal experience the same fading behavior, whereas in the latter the fading levels vary across different frequency components of the transmitted signal.

As fading is a key impairment concern, this chapter focuses on PU/SU modeling for fast-flat fading channels (whereas Chapter 4 looks at the case of slow-flat fading channels). In particular, the Rayleigh fast-flat fading model is treated first and appropriate utility functions defined. The existence and uniqueness of the NE for the modified game are then shown and simulation analysis conducted. The process is then repeated for the Rician fast-flat fading channel and overall conclusions drawn.

3.1 Rayleigh Fast-Flat Fading Channels

Consider some further details of a Rayleigh fast-flat fading channels as introduced in Section 2.1.1. Here, the path fading coefficient α_i is modeled as a Rayleigh random variable with pdf given in Eq. (2.8), and the k-th moment of α_i for n degrees of freedom can be determined as [46]:

$$E[\alpha_i^k] = (2\sigma^2)^{\frac{k}{2}} \frac{\Gamma[\frac{1}{2}(n+k)]}{\Gamma[\frac{1}{2}n]} \tag{3.1}$$

where $\Gamma(.)$ is the Gamma function. Now the expectation of α_i^2 can be evaluated by averaging α_i^2 multiplied by Eq. (2.8) over α_i or by setting $n=2$ in Eq. (3.1), given $2\sigma^2$. Here $\sigma^2 = E[(\alpha_i^2)]/2$ is the measure of the distribution's spread and is further assumed to be 1/2 for the rest of this dissertation. Furthermore, for a given I_i, the expected value of ${\gamma_i}^{(s)}$ given in Eq. (2.16) equals $A_i E[(\alpha_i^2)] = A_i$. Hence by using Eqs. (2.16) and (2.8), and by making a change of variable, the conditional pdf of ${\gamma_i}^{(s)}$ given I_i is defined as follows:

$$p_{{\gamma_i}^{(s)}/I_i}({\gamma_i}^{(s)}/I_i) = \frac{1}{A_i} e^{-\frac{\gamma_i^{(s)}}{A_i}} \tag{3.2}$$

Moreover, by taking the average of $\tilde{P}_b(e)$ given in Eq. (2.17) with respect to $p_{{\gamma_i}^{(s)}/I_i}({\gamma_i}^{(s)}/I_i)$ shown in Eq. (3.2), the *conditioned bit error probability*, termed as

$\tilde{P}_e$, can be derived as follows [47]:

$$\begin{aligned}\tilde{P}_e = E[\tilde{P}_b(e)] &= \int_0^\infty \tilde{P}_b(e) p_{{\gamma_i}^{(s)}/I_i}({\gamma_i}^{(s)}/I_i)\, d{\gamma_i}^{(s)} \\ &= (\frac{1}{2A_i}) \int_0^\infty e^{-(\frac{1}{2}+\frac{1}{A_i})\alpha_i}\, d\alpha_i = \frac{1}{(A_i+2)}\end{aligned} \tag{3.3}$$

Now since P_e does not depend upon m, the bit index m can be dropped. Furthermore, assuming $\tilde{P}_e \approx 1/A_i$ for large SINR values, P_e can be determined by taking the expectation of the approximation of Eq. (3.3) as follows [3], [4]:

$$P_e = E[\tilde{P}_e] = E[1/A_i] = \frac{E[I_i] + \sigma_n^2}{h_{si}^2 p_i} \tag{3.4}$$

Hence, by using Eq. (2.15) and assuming $\sigma^2 = 1/2$, Eq. (3.4) can be simplified and rewritten as [3], [4]:

$$P_e = \frac{\sum_{\substack{j=1\\ j\neq i}}^{N} h_{sj}^2 \rho_{ji}^2 p_j + h_{s0}^2 \rho_{ps}^2 P_0 + \sigma_n^2}{h_{si}^2 p_i} = \frac{1}{\bar{\gamma}_i^{(Ra)}} \tag{3.5}$$

where $\bar{\gamma}_i^{(Ra)}$ is the average SINR for Rayleigh fast-flat fading channels.

3.1.1 Utility Functions

As detailed before, a SU's transmission is considered as interference to the PU. Hence, the SUs should minimize their transmission powers in order to achieve the best transmission quality. Thus a suitable utility function for the i-th SU has been given in [7] and [27] for the case of AWGN channels. To further adapt this average utility function to fit the proposed realistic channel model, some additional changes are needed. Namely, $\tilde{P}_b(e)$, which is defined in Eq. (2.17), and was also used in the utility function of [27], must be replaced with P_e which is defined in Eq. (3.5). Hence the modified utility function of the SUs is written as follows:

$$u_i(p_i, \mathbf{p_{-i}}) = \frac{R_i(1-2P_e)^M}{p_i} = \frac{R_i(1-2/\bar{\gamma}_i^{(Ra)})^M}{p_i} \quad (3.6)$$

where $\mathbf{p_{-i}}$ denotes the action vector excluding the action of the i-th user, for $i = 0, 1, \ldots, N$, and R_i is the transmission rate of the i-th SU.

Now the utility function in Eq. (3.6) quantifies the number of successfully transmitted bits per unit transmission power. In addition $P_c = (1-2P_e)^M = f(\bar{\gamma}_i^{(Ra)})$ represents the probability of correct reception of packets at the receiver, where $f(.)$ is the efficiency function. Hence P_c is basically a function of the average SINR and in this dissertation it is assumed that the approximation of this value is consistent with the AWGN game in [7], see [27] for justification.

Overall the utility function for the PU is given as follows [7]:

$$u_0(Q_0, \mathbf{p_{-0}}) = Q_0 - \mu_1[(Q_0 - I_0)^2 u(Q_0 - I_0)] - \mu_2[(e^{(I_0 - Q_0)} - 1)u(I_0 - Q_0)] \quad (3.7)$$

where μ_1 and μ_2 are positive pricing coefficients and $u(.)$ is the step function.

In general, one can interpret the PU utility as being proportional to the payments the SUs need to make for using its spectrum. Hence Eq. (3.7) shows that if SUs can better manage their transmitted powers, they will reduce the total interference caused to the PU. Thus, the PU's utility is proportional to the amount of interference that the PU is willing to tolerate from all SUs. As a result the new modified non-cooperative game for the proposed realistic Rayleigh fast-flat fading channels, $G_1 = (\mathcal{N}, \mathcal{P}, u_i(.))$, has the following three components:

1) **Players**: $\mathcal{N} = \{0, 1, \ldots, N\}$ is the index set of the users currently in the cell, where 0-th user is taken to be the PU and $i = 1, \ldots, N$ represents the i-th SU.

2) **Action space**: $\mathcal{P} = (\mathcal{Q} \times \mathcal{P}_1 \times \mathcal{P}_2 \times \ldots \times \mathcal{P}_N)$, where $\mathcal{Q} = [0, \bar{Q_0}]$ represents the PU's action set and $\mathcal{P}_i = [p_{i(min)}, p_{i(max)}]$ represents the i-th SU's action set. In particular, $\bar{Q_0}$ represents the maximum allowed interference cap of the PU, and $p_{i(min)}$ and $p_{i(max)}$ respectively, represent the minimum and maximum allowed transmission power of the i-th SU. The action vector of all users is denoted by $\mathbf{p} = [Q_0, p_1, \ldots, p_N]$, where $p_i \in \mathcal{P}_i$ and $Q_0 \in \mathcal{Q}$ for $i = 0, 1, \ldots, N$. The PU's strategy is to choose the best Q_0 at any given time, while that of SUs is to adapt their transmit powers.

3) **Utility functions**: In this game $u_i(p_i, \mathbf{p_{-i}})$, given in Eq. (3.6), is used to represent the i-th SU's utility function for Rayleigh fast-flat fading channels. In addition $u_0(Q_0, \mathbf{p_{-0}})$, which is given in Eq. (3.7), is used to represent the utility function of the PU.

3.1.2 Existence of a Nash Equilibrium

Assuming the secondary system employs a MF receiver, the action space defined in [7] should be modified to guarantee the existence of a NE. Moreover, to show the existence of at least one NE point, it is sufficient to show that the utility function is concave in p_i. Now since the quasi-concavity of the PU's utility function has been proven in [7], one only needs to show the quasi-concavity and the continuity of the utility function of the SUs. Hence from Eq. (3.5) it is easy to show that $\frac{\partial \bar{\gamma}_i^{(Ra)}}{\partial p_i} = \frac{\bar{\gamma}_i^{(Ra)}}{p_i}$. By taking the first derivative of Eq. (3.6) one can also get:

$$\frac{\partial u_i(p_i, \mathbf{p_{-i}})}{\partial p_i} = \frac{R_i}{p_i^2}(1 - \frac{2}{\bar{\gamma}_i^{(Ra)}})^{M-1}(\frac{2(M+1)}{\bar{\gamma}_i^{(Ra)}} - 1) \tag{3.8}$$

Furthermore, by setting the above expression to zero, it is seen that $\bar{\gamma}_i^{(Ra)} = 2(M+1)$, which can be further simplified using Eq. (3.5) to [3]:

$$p_i^{max} = 2(M+1)\frac{\sum_{\substack{j=1\\ j\neq i}}^{N} h_{sj}^2 \rho_{ji}^2 p_j + h_{s0}^2 \rho_{ps}^2 P_0 + \sigma_n^2}{h_{si}^2} \tag{3.9}$$

where p_i^{max} is the maximum level of transmit power within the convex action space $\mathcal{P}_i$. Moreover the second derivative of Eq. (3.6) is given as follows:

$$\frac{\partial^2 u_i(p_i, \mathbf{p_{-i}})}{\partial {p_i}^2} = \frac{R_i}{p_i^3}\frac{(1-\frac{2}{\bar{\gamma}_i^{(Ra)}})^M}{(\bar{\gamma}_i^{(Ra)}-2)^2}(4M^2+12M+8+2(\bar{\gamma}_i^{(Ra)})^2-8(M+1)\bar{\gamma}_i^{(Ra)}) \tag{3.10}$$

Hence, the utility function $u_i(p_i, \mathbf{p_{-i}})$ is concave if:

$$\frac{\partial^2 u_i(p_i, \mathbf{p_{-i}})}{\partial {p_i}^2} < 0, \forall \bar{\gamma}_i^{(Ra)} \in (\bar{\gamma}_{i(min)}^{(Ra)}, \bar{\gamma}_{i(max)}^{(Ra)}) \tag{3.11}$$

where $\bar{\gamma}_{i(max)}^{(Ra)} = 2(M+1) + \sqrt{2(M^2+M)}$ is the maximum average SINR and $\bar{\gamma}_{i(min)}^{(Ra)} = 2(M+1) - \sqrt{2(M^2+M)}$ is the minimum average SINR for the Rayleigh fast-flat fading channels. Thus in order to guarantee that the utility function is concave, the action space in [7] should be modified for Rayleigh fast-flat fading channels as follows [3]:

$$\mathcal{P}_i = \{p_i : \bar{\gamma}_i^{(Ra)} \in (\bar{\gamma}_{i(min)}^{(Ra)}, \bar{\gamma}_{i(max)}^{(Ra)})\} \tag{3.12}$$

As such the utility functions of both the PU and SUs satisfy all the required conditions for the existence of at least one NE in this game. The uniqueness of this NE is shown next.

3.1.3 Uniqueness of the Nash Equilibrium

To test the uniqueness of the NE, $r_i^*(\mathbf{p_{-i}})$ is assumed to be the best-response function of player i [37]. Now the best-response vector over all SUs is denoted by $\mathbf{r_1}(\mathbf{p}) = (r_1^*(\mathbf{p_{-1}}), r_2^*(\mathbf{p_{-2}}), \ldots, r_N^*(\mathbf{p_{-N}}))$, where $r_i^*(\mathbf{p_{-i}}) = \min\ (p_i^{max}, p_{i(max)})$ and p_i^{max} is the i-th SU's transmission power which provides it with the *optimum* SINR (i.e., $\bar{\gamma}_i^{(Ra)*}$). Since it is also assumed that all SUs have the same efficiency function, this implies that the SINR corresponding to the best-response is the same for all SUs, i.e., $r_i^*(\mathbf{p_i})$ $= r_i^*(\mathbf{p_{-i}})$. Hence when some of the SUs cannot achieve $\bar{\gamma}_i^{(Ra)*}$, they will send at their maximum possible transmit power and in this case the NE is still unique.

Now in [37] it was shown that if the best-response of the PU and SUs are *standard* functions, then the NE in the game will be unique. Specifically, a function $\mathbf{r}(\mathbf{p})$ is said to be a standard function if it satisfies the following properties:
1) **Positivity**: $\mathbf{r}(\mathbf{p}) > 0$.

2) **Monotonicity**: If $\mathbf{p} \geq \mathbf{p}'$, then $\mathbf{r}(\mathbf{p}) \geq \mathbf{r}(\mathbf{p}')$.

3) **Scalability**: For all $\mu > 1$, $\mu\mathbf{r}(\mathbf{p}) > \mathbf{r}(\mu\mathbf{p})$.

Hence, the best-response correspondence of the SUs in the game can be obtained by setting $u_i'(p_i, \mathbf{p_{-i}})$ to zero which leads to Eq. (3.9) where $p_i^{max} = r_i^*(\mathbf{p_{-i}})$.

Now earlier in [7] it has been shown that the best-response function of the PU is standard and equals $r_0^*(\mathbf{p_{-0}}) = \frac{1}{2\mu_1} + I_0$. As a result one just needs to prove that the best-response function of the SUs is standard by checking the above-detailed three properties. Foremost, the power action sets of the PU and the SUs are closed subsets of $\mathbb{R}$. Furthermore it is easy to check that the utility functions of the PU and the SUs are continuous in $\mathbf{p}$. Also by examining Eq. (3.9), it is easy to check the monotonicity of $\mathbf{r}(\mathbf{p})$ by showing that $p_i^{max}(\mathbf{p}) > p_i^{max}(\mathbf{p}')$ for all i if $\mathbf{p} > \mathbf{p}'$. Finally, to prove scalability, one must show that $p_i^{max}(\mathbf{p_i})$ is scalable. This can be done by rewriting Eq. (3.9) as follows:

$$p_i^{max}(\mathbf{p_i}) = 2(M+1)\frac{\sum_{\substack{j=1\\ j\neq i}}^{N} h_{sj}^2\rho_{ji}^2 p_j + h_{s0}^2\rho_{ps}^2 P_0 + \sigma_n^2}{h_{si}^2} \tag{3.13}$$

$$p_i^{max}(\mu\mathbf{p_i}) = 2(M+1)\frac{\mu(\sum_{\substack{j=1\\ j\neq i}}^{N} h_{sj}^2\rho_{ji}^2 p_j + h_{s0}^2\rho_{ps}^2 P_0) + \sigma_n^2}{h_{si}^2} \tag{3.14}$$

while

$$\mu p_i^{max}(\mathbf{p_i}) = 2\mu(M+1)\frac{\sum_{\substack{j=1\\ j\neq i}}^{N} h_{sj}^2\rho_{ji}^2 p_j + h_{s0}^2\rho_{ps}^2 P_0 + \sigma_n^2}{h_{si}^2} \tag{3.15}$$

From Eqs. (3.14) and (3.15) it is obvious that $\mu p_i^{max}(\mathbf{p_i}) > p_i^{max}(\mu\mathbf{p_i})$, which completes NE uniqueness proof for Rayleigh fast-flat fading channels model.

3.1.4 Analysis of Simulation Results

Detailed simulations are done to model the performance of the game theoretic scheme. In particular, the following parameters are used: $\bar{Q_0} = 5$, $\rho_{pi} = \rho_{ip} = \rho_{ji} = 0.1$, $h_{pi} = h_{ip} = h_{ji} = 1$ for all i , $j \in \{1, \ldots, N\}$, $M = 80$, $R_i = 1$, $\bar{\gamma_0} = 10$, $\sigma_n^2 = 1$, $\mu_1 = 10$ and $\mu_2 = 100$. First of all, the PU utility at the NE is shown as a function of the number of SUs N in Figure 3.1. Here it is seen that when $\bar{Q_0} < I_0$, the PU's utility is severely penalized by the exponential pricing function. This occurs when $N \geq 26$ for AWGN channel and when $N \geq 17$ for Rayleigh fast-flat fading channels. Meanwhile Figure 3.2 plots I_0 values from all SUs to the PU. Here when $N > 3$ for AWGN channel case, the network cannot support these SUs, and as a result, no SU can achieve its optimal SINR. Thus all SUs are forced to transmit at their maximum power levels, and both the PU's utility at the NE and I_0 increase linearly with N.

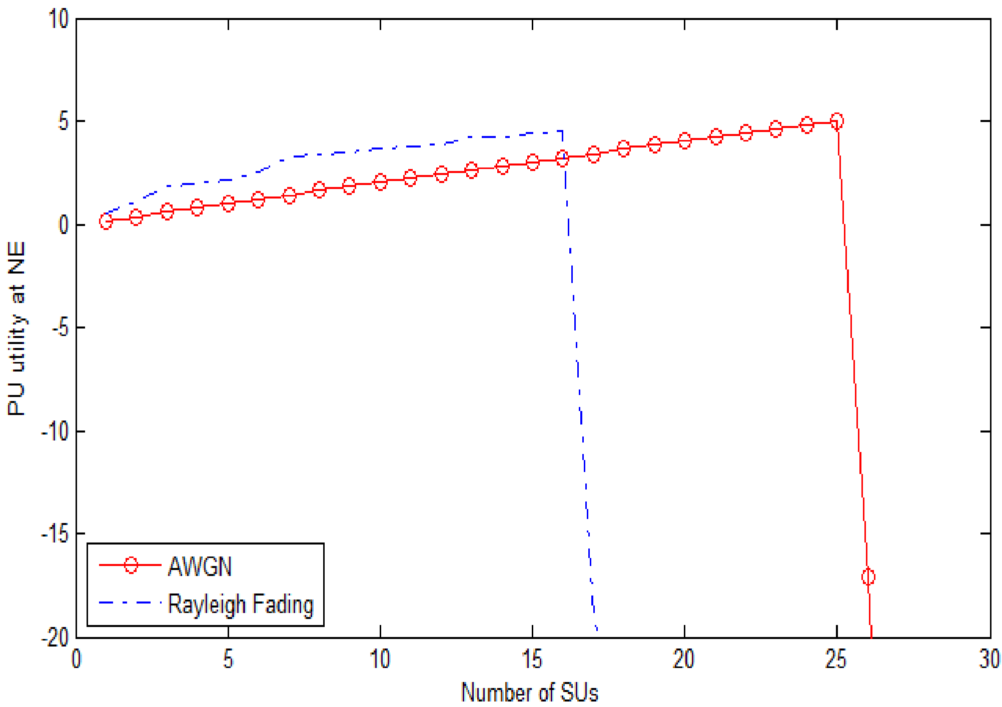

Figure 3.1: Primary user's utility at the NE for Rayleigh fast fading

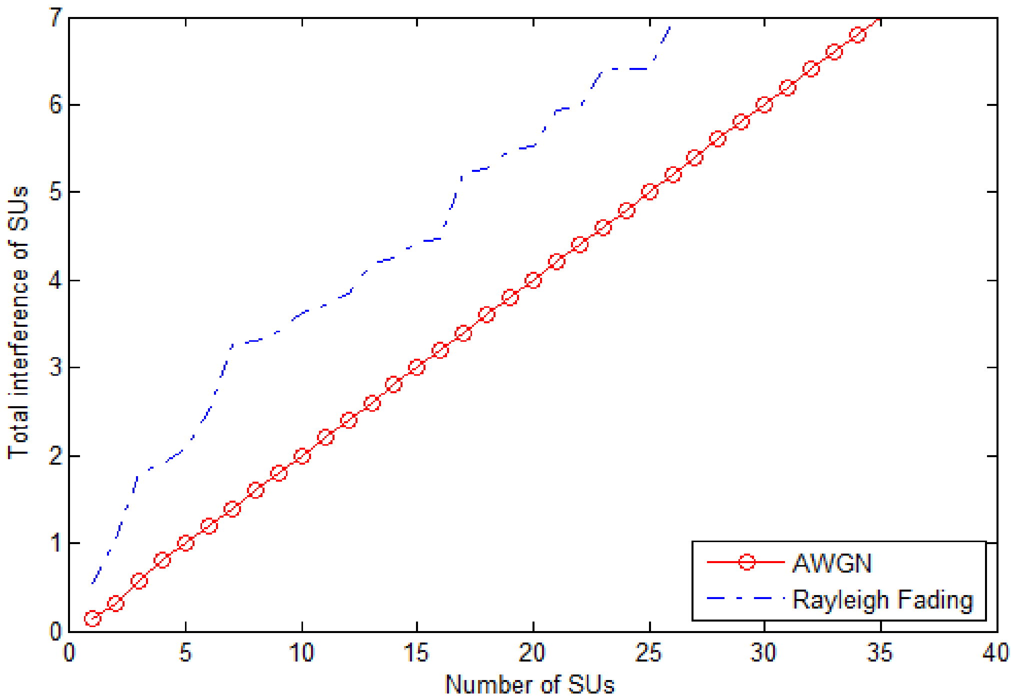

Figure 3.2: Total interference from all secondary users for Rayleigh fast fading

Next, the average SU utility is also shown in Figure 3.3. Here as the number of SUs increases, each SU (as well as the PU) sees more interference due to the added numbers of SUs. Thus each SU has to transmit at a higher power than that with smaller numbers of SUs in the system in order to achieve the same optimum SINR. This reduces the average utility. Figure 3.4 also plots the number of SU's in energy efficient mode. Hence one sees that all SUs will maximize their utility by achieving their optimum SINR, i.e., $\bar{\gamma}_i^*$ and $\bar{\gamma}_i^{(Ra)*}$, when $0 < N \leq 1$ for Rayleigh fast-flat fading channels and when $0 < N \leq 3$ for AWGN channels. Otherwise, the network cannot afford these SUs, i.e., no SU can achieve its optimum SINR. In this case all SUs transmit at their maximum possible power levels, which equals $\bar{P}_i = 20$ for AWGN channels and $P_i^{(max)}$ for Rayleigh fast-flat fading channels.

Finally, Figure 3.5 shows the number of SUs that the PU can afford as a function of the total number of SUs. This could be any number of SUs as long as $\bar{Q}_0 > I_0$, where $N = 25$ for AWGN channel and $N = 17$ for Rayleigh fast-flat fading channels. As expected, the total number of SUs that the PU can afford is lower in the case of Rayleigh fast-flat fading channels. In addition, Figure 3.6 shows the aggregate utility achieved by all SUs at the NE. These results show that the sum of all SUs' utility has a unique maximum when $N = 4$ for AWGN channel and when $N = 6$ for Rayleigh fast-flat fading channels. As the number of SUs increases, average SU utility decreases. Also when $N < 4$ for AWGN channel and $N < 6$ for Rayleigh fast-flat fading channels, the decrease in the average SU utility is dominated by the increase of the number of SUs, and hence the aggregate utility of all SUs still increases. Conversely, the aggregate utility decreases due to the decay of the average SU utility.

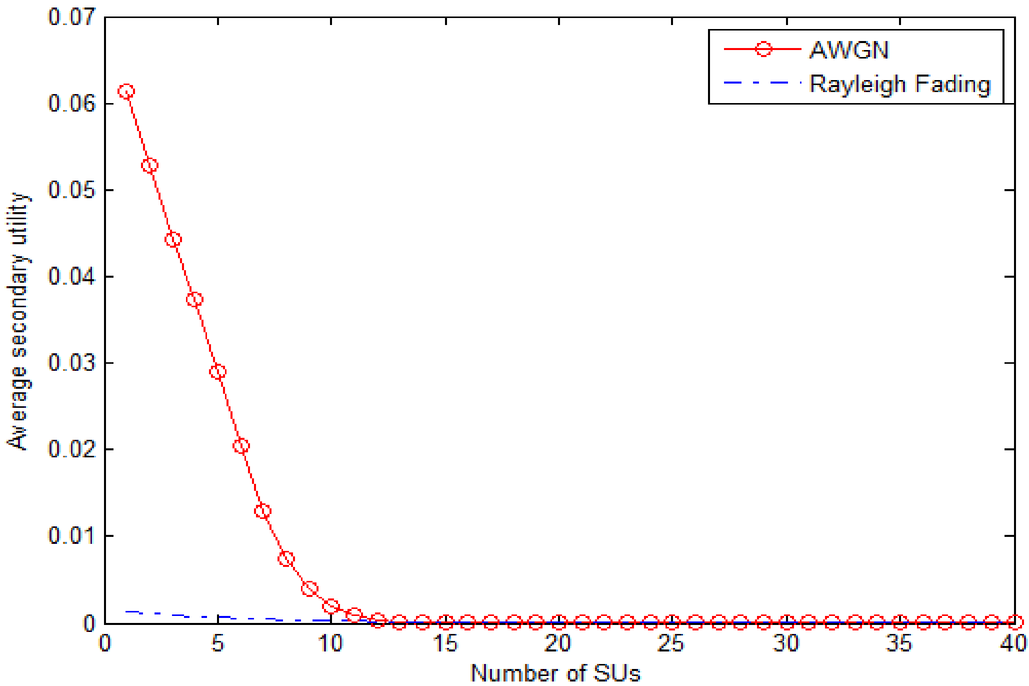

Figure 3.3: Average secondary user's utility at the NE for Rayleigh fast fading

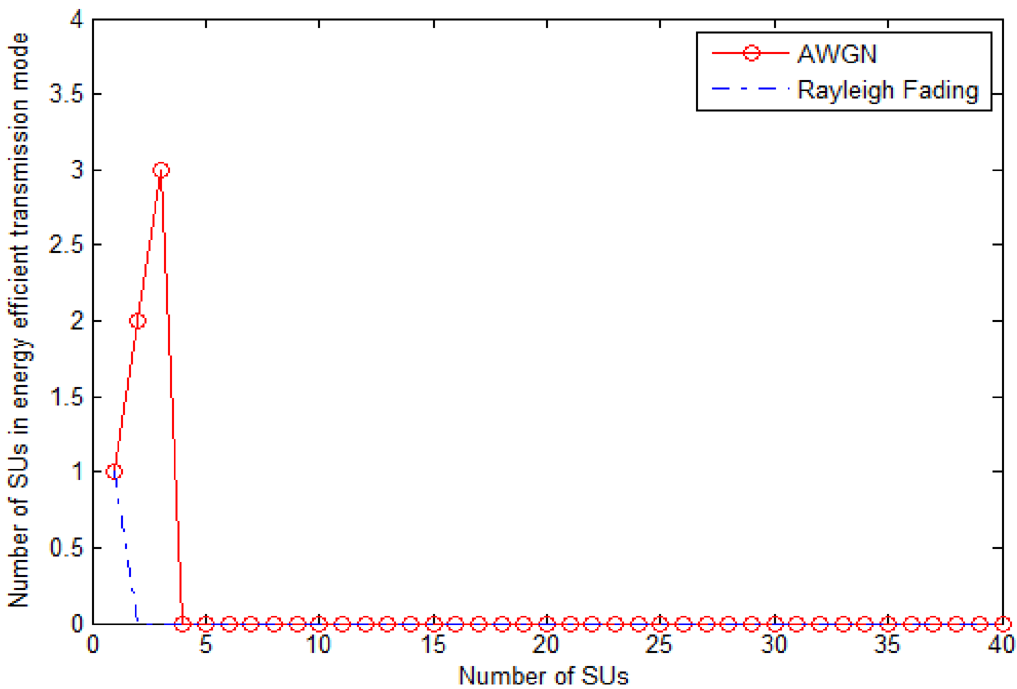

Figure 3.4: Number of SUs in energy-efficient mode for Rayleigh fast fading

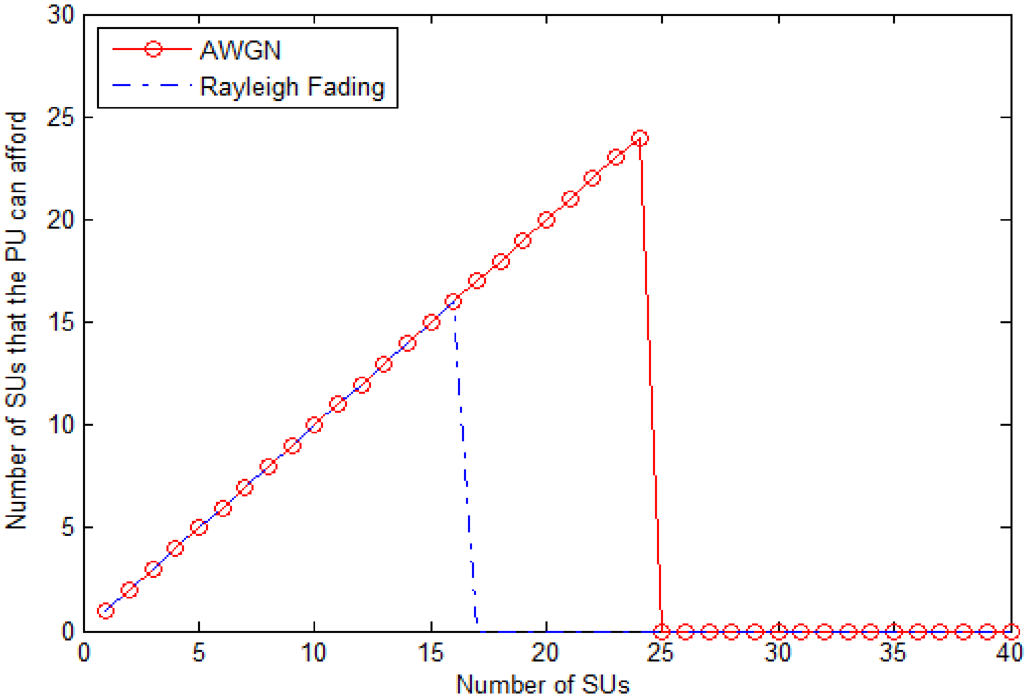

Figure 3.5: The maximum number of SUs that can be supported for Rayleigh fast fading

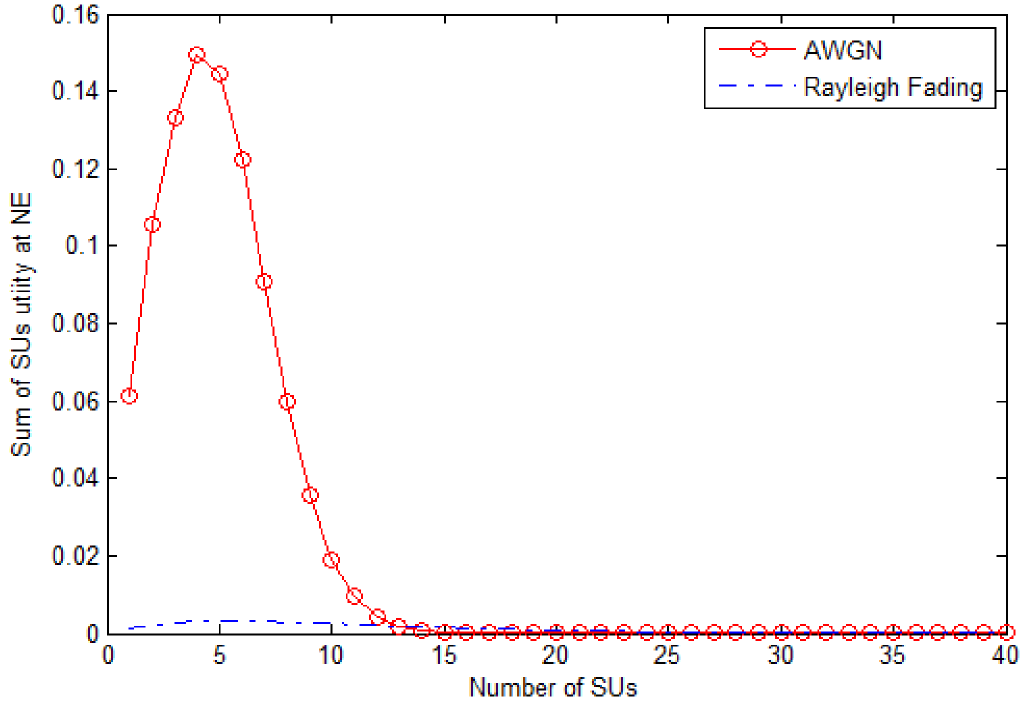

Figure 3.6: Sum of secondary users' utility at the NE for Rayleigh fast fading

3.2 Rician Fast-Flat Fading Channels

The Rician channel is another popular fast-flat fading channel model. In general the performance of wireless telecommunication systems under this channel is better than that with Rayleigh fast-flat fading channels. This is attributed to the existence of the LOS component, i.e., stronger received signal. Along these lines, consider the derivation of the *bit error probability*, P_e, for Rician fast-flat fading channels. First, the path fading coefficient α_i is modeled as a random variable with Rician pdf given by Eq. (2.9). Here $(\alpha_i/\sigma)^2$ has a non-central chi-square distribution with two degrees of freedom and non-centrality parameter $(s/\sigma)^2$. Furthermore, the Rician K-factor, i.e., $0.5(s/\sigma)^2$, is defined as the ratio of signal power in dominant component over the (local-mean) scattered power.

Assuming $\sigma^2 = 1/2$, and using Eqs. (2.16) and (2.9) with a change of variable, the conditional pdf of ${\gamma_i}^{(s)}$ given I_i is defined as follows [4]:

$$p_{{\gamma_i}^{(s)}/I_i}({\gamma_i}^{(s)}/I_i) = \frac{e^{-s^2}}{A_i} e^{-(\frac{\gamma_i^{(s)}}{A_i})} I_0(2s\sqrt{{\gamma_i}^{(s)}/A_i}) \tag{3.16}$$

Furthermore, taking the average of $\tilde{P}_b(e)$ with respect to $p_{{\gamma_i}^{(s)}/I_i}({\gamma_i}^{(s)}/I_i)$, the *conditioned bit error probability*, $(\tilde{P}_e)$, in Eq. (2.17) can be derived as follows [4], [47]:

$$\begin{aligned}\tilde{P}_e = E[\tilde{P}_b(e)] &= \int_0^\infty \tilde{P}_b(e) p_{{\gamma_i}^{(s)}/I_i}({\gamma_i}^{(s)}/I_i)\, d\gamma_i^{(s)} \\ &= \frac{e^{-s^2}}{2A_i} \int_0^\infty e^{-(\frac{1}{2}+\frac{1}{A_i})\gamma_i^{(s)}} I_0(2s\sqrt{{\gamma_i}^{(s)}/A_i})\, d\gamma_i^{(s)}\end{aligned} \tag{3.17}$$

Using the following expansion of the zero-order modified first-kind Bessel function

[46]:

$$I_0(x) = \sum_{k=0}^{\infty} \frac{(\frac{x}{2})^{2k}}{(k!)^2} \tag{3.18}$$

Eq. (3.17) can be further simplified as follows:

$$\tilde{P}_e = \sum_{k=0}^{\infty} \frac{e^{-s^2}}{2A_i} \int_0^{\infty} \frac{(s\sqrt{\gamma_i{}^{(s)}/A_i})^{2k}}{(k!)^2} \; e^{-(\frac{1}{2}+\frac{1}{A_i})\gamma_i^{(s)}} \; d\gamma_i^{(s)} \tag{3.19}$$

Moreover, using the fact that $\int_0^{\infty} x^{(2k+1)} e^{-ax^2}\, dx = k!/2a^{(k+1)}$ and the exponential expansion $e^x = \sum_{k=0}^{\infty} x^k/k!$, the above equation can be simplified to:

$$\tilde{P}_e = \frac{1}{A_i+2}\; e^{s^2(\frac{-A_i}{A_i+2})} \tag{3.20}$$

finally, assuming $\tilde{P}_e \approx e^{-s^2}/A_i$ for large SINR, P_e can be found by taking the expectation of the approximation of Eq. (3.20) as follows:

$$P_e = E[\tilde{P}_e] \approx E[1/A_i]e^{-s^2} = \frac{E[I_i] + \sigma_n^2}{h_{si}^2 p_i} e^{-s^2} \tag{3.21}$$

where the expectation of I_i is defined as [4]:

$$E[I_i] = \sum_{\substack{j=1 \\ j\neq i}}^{N} h_{sj}^2 \rho_{ji}^2 p_j E[\alpha_j^2] + h_{s0}^2 \rho_{ps}^2 P_0 E[\alpha_0^2] \tag{3.22}$$

Carefully note that the bit index m is dropped here since P_e does not depend upon m. Furthermore, the k-th moment of α_j for n degrees of freedom can be found using [46] as:

$$E[\alpha_j^k] = (2\sigma^2)^{\frac{k}{2}} e^{-(\frac{s^2}{2\sigma^2})} \frac{\Gamma[\frac{1}{2}(n+k)]}{\Gamma[\frac{1}{2}n]}\, {}_1F_1(\frac{n+k}{2}, \frac{n}{2}; \frac{s^2}{2\sigma^2}) \tag{3.23}$$

where ${}_1F_1(a, b; c)$ is the confluent hypergeometric function and $\Gamma(.)$ is the Gamma function. Hence for $n = 2$ and assuming $\sigma^2 = 1/2$, Eq. (3.23) can be rewritten as:

$$E[\alpha_j^2] = e^{-s^2} \frac{\Gamma[2]}{\Gamma[1]} {}_1F_1(2, 1; s^2), \quad j = 0, 1, \ldots, N \tag{3.24}$$

Again, using exponential expansion and the fact that [46]:

$${}_1F_1(\alpha, \beta; x) = \sum_{k=0}^{\infty} \frac{\Gamma(\alpha + k)\Gamma(\beta)x^k}{\Gamma(\alpha)\Gamma(\beta + k)k!}, \quad \beta \neq 0, -1, .. \tag{3.25}$$

hence, one can rewrite Eq. (3.24) as:

$$E[\alpha_j^2] = e^{-s^2} (\sum_{k=0}^{\infty} \frac{\Gamma(2 + k)\Gamma(1)s^{2k}}{\Gamma(2)\Gamma(1 + k)k!}) = e^{-s^2} (\sum_{k=0}^{\infty} \frac{k(s)^{2k}}{k!} + \sum_{k=0}^{\infty} \frac{(s)^{2k}}{k!}) \;\; j = 0, 1, \ldots, N \tag{3.26}$$

After some manipulation, the above equation can be rewritten as follows:

$$E[\alpha_j^2] = s^2 + 1, \quad j = 0, 1, \ldots, N \tag{3.27}$$

Furthermore, using Eqs. (3.22) and (3.27) one can simplify (3.21) to [4]:

$$P_e \approx \frac{(\sum_{\substack{j=1, \\ j \neq i}}^{N} h_{sj}^2 \rho_{ji}^2 p_j + h_{s0}^2 \rho_{ps}^2 P_0)(s^2 + 1) + \sigma_n^2}{h_{si}^2 p_i e^{s^2}} \approx \frac{1}{\bar{\gamma}_i^{(Rice)}} \tag{3.28}$$

where $\bar{\gamma}_i^{(Rice)}$ is the average SINR for Rician fast-flat fading channels.

3.2.1 Utility Functions

SU transmissions in CR networks are generally considered as interference to the PU. Hence SUs should maximize their transmission energy efficiency by using the smallest possible amount of transmission power to achieve the best transmission quality. Along these lines, a suitable utility function for the i-th secondary user has been given in [7] and [27]. However, to adapt this average utility function to fit the proposed realistic Rician fast-flat fading channels model, some changes are needed. Namely, $\tilde{P}_b(e)$ which is defined in Eq. (2.17) and was used to define the utility function in [7] and [27], must be replaced with P_e which is defined in Eq. (3.28) for Rician fast-flat fading channels. Hence one can get [4], [48]:

$$u_i(p_i, \mathbf{p_{-i}}) = \frac{R_i(1-2P_e)^M}{p_i} = \frac{R_i(1-2/\bar{\gamma}_i^{(Rice)})^M}{p_i} \tag{3.29}$$

where R_i is the transmission rate of the i-th SU and $\mathbf{p_{-i}}$ denotes the action vector excluding the action of the i-th user, for $i = 0, 1, \ldots, N$.

In general the utility function in Eq. (3.29) quantifies the number of successfully transmitted bits per unit transmission power. Furthermore, in order to be consistent with the AWGN games in [7] and [27], the *probability of correct reception* of packets at the receiver, P_c, which is a function of the average SINR, is defined as $P_c = (1-2P_e)^M = f(\bar{\gamma}_i^{(Rice)})$, where $f(.)$ is the efficiency function, see [27]. Now the utility function for the PU remains the same as that given in Eq. (3.7). Overall, the PU's utility can be interpreted as being proportion to the payments the SUs need to make for using its spectrum. In other words, the PU's utility is proportional to the amount of interference that the PU is willing to tolerate from all SUs. Hence, the new modified non-cooperative game for the proposed realistic Rician fast-flat fading channels, $G_2 = (\mathcal{N}, \mathcal{P}, u_i(.))$, has the following components:

1) **Players**: $\mathcal{N} = \{0, 1, \ldots, N\}$ is the index set of the users currently in the cell, where 0-th user represents the PU and $i = 1, \ldots, N$ represents the i-th SU.

2) **Action space**: $\mathcal{P} = (\mathcal{Q} \times \mathcal{P}_1 \times \mathcal{P}_2 \times \ldots \times \mathcal{P}_N)$, where $\mathcal{Q} = [0, \bar{Q}_0]$ represents the PU's action set and $\mathcal{P}_i = [p_{i(min)}, p_{i(max)}]$ represents the i-th SU's action set. Here

$\bar{Q_0}$ represents the maximum allowed Q_0 of the PU, and $p_{i(min)}$ and $p_{i(max)}$ represent the minimum and maximum allowed transmission power of the i-th SU respectively. The action vector of all users is denoted by $\mathbf{p} = [Q_0, p_1, \dots, p_N]$, where $p_i \in \mathcal{P}_i$ and $Q_0 \in \mathcal{Q}$ for $i = 0, 1, \dots, N$. It is important to note that PU's strategy is to choose the best Q_0 at any given time, while that of SUs is to adapt their transmit powers.

3) **Utility functions**: In this game $u_i(p_i, \mathbf{p_{-i}})$, given in Eq. (3.29) is used to represent the i-th SU's utility function for Rician fast-flat fading channels. Meanwhile $u_0(Q_0, \mathbf{p_{-0}})$, given in Eq. (3.7), is used to represent utility function the PU.

3.2.2 Existence of a Nash Equilibrium

Again, assuming a MF receiver is employed at the SU systems, the action space defined in [7] must be modified to guarantee the existence of NE for realistic Rician fast-flat fading channels. Hence the steps to show the existence and uniqueness of the NE for Rician fast-flat fading channels are now presented. To prove the existence of a NE point, it is again sufficient to show that the all utility functions are concave in p_i. Now given that the quasi-concavity of the PU's utility function has been proven in [7], the only thing that needs to be shown here is the quasi-concavity and the continuity of the utility functions of the SUs. Hence from Eq. (3.28), it is easy to show that $\frac{\partial \bar{\gamma}_i^{(Rice)}}{\partial p_i} = \frac{\bar{\gamma}_i^{(Rice)}}{p_i}$. Moreover by taking the first derivative of Eq. (3.29) one gets [4], [48]:

$$\frac{\partial u_i(p_i, \mathbf{p_{-i}})}{\partial p_i} = \frac{R_i}{p_i^2}(1 - \frac{2}{\bar{\gamma}_i^{(Rice)}})^{M-1}(\frac{2(M+1)}{\bar{\gamma}_i^{(Rice)}} - 1) \tag{3.30}$$

By setting the above expression to zero, it is seen that $\bar{\gamma}_i^{(Rice)} = 2(M+1)$, which can be further simplified using Eq. (3.28) to:

$$p_i^{max} = 2(M+1)\frac{(\sum_{\substack{j=1 \\ j\neq i}}^{N} h_{sj}^2\rho_{ji}^2 p_j + h_{s0}^2\rho_{ps}^2 P_0)(s^2+1)+\sigma_n^2}{h_{si}^2 e^{s^2}} \tag{3.31}$$

where p_i^{max} is the maximum level of transmit power within the convex action space $\mathcal{P}_i$. Furthermore the second derivative of Eq. (3.29) is given as follows:

$$\frac{\partial^2 u_i(p_i, \mathbf{p_{-i}})}{\partial {p_i}^2} = \frac{R_i}{p_i^3}\frac{(1-\frac{2}{\bar{\gamma}_i^{(Rice)}})^M}{(\bar{\gamma}_i^{(Rice)}-2)^2}(4M^2+12M+8+2(\bar{\gamma}_i^{(Rice)})^2-8(M+1)\bar{\gamma}_i^{(Rice)}) \tag{3.32}$$

Hence the utility function $u_i(p_i, \mathbf{p_{-i}})$ is concave if:

$$\frac{\partial^2 u_i(p_i, \mathbf{p_{-i}})}{\partial {p_i}^2} < 0, \quad \forall \bar{\gamma}_i^{(Rice)} \in (\bar{\gamma}_{i(min)}^{(Rice)}, \bar{\gamma}_{i(max)}^{(Rice)}) \tag{3.33}$$

where $\bar{\gamma}_{i(max)}^{(Rice)} = 2(M+1) + \sqrt{2(M^2+M)}$ is the maximum average SINR and $\bar{\gamma}_{i(min)}^{(Rice)} = 2(M+1) - \sqrt{2(M^2+M)}$ is the minimum average SINR for the Rician fast-flat fading channels. Based upon the above, the action space in [7] must be modified to fit Rician fast-flat fading channels as follows [4], [48]:

$$\mathcal{P}_i = \{p_i : \bar{\gamma}_i^{(Rice)} \in (\bar{\gamma}_{i(min)}^{(Rice)}, \bar{\gamma}_{i(max)}^{(Rice)})\} \tag{3.34}$$

This modification will guarantee that the utility function is concave. As such the utility functions of both the PU and SUs satisfy all the required conditions for the existence of at least one NE in this game. The uniqueness of this NE is now shown.

3.2.3 Uniqueness of Nash Equilibrium

The best-response function of player i, $r_i^*(\mathbf{p_{-i}})$, is used to test the uniqueness of the NE [37]. Now the best-response vector over all SUs is given by $\mathbf{r_2}(\mathbf{p}) = (r_1^*(\mathbf{p_{-1}}), r_2^*(\mathbf{p_{-2}}), \ldots, r_N^*(\mathbf{p_{-N}}))$, where $r_i^*(\mathbf{p_{-i}}) = \min\,(p_i^{max}, p_{i(max)})$ and p_i^{max} is the i-th SU's transmission power which gives it the optimum SINR ($\bar{\gamma}_i^{(Rice)*}$) for Rician fast-flat fading channels. Since it is assumed that all SUs have the same efficiency function, this also implies that the SINR corresponding to the best-response is the same for all SUs, i.e., $r_i^*(\mathbf{p_i}) = r_i^*(\mathbf{p_{-i}})$. Hence when some of the SUs cannot achieve their optimum SINR, they will send at their maximum possible transmit power levels and the NE is still unique in this case. Moreover it has been shown in [37] that if the best-response of the PU and SUs are standard functions, then the NE in the game will be unique. Now consider the same conditions for positivity, monotonicity and scalability noted in Section 3.2.3. Hence the best-response correspondence of the SUs in our game can be obtained by setting $u_i^{'}(p_i, \mathbf{p_{-i}})$ to zero, which leads to Eq. (3.31) for Rician fast-flat fading channels, where $p_i^{max} = r_i^*(\mathbf{p_{-i}})$.

As indicated earlier, the best-response function of the PU has been shown to be standard and equals $r_0^*(\mathbf{p_{-0}}) = \frac{1}{2\mu_1} + I_0$. Hence one just needs to prove that the best-response function of the SUs is also standard by checking the three properties listed in Section 3.2.3. Foremost, the power action sets of the PU and the SUs are closed subsets of $\mathbb{R}$. Furthermore, it is easy to check that the utility functions of the PU and the SUs are continuous in $\mathbf{p}$. Also by examining Eq. (3.31), it is easy to check the monotonicity of $\mathbf{r}(\mathbf{p})$ by showing that $p_i^{max}(\mathbf{p}) > p_i^{max}(\mathbf{p}^{'})$ for all i if $\mathbf{p} > \mathbf{p}^{'}$. Finally, to prove scalability, one must show that $p_i^{max}(\mathbf{p_i})$ is scalable. This can be achieved by rewriting Eq. (3.31) as follows:

$$
\begin{aligned}
p_i^{max}(\mathbf{p_{-i}}) &= 2(M+1)\frac{(\sum_{\substack{j=1,\\ j\neq i}}^{N} h_{sj}^2\rho_{ji}^2 p_j + h_{s0}^2\rho_{ps}^2 P_0)(s^2+1)+\sigma_n^2}{h_{si}^2} \\
p_i^{max}(\mu\mathbf{p_{-i}}) &= 2(M+1)\frac{\mu((\sum_{\substack{j=1,\\ j\neq i}}^{N} h_{sj}^2\rho_{ji}^2 p_j + h_{s0}^2\rho_{ps}^2 P_0)(s^2+1))+\sigma_n^2}{h_{si}^2}
\end{aligned}
\tag{3.35}
$$

while

$$
\mu p_i^{max}(\mathbf{p_{-i}}) = 2\mu(M+1)\frac{(\sum_{\substack{j=1,\\ j\neq i}}^{N} h_{sj}^2\rho_{ji}^2 p_j + h_{s0}^2\rho_{ps}^2 P_0)(s^2+1)+\sigma_n^2}{h_{si}^2} \tag{3.36}
$$

From Eqs. (3.35) and (3.36) it is obvious that $\mu p_i^{max}(\mathbf{p_{-i}}) > p_i^{max}(\mu\mathbf{p_{-i}})$, which completes NE uniqueness proof for the case of Rician fast-flat fading channels model.

3.2.4 Analysis and Simulation Results

To model the performance of the proposed game theoretic scheme, detailed simulations are done. Results with the earlier-developed Rayleigh fast-flat fading channels (Section 3.2.4) are also included for comparison purposes. Again, the following parameters are used: $\bar{Q_0} = 5$, $\rho_{pi} = \rho_{ip} = \rho_{ji} = 0.1$, $h_{pi} = h_{ip} = h_{ji} = 1$ for all i , $j \in \{1, \ldots, N\}$, $M = 80$, $R_i = 1$, $\bar{\gamma_0} = 10$, $\sigma_n^2 = 1$, $\mu_1 = 10$ and $\mu_2 = 100$. First of all, the PU utility at the NE is shown as a function of the number of SUs, N, in Figure 3.7. Here it is seen that when $\bar{Q_0} < I_0$, the PU's utility is severely penalized by the exponential pricing function. This happens when $N \geq 26$ for AWGN channel, $N \geq 17$, and $N \geq 14$ for Rayleigh and Rician fast-flat fading channels, respectively. Meanwhile, Figure 3.8 shows the total interference, I_0, from all SUs to the PU. Here when $N > 3$ for AWGN channel case, the network cannot support these SUs, and as a result no SU can achieve its optimal SINR. Hence all SUs are forced to transmit at their maximum possible power levels, and I_0 increases linearly with N. As a result the PU's utility at the NE also increases linearly. Moreover, when $N \geq 9$ for both fast-flat fading channels, I_0 is greater than that for AWGN channel and therefore the PU's utility (proportional to the total amount of interference) is also higher, as shown in Figure 3.8.

Next, the average SU utility is plotted in Figure 3.9. Here as the number of SUs increases, each SU as well as the PU, sees more interference due to the added SUs. Therefore in order to achieve the same optimum SINR, each SU has to transmit at a higher power than that with a smaller number of SUs, and this decreases the average utility. Moreover the average utility in the case of fading is also lower than that for AWGN channels, i.e., due to the interference introduced to the channel by fading. For example, when $N < 4$ for AWGN channel, $N < 9$ for Rayleigh fast-flat fading channels, and $N < 5$ for Rician fast-flat fading channels, the decrease in the average SU utility is dominated by the increase of the number of SUs (Figure 3.9). Here the aggregate utility of all SUs still increases. Conversely, the aggregate utility decreases due to the decay of the average SU utility. Figure 3.10 also shows the number of SUs in energy-efficient mode. Here when $0 < N \leq 3$ for AWGN channel, $0 < N \leq 4$, and $0 < N \leq 1$ for Rayleigh and Rician fast-flat fading channels, respectively, one sees that all SUs maximize their utility by achieving their optimum SINR. Otherwise the network cannot afford these SUs and hence no SU can achieve its optimum SINR. Thus all SUs transmit at their maximum possible power level, which equals $\bar{P}_i = 20$ for AWGN channel and $P_i^{(max)}$ for the both fast-flat fading channels.

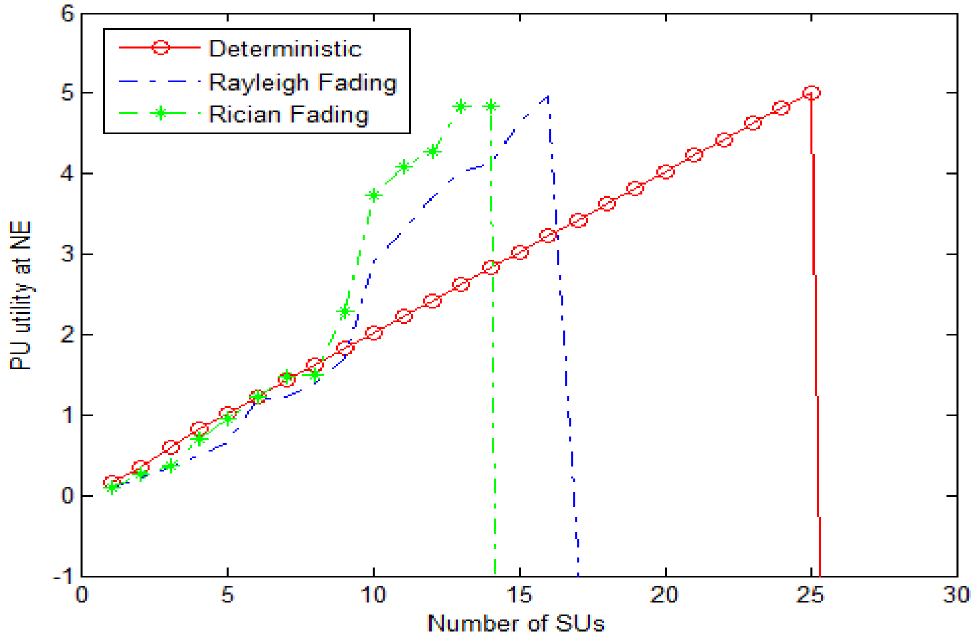

Figure 3.7: Primary user's utility at the NE for Rician fast fading

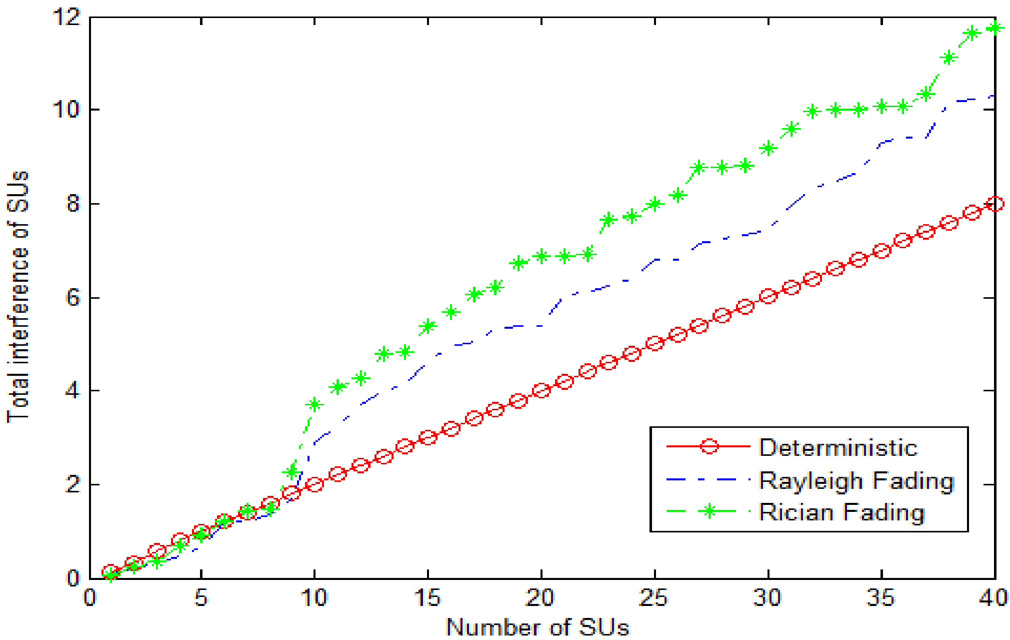

Figure 3.8: Total interference from all secondary users for Rician fast fading

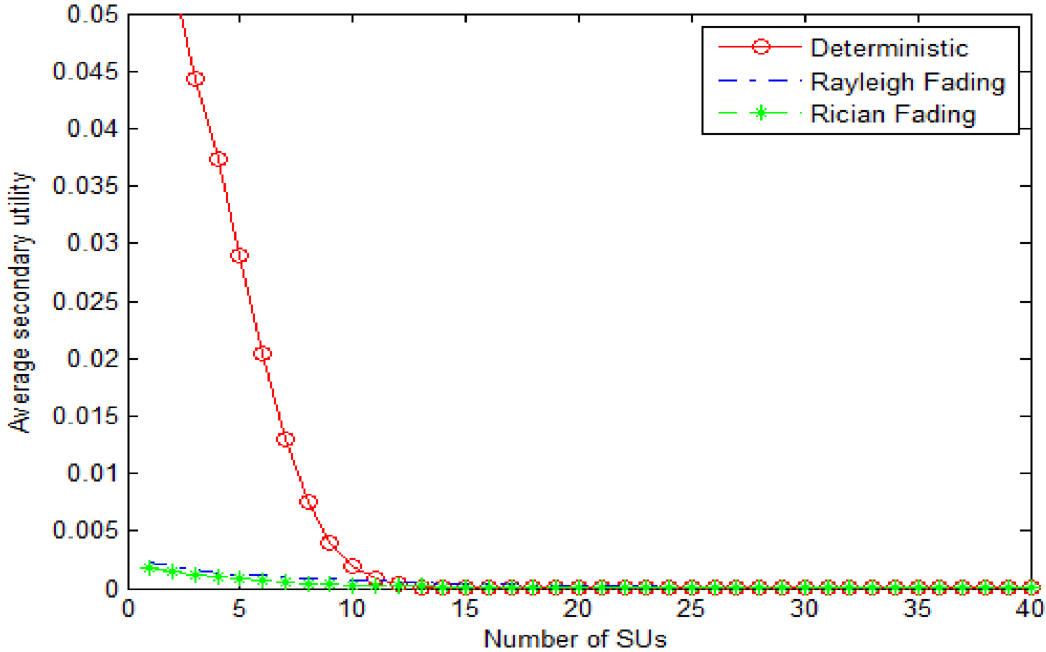

Figure 3.9: Average secondary user's utility at the NE for Rician fast fading

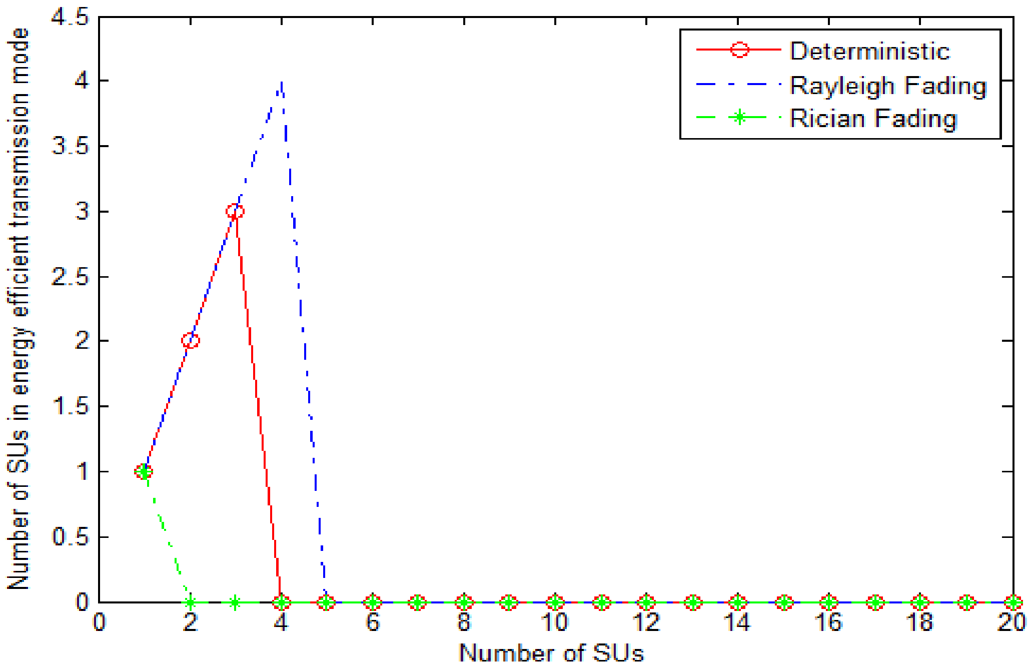

Figure 3.10: Number of SUs in energy-efficient mode for Rician fast fading

Finally, Figure 3.11 plots the number of SUs, N, that the PU can afford as a function of the total number of SUs. In general this can be any number of SUs as long as $\bar{Q}_0 > I_0$, and from the plot we get $N = 25$ for AWGN, $N = 17$ for Rayleigh fast-flat fading channels and $N = 14$ for Rician fast-flat fading channels. As expected, the total number of SUs that the PU can afford is generally lower in fast-flat fading channels. In addition, Figure 3.12 shows the aggregate utility achieved by all SUs at the NE. These results show that the sum of all SUs' utility has a unique maximum when $N = 4$ for AWGN channel, $N = 9$, and $N = 5$ for Rayleigh and Rician fast-flat fading channels, respectively. Also as the number of SUs increases, average SU utility decreases.

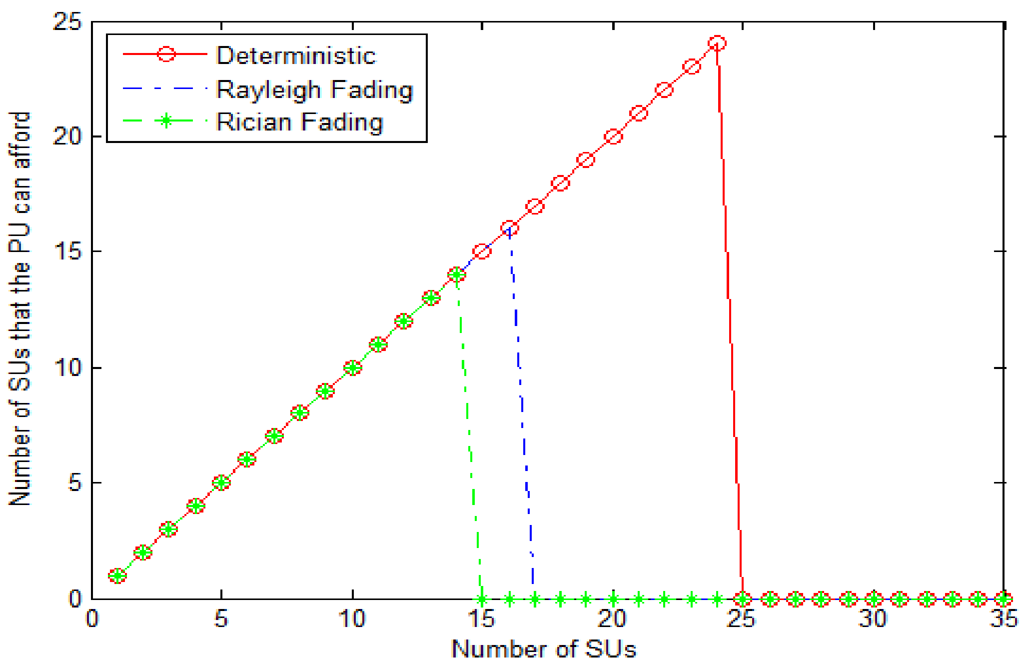

Figure 3.11: The maximum number of SUs that can be supported for Rician fast fading

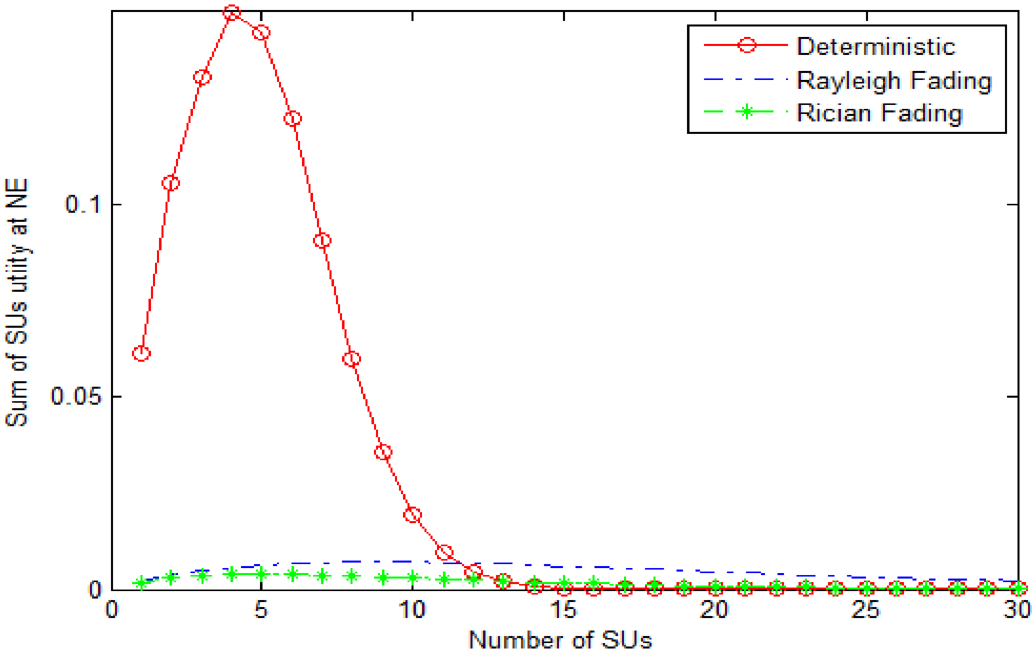

Figure 3.12: Sum of secondary users' utility at the NE for Rician fast fading

3.3 Conclusions

This chapter studies the impact of fast-flat fading on game-theoretic models for CR networks. In particular, the average bit error rate, P_e, is derived for each bit in the packet, and the average utility functions are then evaluated for both Rayleigh and Rician fast-flat fading channels. In these models the path fading coefficient cannot be assumed as constant over the packet duration, albeit it can be over the bit duration. Detailed analytical derivations are performed to show that the modified realistic game can achieve a unique NE point, assuming MF detectors are used at the secondary systems. Overall, the simulations show that the proposed scheme yields realistic energy efficiency for SUs without compromising transmission quality for PUs. The results are also compared with more basic AWGN models. Overall, both Rayleigh and Rician fast-flat fading channels are seen to have a very direct impact upon the performance of the scheme, e.g., in terms of reduced numbers of users supported by the PU (due to higher interference) and lower throughput-per-unit-power (utility).

Chapter 4

Slow Flat-Fading Channels Model

Building upon the work in Chapter 2, the impact of slow-flat fading channels on PU/SU behaviors is now considered. As mentioned in Section 2.1.2, the amplitudes of the fading coefficient in these type of channels have slower rate of changes as compared to fast-flat fading channels. Hence the fading parameter α_i is assumed to change independently for each packet. Herein, both Rayleigh and Rician slow-flat fading channels are considered.

4.1 Rayleigh Slow-Flat Fading Channels

Unlike fast-flat fading channels, the fading coefficient parameters α_i and α_j in slow-flat fading channels are assumed to be independent for $j \neq i$. Moreover, in this work the path fading coefficient of the i-th user, α_i, is modeled for both Rayleigh and Rician random variables. Now consider the derivation of P_e. Here path fading coefficient of the i-th user, α_i, is modeled as a Rayleigh random variable. Furthermore, given $\tilde{P}_b(e)$ in Eq. (2.17) the average correct packet reception, P_c, for M bits in each packet is given by $E[(1 - \tilde{P}_b(e))^M]$, where the expectation is taken with respect to the random variables $\gamma_i^{(s)}$ and I_i. Thus the utility function of the SUs can be written as [49]:

$$u_i(p_i, \mathbf{p_{-i}}/\gamma_i^{(s)}, I_i) = \frac{f(\gamma_i^{(s)})}{p_i} = \frac{R_i P_c}{p_i} \tag{4.1}$$

where R_i is the transmission rate of the i-th SU, $\mathbf{p_{-i}}$ denotes the action vector excluding the action of the i-th user, and $f(\gamma_i^{(s)})$ represents the probability of correct reception of packets at the receiver, where $f(.)$ is the efficiency function. Moreover, it is also assumed that $P_c = (1 - 2P_e)^M$, which is consistent with the AWGN game in [7], i.e., $u_i(p_i, \mathbf{p_{-i}}/\alpha_i, I_i) \to 0$ as $p_i \to \infty$ and $u_i(p_i, \mathbf{p_{-i}}/\alpha_i, I_i) \to 0$ as $p_i \to 0$, see [27] for justification. Therefore by using Eq. (2.17) one can rewrite the above equation as:

$$u_i(p_i, \mathbf{p_{-i}}/\gamma_i^{(s)}, I_i) = \frac{R_i(1 - 2\tilde{P}_b(e))^M}{p_i} = \frac{R_i(1 - e^{-\frac{\gamma_i^{(s)}}{2}})^M}{p_i} \tag{4.2}$$

The above utility function quantifies the number of information bits received successfully at the receiver per joule of expended energy. In other words, it quantifies the number of successfully transmitted bits per unit transmission power. Furthermore, taking the average of $u_i(p_i, \mathbf{p_{-i}}/\gamma_i^{(s)}, I_i)$ in Eq. (4.2) with respect to $p_{\gamma_i^{(s)}/I_i}(\gamma_i^{(s)})$, one can get [49]:

$$\begin{aligned} u_i(p_i, \mathbf{p_{-i}}/I_i) &= E[u_i(p_i, \mathbf{p_{-i}}/\gamma_i^{(s)}, I_i)] \\ &= \int_0^\infty u_i(p_i, \mathbf{p_{-i}}/\gamma_i^{(s)}, I_i) \times p_{\gamma_i^{(s)}/I_i}(\gamma_i^{(s)}) d\gamma_i^{(s)} \\ &= \int_0^\infty (\frac{R_i(1 - e^{-\frac{\gamma_i^{(s)}}{2}})^M}{p_i}) \times (\frac{1}{A_i} e^{-\frac{\gamma_i^{(s)}}{A_i}}) \, d\gamma_i^{(s)} \end{aligned} \tag{4.3}$$

Using the fact that $(1-e^{-\frac{\gamma_i^{(s)}}{2}})^M = \sum_{n=0}^{M} \begin{pmatrix} M \\ n \end{pmatrix} (-1)^n e^{\frac{-n\gamma_i^{(s)}}{2}}$, the above equation can be rewritten as follows:

$$u_i(p_i, \mathbf{p_{-i}}/I_i) = \frac{R_i}{p_i A_i} \sum_{n=0}^{M} \begin{pmatrix} M \\ n \end{pmatrix} (-1)^n \int_0^\infty e^{(-\frac{n}{2}-\frac{1}{A_i})\gamma_i^{(s)}}\, d\gamma_i^{(s)} \qquad (4.4)$$

Furthermore, one can easily check that the integral in the above equation equals $(2A_i)/(nA_i+2)$. Thus

$$u_i(p_i, \mathbf{p_{-i}}/I_i) = \frac{R_i}{p_i} \sum_{n=0}^{M} \begin{pmatrix} M \\ n \end{pmatrix} (-1)^n \frac{2}{nA_i+2} \qquad (4.5)$$

Moreover, one can approximate Eq. (4.5) for large A_i as follows:

$$\begin{aligned} u_i(p_i, \mathbf{p_{-i}}/I_i) &\approx \frac{R_i}{p_i} \sum_{n=0}^{M} \begin{pmatrix} M \\ n \end{pmatrix} (-1)^n \frac{2}{nA_i} \\ &\approx \frac{R_i}{p_i} \{1 + \sum_{n=1}^{M} \begin{pmatrix} M \\ n \end{pmatrix} (-1)^n \frac{2}{nA_i}\} \qquad (4.6) \end{aligned}$$

which also can be rewritten as [49]:

$$u_i(p_i, \mathbf{p_{-i}}/I_i) \approx \frac{R_i}{p_i}(1 - \frac{\psi}{A_i}) \qquad (4.7)$$

where $\psi = -\sum_{n=1}^{M} \begin{pmatrix} M \\ n \end{pmatrix} (-1)^n (\frac{2}{n}) > 0$.

Next, averaging the above equation with respect to I_i, i.e., $E[u_i(p_i, \mathbf{p_{-i}}/I_i)]$, one gets the i-th user's average utility function for high SINR as follows [47], [49]:

$$\begin{aligned}
u_i(p_i, \mathbf{p_{-i}}) &\approx \frac{R_i}{p_i} E\{1 + \sum_{n=1}^{M} \begin{pmatrix} M \\ n \end{pmatrix} (-1)^n \frac{2}{nA_i}\} \\
&= \frac{R_i}{p_i}\{1 + \sum_{n=1}^{M} \begin{pmatrix} M \\ n \end{pmatrix} (-1)^n \frac{2}{n \times E[A_i]}\} \\
&= \frac{R_i}{p_i}\{1 + \sum_{n=1}^{M} \begin{pmatrix} M \\ n \end{pmatrix} (-1)^n \frac{2}{n} \times \frac{E[I_i] + \sigma_n^2}{h_{si}^2 p_i}\}
\end{aligned} \tag{4.8}$$

Recall from Eq. (3.4) that $E[1/A_i] = (E[I_i] + \sigma_n^2)/(h_{si}^2 p_i)$ [3],[4]. Hence the above equation can be rewritten as follows [49]:

$$u_i(p_i, \mathbf{p_{-i}}) \approx \frac{R_i}{p_i}\{1 - \frac{\psi}{\bar{\gamma}_i^{(Ra)}}\} \tag{4.9}$$

Note that the same utility function for the PU which was defined in Eq. (3.7) for Rayleigh fast-flat fading channels case can also be reused here [3],[4].

4.1.1 Realistic Game

In general, SUs' transmissions in the CR networks are considered as interference to the PU. Hence, SUs should minimize the amount of transmission power to achieve the best transmission quality. Thus in Eq. (4.2) a suitable utility function for the i-th SU has been given as in [27]. To adapt the average utility function to fit our model, some modifications must be added, as shown in Eq. (4.9). Therefore, the new modified non-cooperative game for the proposed realistic Rayleigh slow-flat fading channels, $G_3 = (\mathcal{N}, \mathcal{P}, u_i(.))$, has the following components:

1) **<u>Players</u>**: $\mathcal{N} = \{0, 1, \ldots, N\}$ is the index set of the users currently in the cell, where 0-th user represents the PU and $i = 1, \ldots, N$ represents the i-th SU.

2) **<u>Action space</u>**: $\mathcal{P} = (\mathcal{Q} \times \mathcal{P}_1 \times \mathcal{P}_2 \times \ldots \times \mathcal{P}_N)$, where $\mathcal{Q} = [0, \bar{Q_0}]$ represents the PU's action set and $\mathcal{P}_i = [p_{i(min)}, p_{i(max)}]$ represents the i-th SU's action set. Here $\bar{Q_0}$ represents the maximum allowed interference cap of the PU, and $p_{i(min)}$ and $p_{i(max)}$ respectively, represent the minimum and maximum allowed transmission power of the i-th SU. The action vector of all users is denoted by $\mathbf{p} = [Q_0, p_1, \ldots, p_N]$, where $p_i \in \mathcal{P}_i$ and $Q_0 \in \mathcal{Q}$ for $i = 0, 1, \ldots, N$. The PU's strategy is to choose the best Q_0 at any given time, while that of SUs is to adapt their transmit powers.

3) **<u>Utility functions</u>**: In realistic game, the i-th SU's average utility function, $u_i(p_i, \mathbf{p_{-i}})$, is given in Eq. (4.9) while $u_0(Q_0, \mathbf{p_{-0}})$ which is given in Eq. (3.7) represents the utility function of the PU.

4.1.2 Existence of a Nash Equilibrium

Assuming a MF receiver is employed in the secondary system, the realistic action space for AWGN channel should be modified to guarantee the existence of a NE for Rayleigh slow-flat fading channels. Now given that the quasi-concavity of the PU's utility function has been proven in [7], one only needs to show the quasi-concavity and the continuity of the average utility function of the SUs in p_i to prove the existence of at least one NE point. Hence taking the first derivative of $u_i(p_i, \mathbf{p_{-i}})$ with respect to p_i gives:

$$\frac{\partial u_i(p_i, \mathbf{p_{-i}})}{\partial p_i} = \frac{R_i}{p_i^2}(-1 + \frac{2\psi}{\bar{\gamma}_i^{(Ra)}}) \tag{4.10}$$

By setting the above expression to zero, it is seen that $\bar{\gamma}_i^{(Ra)} = 2\psi$ which can be further simplified using Eq. (3.5) to [49]:

$$p_i^{max} = 2\psi \frac{\sum_{\substack{j=1\\j\neq i}}^{N} h_{sj}^2 \rho_{ji}^2 p_j + h_{s0}^2 \rho_{ps}^2 P_0 + \sigma_n^2}{h_{si}^2} \tag{4.11}$$

where p_i^{max} is the maximum level of transmit power within the convex action space $\mathcal{P}_i$. Furthermore, the second derivative of $u_i(p_i, \mathbf{p_{-i}})$ with respect to p_i is given as follows:

$$\frac{\partial^2 u_i(p_i, \mathbf{p_{-i}})}{\partial {p_i}^2} = \frac{2R_i}{p_i^3}(1 - \frac{3\psi}{\bar{\gamma}_i^{(Ra)}}) \tag{4.12}$$

Hence, the utility function $u_i(p_i, \mathbf{p_{-i}})$ is concave if:

$$\frac{\partial^2 u_i(p_i, \mathbf{p_{-i}})}{\partial {p_i}^2} < 0, \quad \forall \bar{\gamma}_i^{(Ra)} \in (\bar{\gamma}_{i(min)}^{(Ra)}, \bar{\gamma}_{i(max)}^{(Ra)}) \tag{4.13}$$

where $\bar{\gamma}_{i(max)}^{(Ra)} = 3\psi$ and $\bar{\gamma}_{i(min)}^{(Ra)} = 1$ are the maximum and minimum average SINR for the Rayleigh slow flat fading channel respectively. Thus in order to guarantee that the utility function is concave, the AWGN action space should be modified to fit the Rayleigh slow-flat fading channels as follows [49]:

$$\mathcal{P}_i = \{p_i : \bar{\gamma}_i^{(Ra)} \in (\bar{\gamma}_{i(min)}^{(Ra)}, \bar{\gamma}_{i(max)}^{(Ra)})\} \tag{4.14}$$

Therefore the PU's utility function and SUs average utility function satisfy all the required conditions for the existence of at least one NE in this game. The uniqueness of this NE is shown next.

4.1.3 Uniqueness of a the Nash Equilibrium

To test the uniqueness of the NE under Rayleigh slow-flat fading channel, $r_i^*(\mathbf{p_{-i}})$ is assumed to be the best-response function of player i [37]. The best-response vector over all SUs, $\mathbf{r_3}(\mathbf{p}) = (r_1^*(\mathbf{p_{-1}}), r_2^*(\mathbf{p_{-2}}), \ldots, r_N^*(\mathbf{p_{-N}}))$, where $r_i^*(\mathbf{p_{-i}}) = \min$ $(p_i^{max}, p_{i(max)})$ and $p_i^{(max)}$ is the i-th SU's transmission power which provides it with the *optimum* SINR (i.e., $\bar{\gamma}_i^{(Ra)*}$). Moreover, the SINR corresponding to the best-response is the same for all SUs because all SUs are assumed to have the same efficiency function. This implies that $r_i^*(\mathbf{p_i}) = r_i^*(\mathbf{p_{-i}})$. Hence when some of the SUs cannot achieve $\bar{\gamma}_i^{(Ra)*}$, they will transmit at their maximum possible transmit power and in this case the NE is still unique. Moreover, if the best-response of the PU and SUs are *standard* functions, then the NE in the game will be unique. Now consider the properties of a standard function as listed in Section 3.1.3. Here the best-response correspondence of the SUs in our game can be obtained by setting $u_i'(p_i, \mathbf{p_{-i}})$ to zero which leads to Eq. (4.11) where $p_i^{(max)} = r_i^*(\mathbf{p_{-i}})$ [49].

Now earlier in [7] it has also been shown that the best-response function of the PU is standard and equals $r_0^*(\mathbf{p_{-0}}) = \frac{1}{2\mu_1} + I_0$. Hence one just needs to prove that the best-response function of the SUs is standard by checking the three standard function properties (Section 3.1.3). Foremost, the power action sets of the PU and the SUs are closed subsets of $\mathbb{R}$. Furthermore, it is easy to check that the utility function of the PU and the average utility functions of SUs are continuous in $\mathbf{p}$. Also by examining Eq. (4.11), it is easy to check the monotonicity of $\mathbf{r}(\mathbf{p})$ by showing that $p_i^{max}(\mathbf{p}) > p_i^{max}(\mathbf{p}')$ for all i if $\mathbf{p} > \mathbf{p}'$. Finally, to prove scalability, it is enough to show that $p_i^{max}(\mathbf{p_{-i}})$ is scalable. This can be achieved by rewriting Eq. (4.11) as follows [49]:

$$p_i^{max}(\mathbf{p_{-i}}) = 2\psi \frac{\sum_{\substack{j=1\\j\neq i}}^{N} h_{sj}^2\rho_{ji}^2 p_j + h_{s0}^2\rho_{ps}^2 P_0 + \sigma_n^2}{h_{si}^2}$$
$$p_i^{max}(\mu\mathbf{p_{-i}}) = 2\psi \frac{\mu(\sum_{\substack{j=1\\j\neq i}}^{N} h_{sj}^2\rho_{ji}^2 p_j + h_{s0}^2\rho_{ps}^2 P_0) + \sigma_n^2}{h_{si}^2} \tag{4.15}$$

while

$$\mu p_i^{max}(\mathbf{p_{-i}} = (2\mu)\psi \frac{\sum_{\substack{j=1\\j\neq i}}^{N} h_{sj}^2\rho_{ji}^2 p_j + h_{s0}^2\rho_{ps}^2 P_0 + \sigma_n^2}{h_{si}^2} \tag{4.16}$$

From the above equations, it is obvious that $\mu p_i^{max}(\mathbf{p_{-i}}) > p_i^{max}(\mu\mathbf{p_{-i}})$, which completes NE uniqueness proof Rayleigh slow-flat fading channels.

4.1.4 Analysis of Simulation Results

Detailed simulations are also done to model the performance of the game theoretic scheme under Rayleigh slow-flat fading channels. Again, the following parameters are used: $\bar{Q_0} = 5$, $\rho_{pi} = \rho_{ip} = \rho_{ji} = 0.1$, $h_{pi} = h_{ip} = h_{ji} = 1$ for all i , $j \in \{1, \ldots, N$ $\}$, $M = 50$, $R_i = 1$, $\bar{\gamma_0} = 10$, $\sigma_n^2 = 1$, $\mu_1 = 10$ and $\mu_2 = 100$. First of all, Figure 4.1 shows the PU utility at the NE as a function of the number of SUs N. One can see that the PU's utility is severely penalized by the exponential pricing function when $\bar{Q_0} < I_0$. This happens when $N \geq 26$ for AWGN channel and when $N \geq 22$ for Rayleigh slow-flat fading channels. Meanwhile, the total interference from all SUs to the PU is shown in Figure 4.2. When $N > 3$ for AWGN channel case, the network cannot support these SUs, and as a result, no SU can achieve the optimal SINR. Thus all SUs are forced to transmit at their maximum possible power levels, and I_0 increases linearly with N. As a result the PU's utility at the NE also increases linearly.

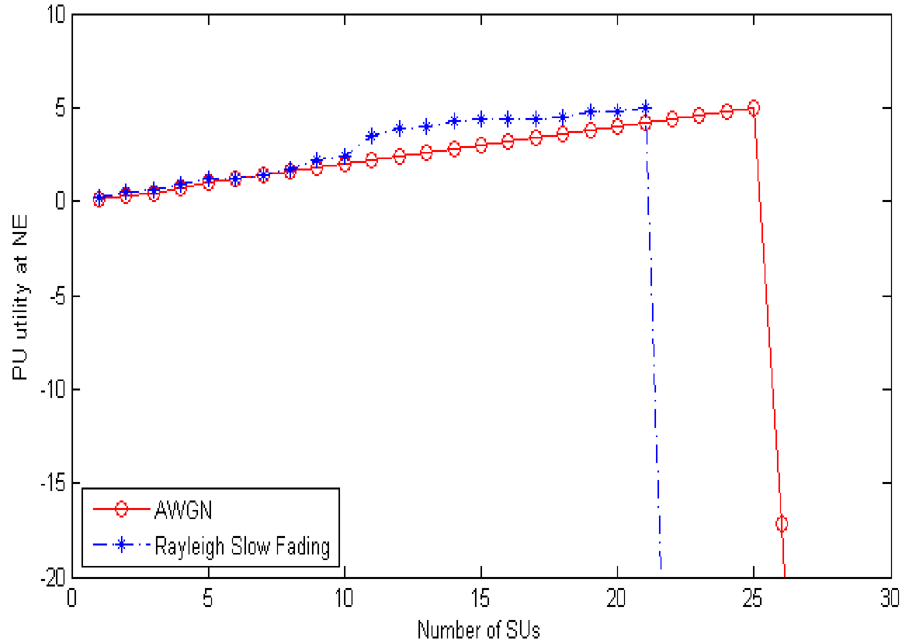

Figure 4.1: Primary user's utility at the NE for Rayleigh slow fading

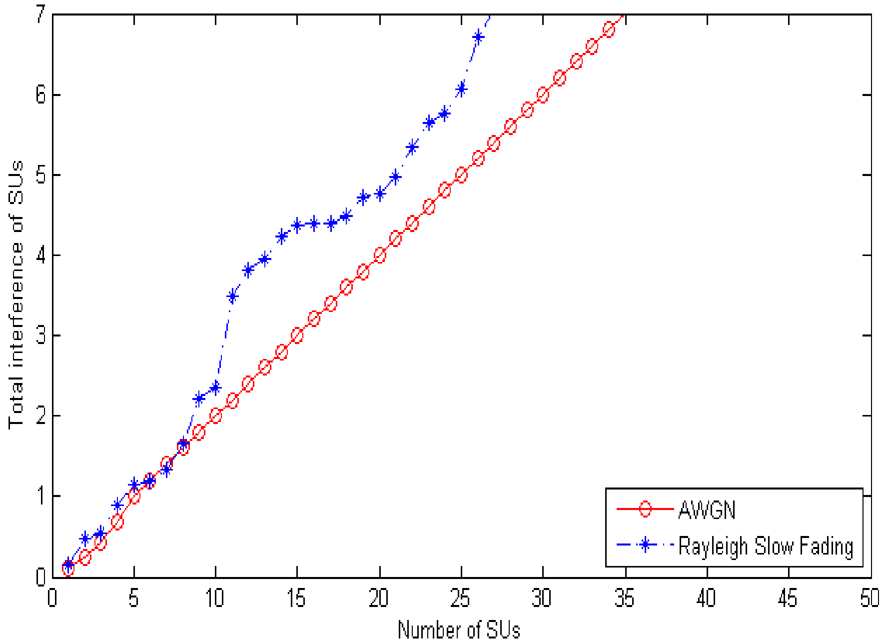

Figure 4.2: Total interference from all secondary users for Rayleigh slow fading

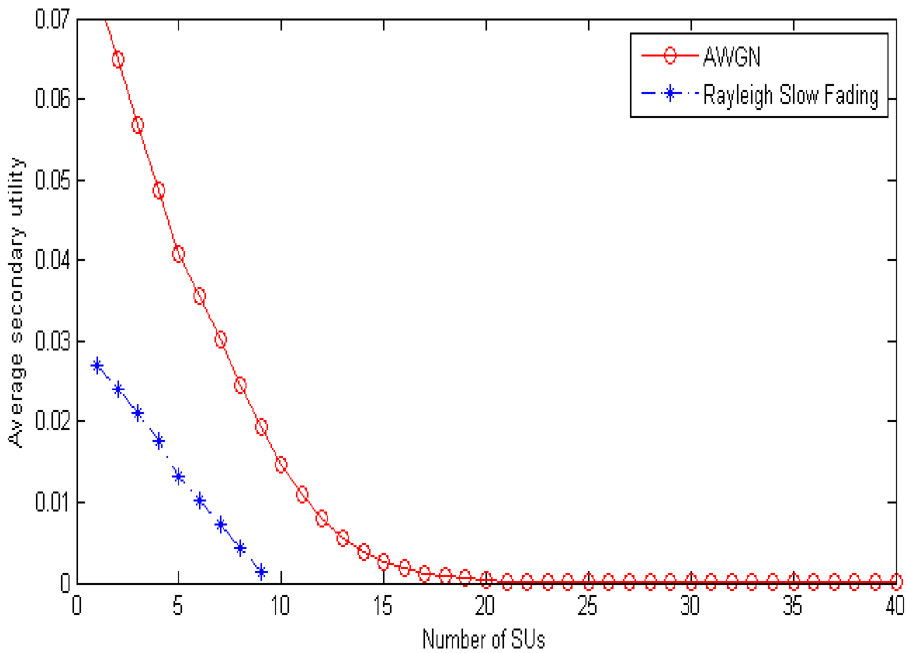

Figure 4.3: Average secondary user's utility at the NE for Rayleigh slow fading

Next, the average SU utility is shown in Figure 4.3. Here as the number of SUs increases, each SU and the PU sees more interference due to the added SUs. Therefore each SU has to transmit at a higher power than that with smaller number of SUs in the system in order to achieve the same optimum SINR. This reduces the average utility. Moreover, the number of SU's in energy efficient mode is plotted in Figure 4.4. Here, when $0 < N \leq 4$ for AWGN channel and when $0 < N \leq 3$ for Rayleigh slow-flat fading channel, one sees that all SUs will maximize their utility by achieving their optimum SINR. i.e., $\bar{\gamma}_i^*$ and $\bar{\gamma}_i^{(Ra)*}$, respectively. Otherwise, the network cannot afford these SUs (i.e., no SU can achieve its optimum SINR) and they all transmit at their maximum possible power level, i.e., $\bar{P}_i = 20$ for AWGN channel and $P_i^{(max)}$ for Rayleigh slow-flat fading channels.

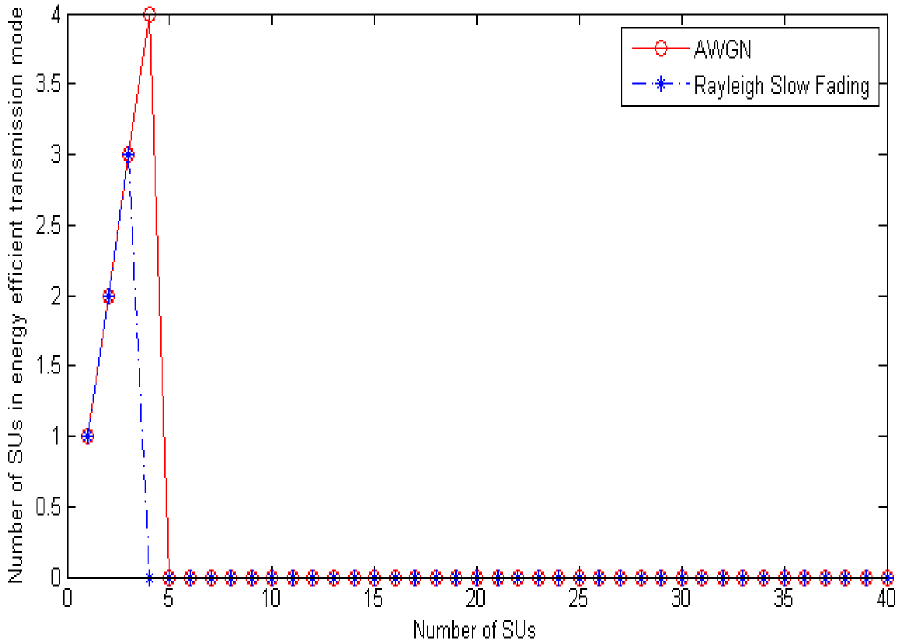

Figure 4.4: Number of SUs in energy-efficient mode for Rayleigh slow fading

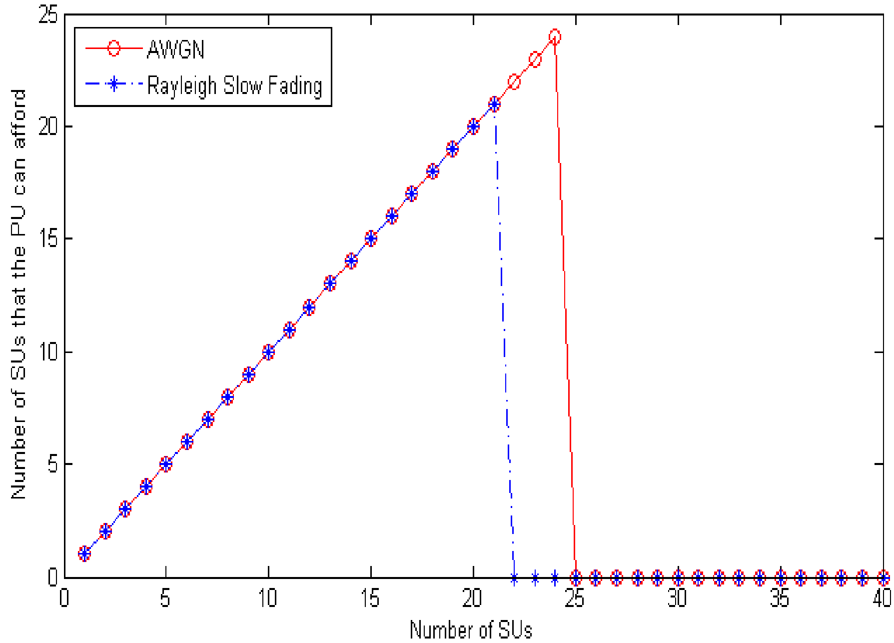

Figure 4.5: The maximum number of SUs that can be supported for Rayleigh slow fading

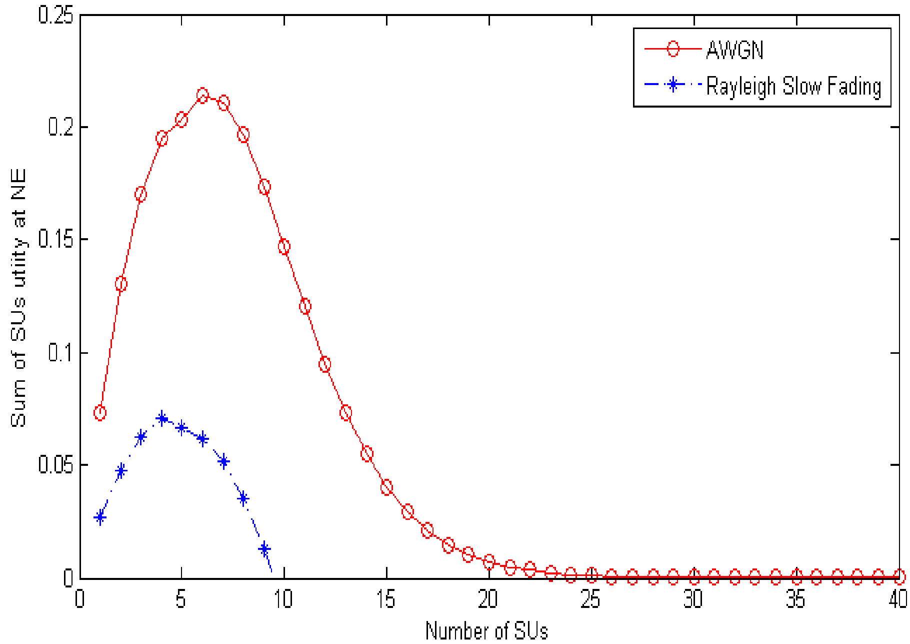

Figure 4.6: Sum of SUs' utility at the NE for Rayleigh slow fading

Finally, Figure 4.5 shows the number of SUs that the PU can afford as a function of the total number of SUs. This could be any number of SUs as long as $\bar{Q}_0 > I_0$, where $N = 25$ for AWGN channel and $N = 22$ for Rayleigh slow-fading channels. As expected, the total number of SUs that the PU can afford is lower in the cases of Rayleigh slow-flat fading channel. In addition, the sum of the utility achieved by all SUs at the NE is shown in Figure 4.6. Results show that the sum of all SUs' utility has a unique maximum when $N = 6$ for AWGN channel and when $N = 4$ for Rayleigh slow-fading channels. As the number of SUs increases, average SU utility decreases. Also when $N < 6$ for AWGN channel and $N < 4$ for Rayleigh slow-flat fading channels, the decrease in the average SU utility is dominated by the increase of the number of SUs, and hence the aggregate utility of all SUs still increases. Conversely, the aggregate utility decreases due to the decay of the average SU utility. In general, one can see that the Rayleigh slow-flat fading channels have a key direct impact upon the performance of the scheme, i.e., in terms of reduced numbers SUs supported by the PU (due to higher interference) and lower utility as compared to AWGN channel.

4.2 Rician Slow-Flat Fading Channels

Consider the derivation of P_e for slow-flat fading channels. First, the path fading coefficient α_i is modeled as a random variable with Rician pdf. Furthermore, taking the average of $u_i(p_i, \mathbf{p_{-i}}/\gamma_i^{(s)}, I_i)$ in Eq. (4.2) with respect to $p_{\gamma_i{}^{(s)}/I_i}(\gamma_i^{(s)})$, one gets [50]:

$$u_i(p_i, \mathbf{p_{-i}}/I_i) = E[u_i(p_i, \mathbf{p_{-i}}/\gamma_i^{(s)}, I_i)]$$
$$= \int_0^\infty u_i(p_i, \mathbf{p_{-i}}/\gamma_i^{(s)}, I_i) \times p_{\gamma_i{}^{(s)}/I_i}(\gamma_i{}^{(s)})\, d\gamma_i^{(s)} \tag{4.17}$$

By making suitable substitutions, the above equation can be rewritten as follows [50]:

$$u_i(p_i, \mathbf{p_{-i}}/I_i) = \int_0^\infty (\frac{R_i(1-e^{-\frac{\gamma_i^{(s)}}{2}})^M}{p_i})\frac{e^{-s^2}}{A_i}e^{-(\frac{\gamma_i^{(s)}}{A_i})} I_0(2s\sqrt{\gamma_i{}^{(s)}/A_i})\, d\gamma_i^{(s)}$$
$$= \frac{R_i e^{-s^2}}{p_i A_i}\sum_{n=0}^{M}\begin{pmatrix} M \\ n \end{pmatrix}(-1)^n \int_0^\infty e^{(-\frac{n}{2}-\frac{1}{A_i})\gamma_i^{(s)}}\, d\gamma_i^{(s)} \tag{4.18}$$

Next, using expansion of a zero-order modified first kind Bessel function which is shown in Eq. (3.18), the fact that $\int_0^\infty x^{(2k+1)}e^{-ax^2}\,dx = k!/2a^{(k+1)}$, the exponential expansion $e^x = \sum_{k=0}^\infty x^k/k!$ and Binomial series expansion (i.e., $(1-e^{-\frac{\gamma_i^{(s)}}{2}})^M = \sum_{n=0}^M \begin{pmatrix} M \\ n \end{pmatrix} e^{\frac{-n\gamma_i^{(s)}}{2}}(-1)^n$), one can check to see that the integral in the above equation equals $(2A_i)e^{s^2(\frac{2}{nA_i+2}-1)}/(nA_i+2)$. Thus

$$u_i(p_i, \mathbf{p_{-i}}/I_i) = \frac{R_i}{p_i}\sum_{n=0}^{M}\begin{pmatrix} M \\ n \end{pmatrix}\frac{2e^{s^2(\frac{2}{nA_i+2}-1)}}{nA_i+2}(-1)^n \tag{4.19}$$

Moreover, Eq. (4.19) can be approximated for large A_i by:

$$\begin{aligned} u_i(p_i, \mathbf{p_{-i}}/I_i) &\approx \frac{2R_i}{p_i}\sum_{n=0}^{M}\begin{pmatrix} M \\ n \end{pmatrix}\frac{2e^{s^2(\frac{2}{nA_i+2}-1)}}{nA_i}(-1)^n \\ &\approx \frac{R_i}{p_i}\{1+\sum_{n=1}^{M}\begin{pmatrix} M \\ n \end{pmatrix}\frac{2e^{-s^2}}{nA_i}(-1)^n\} \end{aligned} \tag{4.20}$$

which also can be rewritten as [50]:

$$u_i(p_i, \mathbf{p_{-i}}/I_i) \approx \frac{R_i}{p_i}(1-\frac{\psi e^{-s^2}}{A_i}) \tag{4.21}$$

where $\psi = -\sum_{n=1}^{M}\begin{pmatrix} M \\ n \end{pmatrix}(-1)^n(\frac{2}{n}) > 0$. Next, averaging the above equation with respect to I_i, i.e., $E(u_i(p_i, \mathbf{p_{-i}}/I_i))$, one gets the i-th user's average utility function for high SINR as follows [47], [50]:

$$\begin{aligned} u_i(p_i, \mathbf{p_{-i}}) &\approx \frac{R_i}{p_i}E\{1+\sum_{n=1}^{M}\begin{pmatrix} M \\ n \end{pmatrix}(-1)^n\frac{2e^{-s^2}}{nA_i}\} \\ &= \frac{R_i}{p_i}\{1+\sum_{n=1}^{M}\begin{pmatrix} M \\ n \end{pmatrix}(-1)^n\frac{2e^{-s^2}}{n\times E(A_i)}\} \\ &= \frac{R_i}{p_i}\{1+\sum_{n=1}^{M}\begin{pmatrix} M \\ n \end{pmatrix}(-1)^n\frac{2e^{-s^2}}{n}\times\frac{E[I_i]+\sigma_n^2}{h_{si}^2 p_i}\} \\ u_i(p_i, \mathbf{p_{-i}}) &\approx \frac{R_i}{p_i}\{1-\frac{\psi}{\bar{\gamma}_i^{(Rice)}}\} \end{aligned} \tag{4.22}$$

where $E[1/A_i] = (E[I_i]+\sigma_n^2)/(h_{si}^2 p_i)$ and $\bar{\gamma}_i^{(Rice)}$ is the average SINR for Rician fast-flat fading channels [4].

4.2.1 Realistic Game

Overall, a suitable utility function for the i-th SU has been given as in [27]. However, some modifications must be added to this utility function in order to adapt it to fit the proposed model as shown in Eq. (4.22). Namely, the new non-cooperative game for the proposed realistic Rician slow-flat fading channel, $G_4 = (\mathcal{N}, \mathcal{P}, u_i(.))$, has the following components [50]:

1) **Players**: $\mathcal{N} = \{0, 1, \ldots, N\}$ is the index set of the users currently in the cell, where 0-th user represents the PU and $i = 1, \ldots, N$ represents the i-th SU.

2) **Action space**: $\mathcal{P} = (\mathcal{Q} \times \mathcal{P}_1 \times \mathcal{P}_2 \times \ldots \times \mathcal{P}_N)$, where $\mathcal{P}_i = [p_{i(min)}, p_{i(max)}]$ represents the i-th SU's action set and $\mathcal{Q} = [0, \bar{Q_0}]$ represents the PU's action set. Moreover, $p_{i(min)}$ and $p_{i(max)}$ represent the minimum and maximum allowed transmission power of the i-th SU respectively, and $\bar{Q_0}$ represents the maximum allowed interference cap of the PU. The action vector of all users is denoted by $\mathbf{p} = [Q_0, p_1, \ldots, p_N]$, where $p_i \in \mathcal{P}_i$ and $Q_0 \in \mathcal{Q}$ for $i = 0, 1, \ldots, N$. Thus the strategy of the PU's is to choose the best Q_0 all the time, while that of SUs is to adapt their transmit powers.

3) **Utility functions**: In a realistic game the i-th SU's average utility function is given by $u_i(p_i, \mathbf{p_{-i}})$ in Eq. (4.22). Meanwhile, $u_0(Q_0, \mathbf{p_{-0}})$, which is given in Eq. (3.7), represents the utility function of the PU.

4.2.2 Existence of the Nash Equilibrium

Assuming that a MF receiver is used in the secondary system, the realistic action space for AWGN channel must be modified to guarantee the existence of the NE for a Rician slow-flat fading channel. Now the authors in [7] have proven the quasi-concavity of the PU's utility function. Thus one only needs to show the quasi-concavity and the continuity of the average utility function of the SUs in p_i, i.e., to show that there exists at least one NE point. Hence by taking the first derivative of $u_i(p_i, \mathbf{p_{-i}})$ given in Eq. (4.22) with respect to p_i, one gets:

$$\frac{\partial u_i(p_i, \mathbf{p_{-i}})}{\partial p_i} = \frac{R_i}{p_i^2}(-1 + \frac{2\psi}{\bar{\gamma}_i^{(Rice)}}) \tag{4.23}$$

By setting the above expression to zero, it is seen that $\bar{\gamma}_i^{(Rice)} = 2\psi$. Moreover, by using Eq. (3.28), Eq. (4.23) simplifies to [50]:

$$p_i^{max} = 2\psi \frac{(\sum_{\substack{j=1 \\ j\neq i}}^{N} h_{sj}^2 \rho_{ji}^2 p_j + h_{s0}^2 \rho_{ps}^2 P_0)(s^2+1) + \sigma_n^2}{h_{si}^2 e^{s^2}} \tag{4.24}$$

where p_i^{max} is the maximum level of transmit power within the convex action space $\mathcal{P}_i$. Moreover by taking the second derivative of $u_i(p_i, \mathbf{p_{-i}})$ with respect to p_i one can get:

$$\frac{\partial^2 u_i(p_i, \mathbf{p_{-i}})}{\partial {p_i}^2} = \frac{2R_i}{p_i^3}(1 - \frac{3\psi}{\bar{\gamma}_i^{(Rice)}}) \tag{4.25}$$

Hence, the utility function $u_i(p_i, \mathbf{p_{-i}})$ is concave if:

$$\frac{\partial^2 u_i(p_i, \mathbf{p_{-i}})}{\partial {p_i}^2} < 0, \quad \forall \bar{\gamma}_i^{(Rice)} \in (\bar{\gamma}_{i(min)}^{(Rice)}, \bar{\gamma}_{i(max)}^{(Rice)}) \tag{4.26}$$

where $\bar{\gamma}_{i(max)}^{(Rice)} = 3\psi$ and $\bar{\gamma}_{i(min)}^{(Rice)} = 1$ are the maximum and minimum average SINR for the Rician slow-flat fading channel, respectively. Thus in order to guarantee the concavity of the utility function, the AWGN action space must be modified to fit the Rician slow-flat fading channel as follows [50]:

$$\mathcal{P}_i = \{p_i : \bar{\gamma}_i^{(Rice)} \in (\bar{\gamma}_{i(min)}^{(Rice)}, \bar{\gamma}_{i(max)}^{(Rice)})\} \tag{4.27}$$

Therefore the average utility functions of PUs and SUs satisfy all the required conditions for the existence of at least one NE in this game. The uniqueness of this NE is shown next.

4.2.3 Uniqueness of the Nash Equilibrium

To test the uniqueness of the NE under the Rician slow-flat fading channel, $r_i^*(\mathbf{p_{-i}})$ is assumed to be the best-response function of player i [37]. Also the best-response vector over all SUs is $\mathbf{r_4}(\mathbf{p}) = (r_1^*(\mathbf{p_{-1}}), r_2^*(\mathbf{p_{-2}}), \ldots, r_N^*(\mathbf{p_{-N}}))$, where $r_i^*(\mathbf{p_{-i}}) = \min\,(p_i^{max}, p_{i(max)})$ and $p_i^{(max)}$ is the i-th SU's transmission power which provides it with the optimum SINR (i.e., $\bar{\gamma}_i^{(Rice)*}$). Moreover, the SINR corresponding to the best-response is the same for all SUs because all SUs are assumed to have the same efficiency function. This implies that $r_i^*(\mathbf{p_i}) = r_i^*(\mathbf{p_{-i}})$. Hence some of the SUs will send at their maximum possible transmit power when they cannot achieve $\bar{\gamma}_i^{(Rice)*}$ and in this case the NE is still unique. Again, as shown in Section 3.2.3, if the best-responses of the PU and SUs are standard functions, then the NE in the game will be unique. Hence the best-response correspondence of the SUs in the proposed game can be obtained by setting $u_i^{'}(p_i, \mathbf{p_{-i}})$ to zero, which leads to Eq. (4.24) where $p_i^{(max)} = r_i^*(\mathbf{p_{-i}})$ [50]. Furthermore, the authors in [7] have also shown that the best-response function of the PU is standard and equals $r_0^*(\mathbf{p_{-0}}) = \frac{1}{2\mu_1} + I_0$. Therefore, one only needs to prove that the best-response function of the SUs is standard by checking the three properties above. By doing so, it is shown that the NE is unique.

4.2.4 Analysis of Simulation Results

In order to model the performance of the game theoretic scheme under realistic Rician slow-flat fading channel model, detailed simulations are done in *MATLAB* using the following parameters: $\bar{Q}_0 = 5$, $\rho_{pi} = \rho_{ip} = \rho_{ji} = 0.1$, $h_{pi} = h_{ip} = h_{ji} = 1$ for all i ,

$j \in \{1, \ldots, N\}$, $M = 50$, $R_i = 1$, $\bar{\gamma}_0 = 10$, $\sigma_n^2 = 1$, $\mu_1 = 10$ and $\mu_2 = 100$. First of all, Figure 4.7 shows the number of SUs that the PU can afford as a function of the total number of SUs. This can be any number of SUs as long as $\bar{Q}_0 > I_0$, and results show $N = 25$ for AWGN channel and $N = 19$ for Rician slow-flat fading channels. Thus in the Rician slow-flat fading channels case, the PU can afford lower number of SUs as compared to the AWGN channel case. However, the general performance is better than that for the case of Rician fast-flat fading channel, i.e., $N = 12$.

Furthermore, Figure 4.8 plots the sum of the utility achieved by all SUs at the NE. These results show that the sum of all SUs' utility has a unique maximum when $N = 6$ for AWGN channel and when $N = 19$ for Rician slow-flat fading channels. Hence as the number of SUs increases, the average SU utility decreases. Also the decrease in the average SU utility is dominated by the increase in the number of SUs, and hence the total utility of all SUs still increases when $N < 6$ for AWGN channel and $N < 19$ for Rician slow-flat fading channel. Conversely, the aggregate utility decreases due to the decay of the average SU utility.

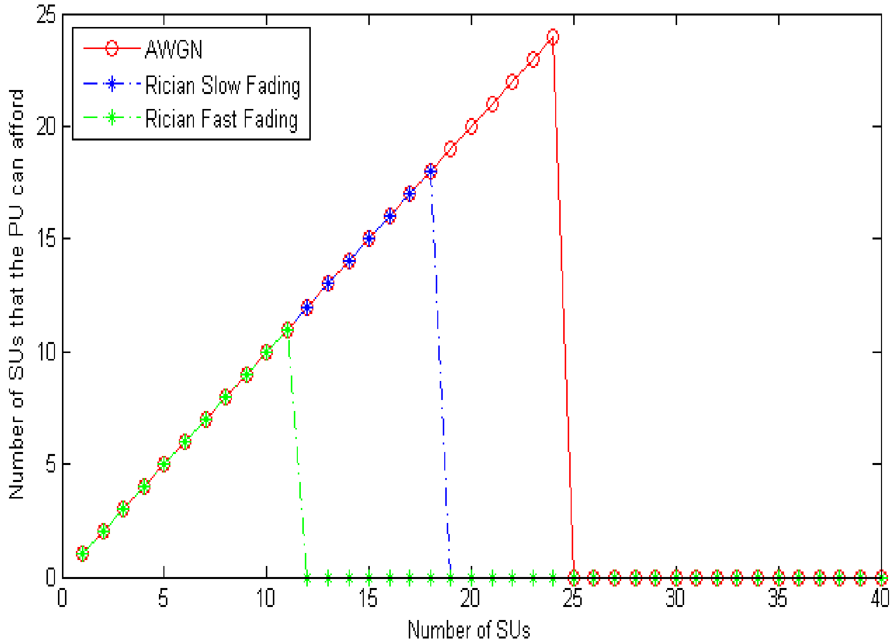

Figure 4.7: The maximum number of SUs that can be supported for Rician slow fading

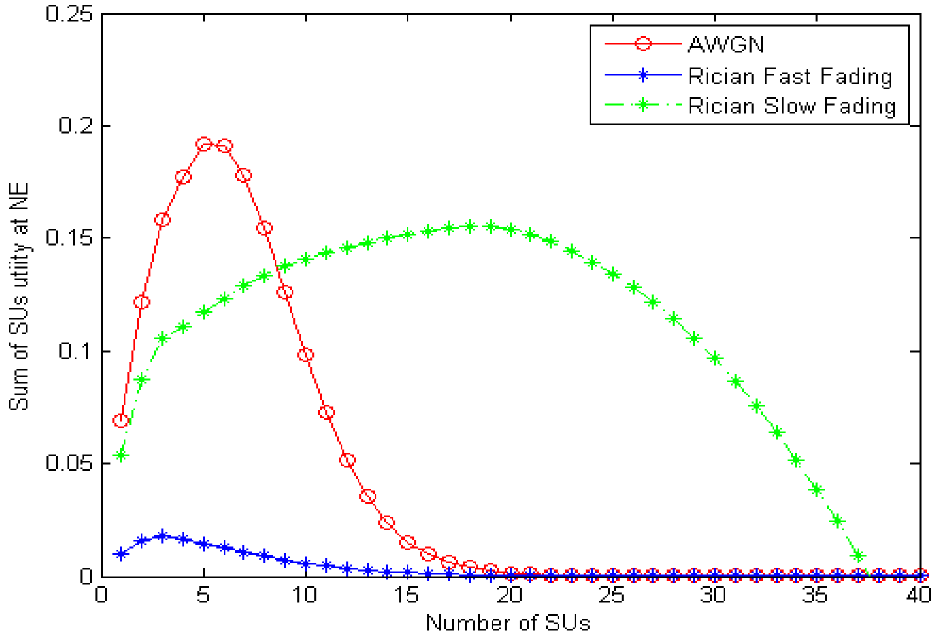

Figure 4.8: Sum of SUs' utility at the NE for Rician slow fading

Next, the average SU utility is shown in Figure 4.9. Here each SU and the PU see more interference as the number of SUs increases due to the added SUs. Hence the high interference generated from larger number of SUs in the system forces each SU to transmit at higher power in order to achieve the same optimum SINR. This reduces the average utility. Moreover, Figure 4.10 plots the total interference, I_0, from all SUs to the PU for AWGN channel and for both Rician slow-flat fading and Rayleigh slow-flat fading channels. Here the Rician slow-flat fading channels have superior performance as compared to Rayleigh slow-flat fading channels. Namely, when $N > 3$ for AWGN channel case, the network cannot support these SUs, and as a result, no SU can achieve the optimal SINR. Thus all SUs are forced to transmit at their maximum possible power level and I_0 increases linearly with N. As a result the PU's utility at the NE also increases linearly. The same is true for Rayleigh slow-flat fading channels.

Finally, the utility of the PU at the NE is plotted in Figure 4.11 as a function of the number of SUs, N, where the PU's utility is severely penalized by the exponential pricing function when $\bar{Q_0} < I_0$. This happens when $N \geq 26$ for AWGN channel, when $N \geq 20$ for Rician slow-flat fading channel and when $N \geq 12$ for Rician fast-flat fading channel. To conclude, Rician slow-flat fading channels have a direct impact in terms of reducing the number of SUs that can be supported by the PU due to higher interference levels. This minimizes the utility as compared to the AWGN channels case. However, the overall performance is still better than that for fast-flat fading channels scheme proposed in [4].

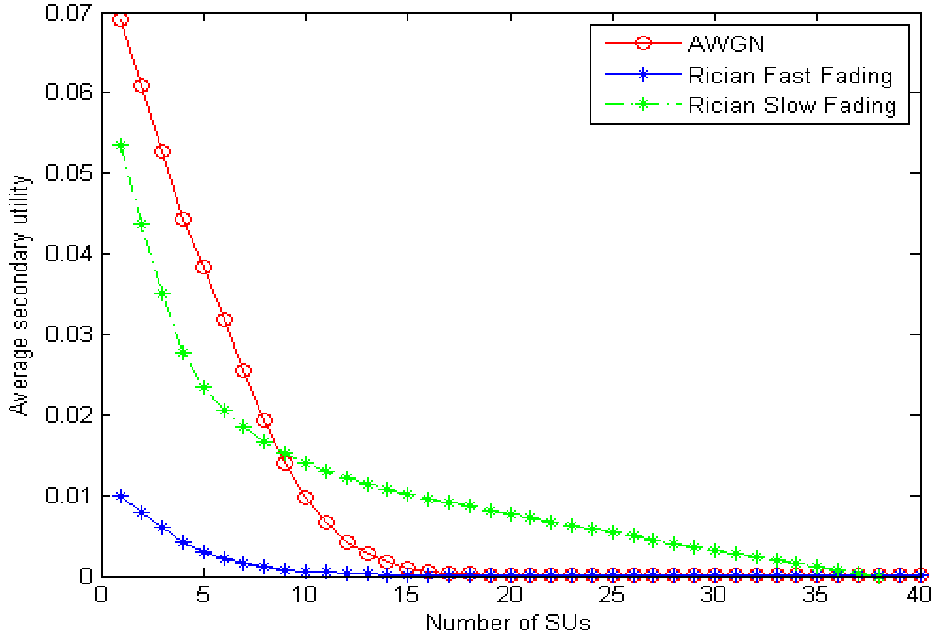

Figure 4.9: Average secondary user's utility at the NE for Rician slow fading

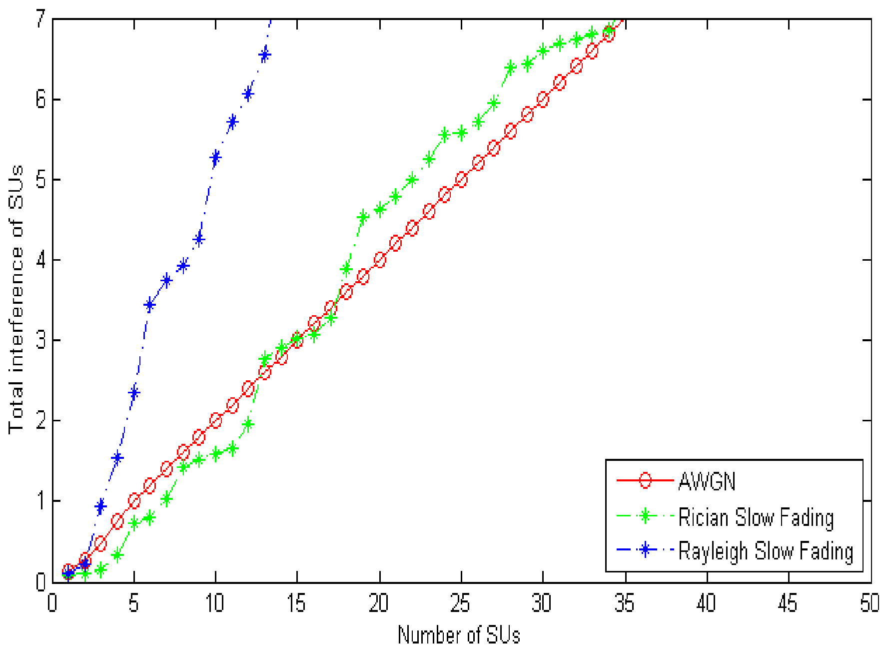

Figure 4.10: Total interference from all secondary users for Rician slow fading

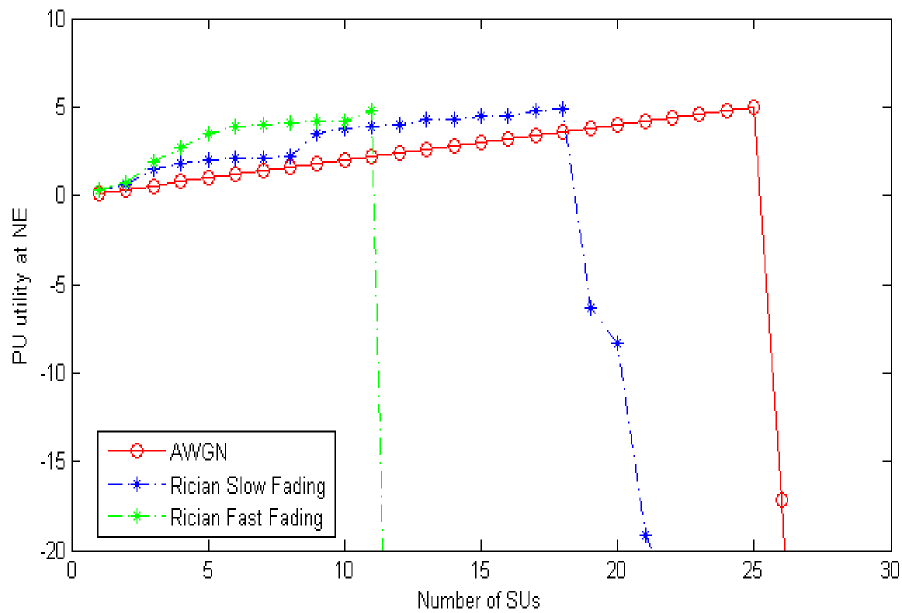

Figure 4.11: Primary user's utility at the NE for Rician slow fading

4.3 Conclusion

A novel realistic game theoretic scheme is proposed for primary-secondary user power control in CR networks with slow-flat fading channels. The formulation builds upon the work in Chapter 3 and proceeds to analyze the power and utilities performance of the scheme for Rician and Rayleigh fast-flat fading channels. In particular, assuming that a MF detector is used at the secondary systems, detailed analytical derivations are done to show that the modified game can achieve a unique NE. Overall, the simulations show that the proposed scheme yields good increases in energy efficiency for SUs without compromising the QoS for PU. However, Rician and Rayleigh fading channels have a very direct impact upon the performance of the scheme in terms of reduced numbers of SUs supported by the PU due to higher interference and lower utility as compared to AWGN channel.

Chapter 5

Fast Flat-Fading Channels Model with Pricing

Pricing models are now considered to help improve the game formulation. The goal with this approach is to allow users in non-cooperative (power control) games to maximize the difference between their utility functions and the chosen pricing function. Therefore more efficient resource allocation can be achieved as SUs will only be penalized for aggressive power usage. Along these lines, this treatment builds upon the work in Chapter 3 by focusing on fast flat-fading models. In particular, linear pricing functions are used, i.e., pricing factor is multiplied by the transmit power. Namely this factor is announced by the BS/AP to all users (in the cell) in order to enforce a NE that improves the aggregate utility of all users at lower power levels. Thus, the resulting power vector with pricing is Pareto-dominant compared to that without pricing, but still not Pareto optimal in the sense that one can multiply the resulting power vector with pricing by a constant, i.e., $0 < \beta < 1$, to achieve higher utilities for all users. Recall from paper [4] that non-cooperative power control game without pricing has a quasi-concave utility function for all SUs. Moreover, as the pricing function is a linear function, it has no impact on the concavity feature as shown in [25] and [47].

5.1 Rayleigh Fast-Flat Fading Channels with Pricing

Now in Chapter 3 the derivation of P_e was conducted for Rayleigh fast-flat fading channels with pricing. Here the path fading coefficient α_i was modeled as a Rayleigh random variable with probability distribution function given in (2.8). Then assuming BFSK transmission, the P_e for Rayleigh fast-flat fading channels was computed and a modified utility function derived. Extending upon this, a utility function with pricing is introduced to help increase the number of supported users in the game.

5.1.1 Utility Functions

Generally, SUs should minimize their transmission powers to achieve the best transmission quality. Hence, for the pricing model, the utility function of the i-th SU is given by [51]:

$$u_i^c(p_i, \mathbf{p_{-i}}) = \frac{R_i(1-2P_e)^M}{p_i} - cp_i = \frac{R_i(1-2/\bar{\gamma}_i^{(Ra)})^M}{p_i} - cp_i \qquad (5.1)$$

where $\mathbf{p_{-i}}$ denotes the action vector excluding the action of the i-th user, $(i = 0, 1, \ldots, N)$, R_i is the transmission rate of the i-th SU, and c is positive scalar pricing factor. This factor is chosen properly to achieve the best possible improvement in the performance. However, carefully note that the utility function for the PU is still the same as that in Eq. (3.7). Hence the new modified non-cooperative power control game with pricing for the proposed realistic channel, $G_5^c = (\mathcal{N}, \mathcal{P}_c, u_i^c(.))$, has the following components:

1) **Players**: $\mathcal{N} = \{0, 1, \ldots, N\}$ is the index set of the users currently in the cell, where the 0-th user is assumed to be the PU and $i = 1, \ldots, N$ represents the i-th SU.

2) **Action space**: $\mathcal{P}_c = (\mathcal{Q} \times \mathcal{P}_{1c} \times \mathcal{P}_{2c} \times \ldots \times \mathcal{P}_{Nc})$, where $\mathcal{Q} = [0, \bar{Q}_0]$ represents the PU's action set and $\mathcal{P}_{ic} = [p_{ic(min)}, p_{ic(max)}]$ represents the i-th SU's action set. Here $\bar{Q}_0$ represents the maximum allowed interference cap of the PU, and $p_{ic(min)}$ and $p_{ic(max)}$ respectively, represent the minimum and maximum allowed transmission power of the i-th SU. The action vector of all users is also denoted by $\mathbf{p} = [Q_0, p_1, \ldots, p_N]$, where $p_i \in \mathcal{P}_{ic}$ and $Q_0 \in \mathcal{Q}$ for $i = 0, 1, \ldots, N$. The PU's strategy is to choose the best Q_0 at any time, while that of SUs is to adapt their transmit powers.

3) **Utility functions**: In this game, $u_i^c(p_i, \mathbf{p_{-i}})$, given in Eq. (5.1), is used to represent the i-th SU's utility function for Rayleigh fast-flat fading channels without pricing. In addition, $u_0(Q_0, \mathbf{p_{-0}})$, given in Eq. (3.7), is also used to represent the utility function of the PU.

5.1.2 Existence and Uniqueness of the NE

Assuming that a MF is employed at the SU receivers, the action space defined in [7] should be modified to guarantee the existence of at least one NE point. Moreover, it is also sufficient to show that the utility function is concave in p_i. Now since the quasi-concavity of the PU's utility function has not been changed, one only needs to show here is the quasi-concavity and the continuity of the utility function of the SUs. Hence by taking the first derivative of Eq. (5.1) with respect to p_i one gets:

$$\frac{\partial u_i^c(p_i, \mathbf{p_{-i}})}{\partial p_i} = \frac{R_i}{p_i^2}(1 - \frac{2}{\bar{\gamma}_i^{(Ra)}})^{M-1}(\frac{2(M+1)}{\bar{\gamma}_i^{(Ra)}} - 1) - c \tag{5.2}$$

Then by setting the above expression to zero, one gets [51]:

$$p_i^{c_{max}} = \sqrt{\frac{R_i}{c}(1 - \frac{2}{\bar{\gamma}_i^{(Ra)}})^{M-1}(\frac{2(M+1)}{\bar{\gamma}_i^{(Ra)}} - 1)} \tag{5.3}$$

where $p_i^{c_{max}}$ is the maximum level of transmit power within the action space $\mathcal{P}_{ic}$. In order to have feasible (i.e., positive and real) values for $p_i^{c_{max}}$, the strategy space must be defined as follows [51]:

$$\mathcal{P}_i = \{p_i : \bar{\gamma}_i^{(Ra)} \in (2, 2(M+1))\} \tag{5.4}$$

Moreover, the second derivative of Eq. (5.1) is given by:

$$\frac{\partial^2 u_i^c(p_i, \mathbf{p_{-i}})}{\partial {p_i}^2} = \frac{R_i}{p_i^3}\frac{(1 - \frac{2}{\bar{\gamma}_i^{(Ra)}})^M}{(\bar{\gamma}_i^{(Ra)} - 2)^2}(4M^2+12M+8+2(\bar{\gamma}_i^{(Ra)})^2-8(M+1)\bar{\gamma}_i^{(Ra)}) \tag{5.5}$$

Hence $u_i^c(p_i, \mathbf{p_{-i}})$ is guaranteed to be concave if [51]:

$$\frac{\partial^2 u_i^c(p_i, \mathbf{p_{-i}})}{\partial {p_i}^2} < 0, \quad \forall \bar{\gamma}_i^{(Ra)} \in (\bar{\gamma}_{i(min)}^{(Ra)}, \bar{\gamma}_{i(max)}^{(Ra)}) \tag{5.6}$$

where $\bar{\gamma}_{i(max)}^{(Ra)} = 2(M+1) + \sqrt{2(M^2+M)}$ is the maximum average SINR and $\bar{\gamma}_{i(min)}^{(Ra)} = 2(M+1) - \sqrt{2(M^2+M)}$ is the minimum average SINR for a Rayleigh fast-flat fading channel. Therefore to fulfill both conditions, the action space of the power control control game with pricing under Rayleigh fast-flat fading channels (i.e., $G_5^c = (\mathcal{N}, \mathcal{P}, u_i^c(.))$) should be modified to be the intersection of the two sets, that is:

$$\mathcal{P}_{ic} = \{p_i : \bar{\gamma}_i^{(Ra)} \in (\bar{\gamma}_{ic(min)}^{(Ra)}, \bar{\gamma}_{ic(max)}^{(Ra)})\} \tag{5.7}$$

where $\bar{\gamma}_{ic(max)}^{(Ra)} = 2(M+1)$ and $\bar{\gamma}_{ic(min)}^{(Ra)} = 2(M+1) - \sqrt{2(M^2+M)}$. Now since $\bar{\gamma}_i^{(Ra)} >> 1$ (i.e., large $\bar{\gamma}_i^{(Ra)}$) does exist in the above strategy space, one can approximate Eq. (5.3) as follows [51]:

$$p_i^{c_{max}} \approx \sqrt{\frac{R_i}{c}\left(\frac{2(M+1)}{\bar{\gamma}_i^{(Ra)}} - 1\right)} \tag{5.8}$$

Now assuming that $I_{xi} = \sum_{\substack{j=1 \\ j\neq i}}^{N} h_{sj}^2 \rho_{ji}^2 p_j + h_{s0}^2 \rho_{ps}^2 P_0$, one can rewrite Eq. (3.5) as $\bar{\gamma}_i^{(Ra)} = (h_{si}^2 p_i)/(I_{xi} + \sigma_n^2)$, where $\bar{\gamma}_i^{(Ra)}$ is the average SINR for Rayleigh fast-flat fading channels. Therefore one can rewrite the above equation as follows:

$$(p_i^{c_{max}})^3 + \frac{R_i h_{si}^2}{c}(p_i^{c_{max}})^2 - \frac{R_i}{c}\frac{2(M+1)(I_{xi}+\sigma_n^2)}{h_{si}^2} \approx 0 \tag{5.9}$$

Furthermore, assume that $a = \frac{R_i h_{si}^2}{c}$ and $b = \frac{R_i}{c}\frac{2(M+1)(I_{xi}+\sigma_n^2)}{h_{si}^2}$, the only positive and real solution for Eq. (5.9) is given by [51]:

$$p_i^{c_{max}} \approx \frac{(108b + 12\sqrt{12a^3 + 81b^2})^{\frac{2}{3}} - 12a}{6(108b + 12\sqrt{12a^3 + 81b^2})^{\frac{1}{3}}} \tag{5.10}$$

which is a standard vector function i.e., one can follow the same steps as shown in Eqs. (3.13), (3.14) and (3.15). Thus the NE point is unique and the utility functions of the SUs satisfy all the required conditions for the existence and uniqueness of at least one NE in the pricing game. Moreover, since $r_{ic}^*(\mathbf{p_{-i}})$ is assumed to be the best-response function of player i [37], $\mathbf{r}_c(\mathbf{p}) = (r_{1c}^*(\mathbf{p_{-1}}), r_{2c}^*(\mathbf{p_{-2}}), \ldots, r_{Nc}^*(\mathbf{p_{-N}}))$ is the best-response vector over all SUs, where $r_{ic}^*(\mathbf{p_{-i}}) = \min\,(p_i^{c_{max}}, p_{ic(max)})$ and $p_i^{c_{max}}$ is the i-th SU's transmission power which provides it with the *optimum* SINR (i.e., $\bar{\gamma}_i^{(Ra)*}$). Since it is also assumed that all SUs have the same efficiency function, this implies that the SINR corresponding to the best-response is the same for all SUs, i.e., $r_{ic}^*(\mathbf{p_i}) = r_{ic}^*(\mathbf{p_{-i}})$. Hence when some of the SUs cannot achieve $\bar{\gamma}_i^{(Ra)*}$, they will transmit at their maximum possible transmission powers, and in this case the NE is still unique.

5.1.3 Analysis of Simulation Results

Detailed simulations are also done to model the performance of the Rayleigh channel game theoretic scheme with pricing. In particular, the following parameters are used: $\bar{Q}_0 = 5$, $\rho_{pi} = \rho_{ip} = \rho_{ji} = 0.1$, $h_{pi} = h_{ip} = h_{ji} = 1$ for all i , $j \in \{1, \ldots, N\}$, $M = 80$, $R_i = 1$, $\bar{\gamma}_0 = 10$, $\sigma_n^2 = 1$, $\mu_1 = 10$, $\mu_2 = 100$ and $c = 10^{+5}$. First of all, the PU utility at the NE is plotted as a function of the number of SUs, N, in Figure 5.1. Here it is seen that when $\bar{Q}_0 < I_0$, the PU's utility is severely penalized by the exponential pricing function. In particular, this happens when $N \geq 26$ for AWGN channel, $N \geq 19$ for Rayleigh fast-flat fading channels with pricing, and $N \geq 17$ for Rayleigh fast-flat fading channels without pricing. Meanwhile Figure 5.2 shows the total interference I_0 from all SUs to the PU. As expected, the total interference is higher for the power control game without pricing due to higher transmit powers.

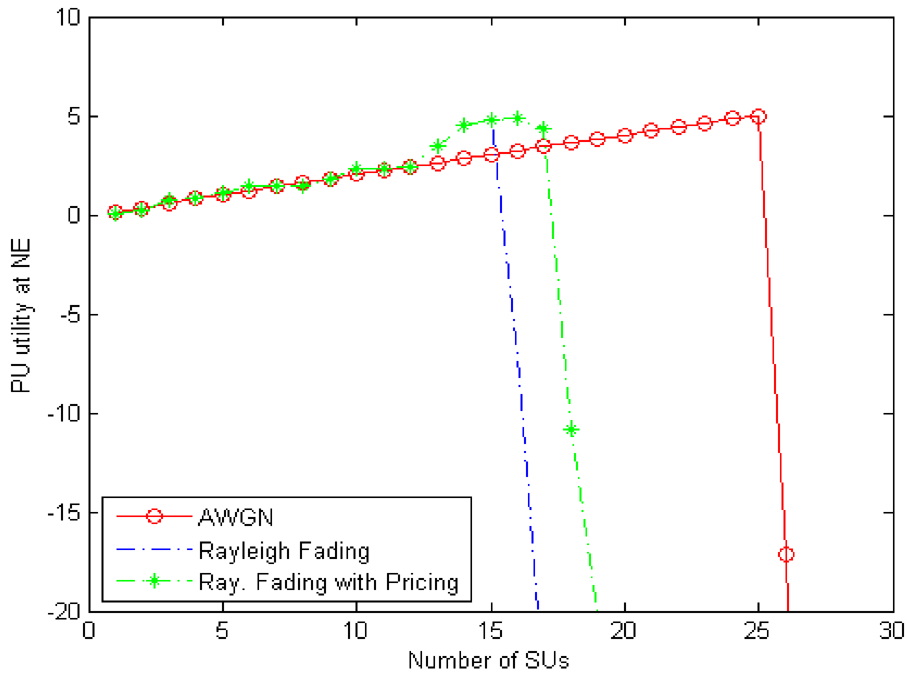

Figure 5.1: Primary user's utility at the NE for Rayleigh fast fading with pricing

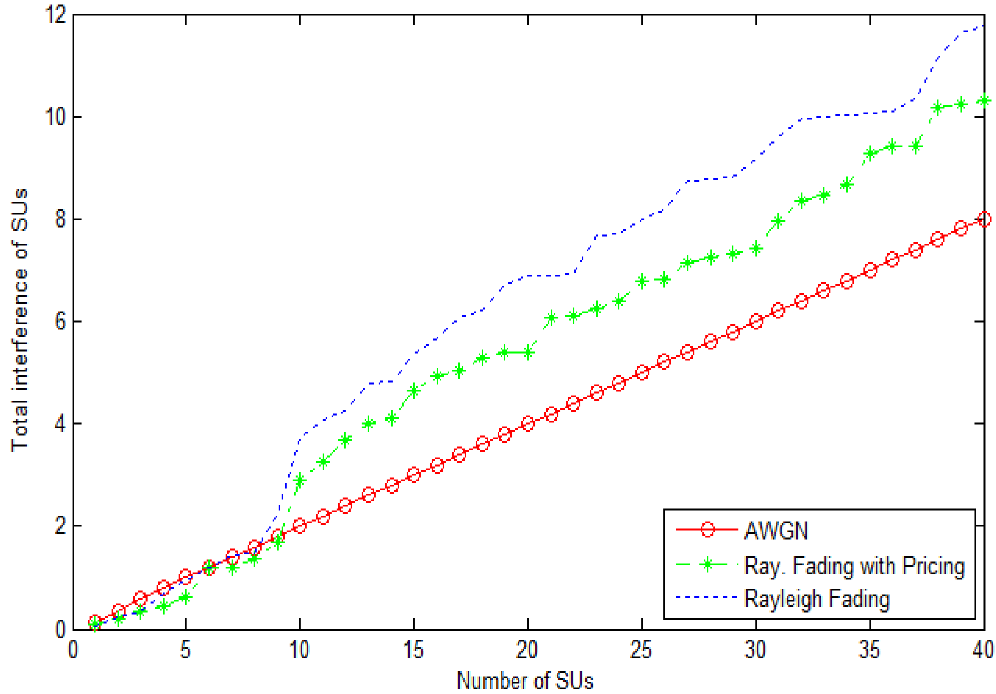

Figure 5.2: Total interference from all SUs for Rayleigh fast fading with pricing

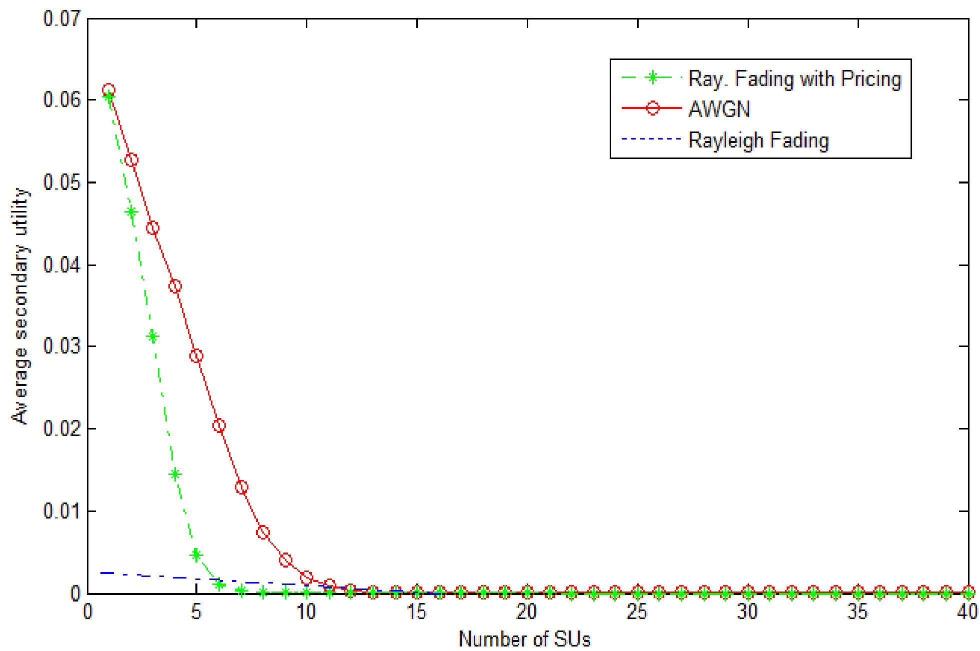

Figure 5.3: Average SU's utility at the NE for Rayleigh fast fading with pricing

Next, the average utility of all SUs is shown in Figure 5.3. Here as the number of SUs increases, each SU (as well as the PU) sees more interference due to the added SUs. Here each SU has to transmit at a higher power (than that with smaller number of SUs in the system) in order to achieve the same optimum SINR. In turn, this reduces the average utility. Once again, the results show that the total performance of the power control game with pricing is better than that one without pricing. For example, Figure 5.4 plots the number of SU's in energy efficient mode. Here one can see that all SUs will maximize their utility by achieving their optimum SINR i.e., $\bar{\gamma}_i^*$ and $\bar{\gamma}_i^{(Ra)*}$, when $0 < N \leq 4$ for AWGN channel, when $0 < N \leq 3$ for Rayleigh fast-flat fading channels with pricing, and when $0 < N \leq 1$ for Rayleigh fast-flat fading channels without pricing. Otherwise the network cannot afford these SUs (i.e., no SU can achieve its optimum SINR), and they all transmit at their maximum possible power level. Finally, Figure 5.5 shows that the sum of the utility achieved by all SUs at the NE decreases as the number of SUs increases. Overall, the total performance for power games with pricing is superior to the ones without pricing.

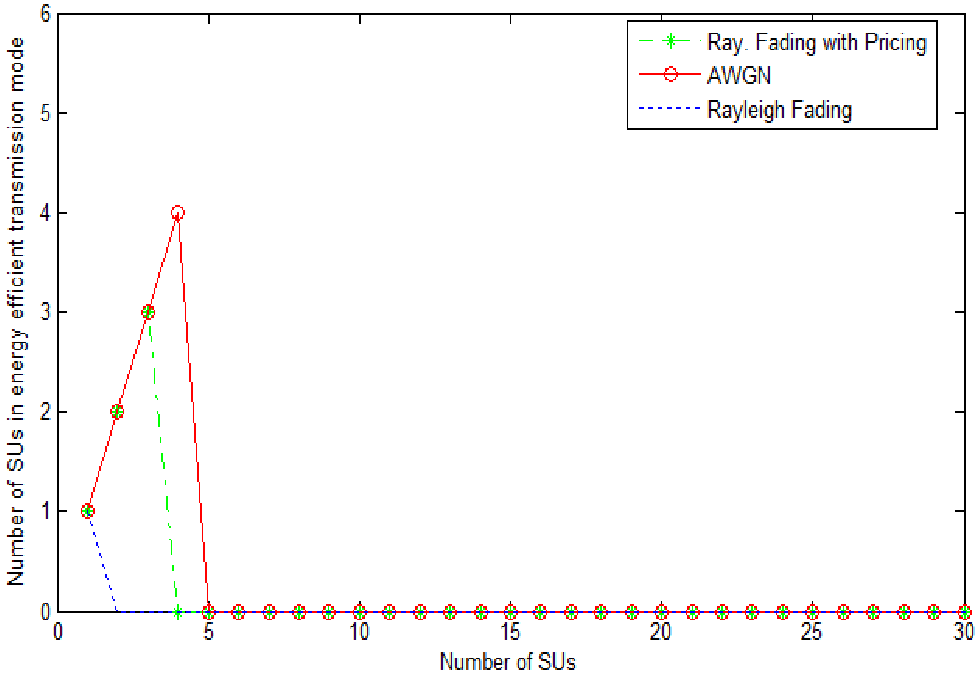

Figure 5.4: Number of SUs in energy-efficient mode for Rayleigh fast fading with pricing

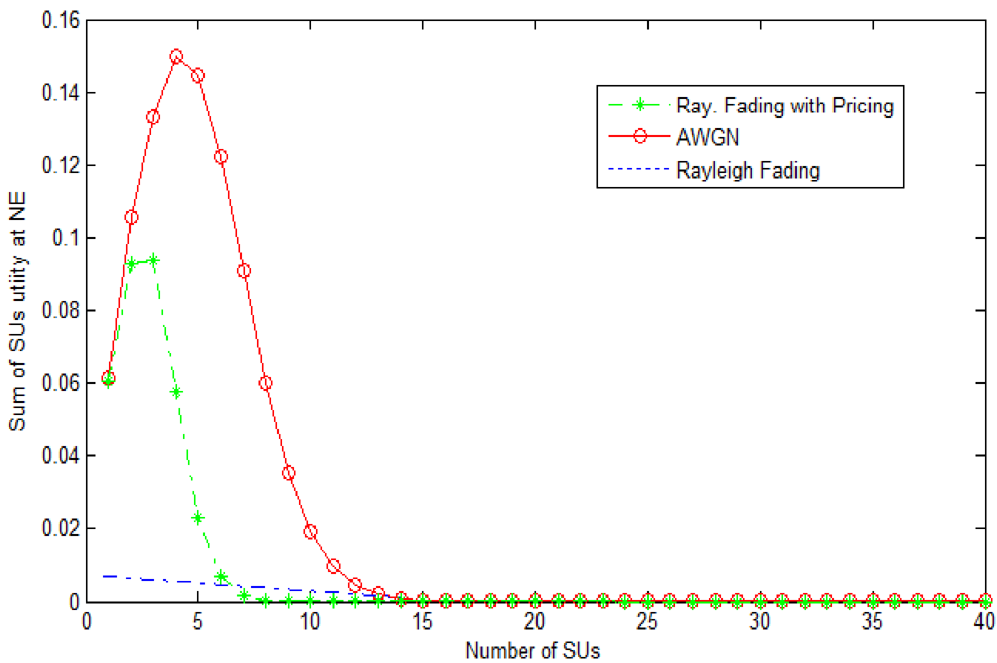

Figure 5.5: Sum of secondary users' utility at the NE for Rayleigh fast fading with pricing

5.2 Rician Fast-Flat Fading Channels with Pricing

Consider the case of Rician fast-flat fading channels now. Here, the derivation of P_e for these channels (without pricing) was considered in Chapter 3 using BFSK modulation, i.e., the path fading coefficient α_i modeled as a Rician random variable with probability density function which is given in Eq. (2.9). Leveraging this baseline, a modified utility function with pricing is now introduced to help boost the total number of SUs that the system can support.

5.2.1 Utility Functions with Pricing

The utility function of the i-th SU with pricing is given as follows:

$$u_i^{\hat{c}}(p_i, \mathbf{p_{-i}}) = \frac{R_i(1-2P_e)^M}{p_i} - \hat{c}p_i = \frac{R_i(1-2/\bar{\gamma}_i^{(Rice)})^M}{p_i} - \hat{c}p_i \quad (5.11)$$

where $\hat{c}$ is positive scalar pricing factor which is chosen to achieve the best possible improvement in the performance. However, since the utility function for the PU is still the same as given in Eq. (3.7), the new modified power control game with pricing for the proposed realistic channel, $G_6^{\hat{c}} = (\mathcal{N}, \mathcal{P}_{\hat{c}}, u_i^{\hat{c}}(.))$ has the following components:

1) **Players**: $\mathcal{N} = \{0, 1, \ldots, N\}$ is the index set of the users currently in the cell, where the 0-th user is assumed to be the PU and $i = 1, \ldots, N$ represents the i-th SU.

2) **Action space**: $\mathcal{P}_{\hat{c}} = (\mathcal{Q} \times \mathcal{P}_{1\hat{c}} \times \mathcal{P}_{2\hat{c}} \times \ldots \times \mathcal{P}_{N\hat{c}})$, where $\mathcal{Q} = [0, \bar{Q_0}]$ represents the PU's action set and $\mathcal{P}_{i\hat{c}} = [p_{i\hat{c}(min)}, p_{i\hat{c}(max)}]$ represents the i-th SU's action set. Here $\bar{Q_0}$ represents the maximum allowed interference cap of the PU, and

$p_{i\hat{c}(min)}$ and $p_{i\hat{c}(max)}$ respectively, represent the minimum and maximum allowed transmission power of the i-th SU. The action vector of all users is also denoted by $\mathbf{p} = [Q_0, p_1, \ldots, p_N]$, where $p_i \in \mathcal{P}_{i\hat{c}}$ and $Q_0 \in \mathcal{Q}$ for $i = 0, 1, \ldots, N$. Overall, the PU's strategy is to choose the best Q_0 whereas that of SUs is to adapt their transmit powers.

3) **Utility functions**: In this game the utility function $u_i^{\hat{c}}(p_i, \mathbf{p_{-i}})$, given in Eq. (5.11), is used to represent the i-th SU's utility function for Rician fast-flat fading channels. In addition, $u_0(Q_0, \mathbf{p_{-0}})$, given in Eq. (3.7), is also used to represent the utility function of the PU.

5.2.2 Existence and Uniqueness of the NE

Assuming MF receivers are used at SUs system, the action space defined for Rician fast-flat fading channels can be modified to guarantee the existence of at least one NE point for the pricing game. Moreover, it is also sufficient to show that the utility function is concave in p_i. Now since the PU's utility function has not been changed, and the authors in [7] have proven its quasi-concavity, one only needs to show the quasi-concavity and the continuity of the utility function of the SUs. Therefore by taking the first derivative of Eq. (5.11) with respect to p_i one gets:

$$\frac{\partial u_i^{\hat{c}}(p_i, \mathbf{p_{-i}})}{\partial p_i} = \frac{R_i}{p_i^2}(1 - \frac{2}{\bar{\gamma}_i^{(Rice)}})^{M-1}(\frac{2(M+1)}{\bar{\gamma}_i^{(Rice)}} - 1) - \hat{c} \tag{5.12}$$

By further setting the above expression to zero, one obtains:

$$p_i^{c_{max}} = \sqrt{\frac{R_i}{\hat{c}}(1 - \frac{2}{\bar{\gamma}_i^{(Rice)}})^{M-1}(\frac{2(M+1)}{\bar{\gamma}_i^{(Rice)}} - 1)} \tag{5.13}$$

where $p_i^{\hat{c}_{max}}$ is the maximum transmission power within the action space $\mathcal{P}_{i\hat{c}}$. Now in order to have feasible (i.e., positive and real) values for $p_i^{\hat{c}_{max}}$, the strategy space for the realistic channels model must be defined as follows:

$$\mathcal{P}_i = \{p_i : \bar{\gamma}_i^{(Rice)} \in (2, 2(M+1))\} \tag{5.14}$$

Moreover, the second derivative of Eq. (5.11) is given by:

$$\frac{\partial^2 u_i^{\hat{c}}(p_i, \mathbf{p_{-i}})}{\partial {p_i}^2} = \frac{R_i}{p_i^3} \frac{(1 - \frac{2}{\bar{\gamma}_i^{(Rice)}})^M}{(\bar{\gamma}_i^{(Rice)} - 2)^2} (4M^2+12M+8+2(\bar{\gamma}_i^{(Rice)})^2 - 8(M+1)\bar{\gamma}_i^{(Rice)}) \tag{5.15}$$

Hence, $u_i^{\hat{c}}(p_i, \mathbf{p_{-i}})$ is concave if:

$$\frac{\partial^2 u_i^{\hat{c}}(p_i, \mathbf{p_{-i}})}{\partial {p_i}^2} < 0, \quad \forall \bar{\gamma}_i^{(Rice)} \in (\bar{\gamma}_{i(min)}^{(Rice)}, \bar{\gamma}_{i(max)}^{(Rice)}) \tag{5.16}$$

where $\bar{\gamma}_{i(max)}^{(Rice)}$ and $\bar{\gamma}_{i(min)}^{(Rice)}$ are as defined earlier in Section 3.2.2 for the game without pricing. Therefore to fulfill both conditions, the action space of the power control control game with pricing under Rician fast-flat fading channel, i.e., $G_6^{\hat{c}} = (\mathcal{N}, \mathcal{P}, u_i^{\hat{c}}(.))$, should be modified to be the intersection of the two sets, that is:

$$\mathcal{P}_{i\hat{c}} = \{p_i : \bar{\gamma}_i^{(Rice)} \in (\bar{\gamma}_{i\hat{c}(min)}^{(Rice)}, \bar{\gamma}_{i\hat{c}(max)}^{(Rice)})\} \tag{5.17}$$

where $\bar{\gamma}_{i\hat{c}(max)}^{(Rice)} = 2(M+1)$ and $\bar{\gamma}_{i\hat{c}(min)}^{(Rice)} = 2(M+1) - \sqrt{2(M^2+M)}$. Now, since $\bar{\gamma}_i^{(Rice)} >> 1$, (i.e., large $\bar{\gamma}_i^{(Rice)}$) does exist in the strategy space shown in Eq. (5.17), one can approximate Eq. (5.13) by:

$$p_i^{\hat{c}max} \approx \sqrt{\frac{R_i}{\hat{c}} (\frac{2(M+1)}{\bar{\gamma}_i^{(Rice)}} - 1)} \tag{5.18}$$

Assuming that $I_{Rice(i)} = (\sum_{\substack{j=1,\\ j\neq i}}^{N} h_{sj}^2 \rho_{ji}^2 p_j + h_{s0}^2 \rho_{ps}^2 P_0)(s^2+1)$, then one can rewrite Eq. (3.5) as follows:

$$\bar{\gamma}_i^{(Rice)} = \frac{h_{si}^2 p_i e^{s^2}}{I_{Rice(i)} + \sigma_n^2} \tag{5.19}$$

where $\bar{\gamma}_i^{(Rice)}$ is the average SINR for Rician fast-flat fading channels.
Also by using Eq. (5.19), one can rewrite the above equation as follows:

$$(p_i^{\hat{c}_{max}})^3 + \frac{R_i}{\hat{c}} p_i^{\hat{c}_{max}} - \frac{R_i}{\hat{c}} \frac{2(M+1)(I_{Rice(i)} + \sigma_n^2)}{h_{si}^2 e^{s^2}} \approx 0 \tag{5.20}$$

Assuming that $a = \frac{R_i}{\hat{c}}$ and $b = \frac{R_i}{\hat{c}} \frac{2(M+1)(I_{Rice(i)}+\sigma_n^2)}{h_{si}^2 e^{s^2}}$, the only positive and real solution for Eq. (5.20) is given by:

$$p_i^{\hat{c}_{max}} \approx \frac{(108b + 12\sqrt{12a^3 + 81b^2})^{\frac{2}{3}} - 12a}{6(108b + 12\sqrt{12a^3 + 81b^2})^{\frac{1}{3}}} \tag{5.21}$$

which is a standard vector function, i.e., one can follow the same steps which are shown in Eqs. (3.13), (3.14), and (3.15). Thus the NE point is unique, and the utility functions of the SUs satisfy all the required conditions for the existence and uniqueness of at least one NE in the power control game with pricing for Rician fast-flat fading channels. Moreover, since $r_{i\hat{c}}^*(\mathbf{p_{-i}})$ is assumed to be the best-response function of player i [37], $\mathbf{r}_{\hat{c}}(\mathbf{p}) = (r_{1\hat{c}}^*(\mathbf{p_{-1}}), r_{2\hat{c}}^*(\mathbf{p_{-2}}), \ldots, r_{N\hat{c}}^*(\mathbf{p_{-N}}))$ is the best-response vector over all SUs, where $r_{i\hat{c}}^*(\mathbf{p_{-i}}) = \min\ (p_i^{\hat{c}_{max}}, p_{i\hat{c}(max)})$ and $p_i^{\hat{c}_{max}}$ is the i-th SU's transmission power which provides it with the *optimum* SINR (i.e., $\bar{\gamma}_i^{(Rice)*}$). Since it is assumed that all SUs have the same efficiency function, this implies that the SINR corresponding to the best-response is the same for all SUs, i.e., $r_{i\hat{c}}^*(\mathbf{p_i}) = r_{i\hat{c}}^*(\mathbf{p_{-i}})$. Hence when some of the SUs cannot achieve $\bar{\gamma}_i^{(Rice)*}$, they will send at their maximum possible transmission powers, and in this case the NE is still unique.

5.2.3 Analysis of Simulation Results

Detailed simulations are done in *MATLAB* to model the performance of the Rician channel game theoretic scheme with pricing. In particular, the following parameters are used: $\bar{Q_0} = 5$, $\rho_{pi} = \rho_{ip} = \rho_{ji} = 0.1$, $h_{pi} = h_{ip} = h_{ji} = 1$ for all i , $j \in \{1, \ldots, N$ $\}$, $M = 80$, $R_i = 1$, $\bar{\gamma_0} = 10$, $\sigma_n^2 = 1$, $\mu_1 = 10$, $\mu_2 = 100$, $s = 1$ and $\hat{c} = 10^{+5}$. First, Figure 5.6 plots the utility of the PU at the NE as a function of the number of SUs, N. Here it is seen that when $\bar{Q_0} < I_0$, the PU's utility is severely penalized by the exponential pricing function. Namely, this occurs when $N \geq 26$ for the AWGN channel, $N \geq 21$ for Rician fast-flat fading channels with pricing, and $N \geq 19$ for Rayleigh fast-flat fading channel with pricing. However, the total performance is better than that for the Rician fast-flat fading channels game without pricing which was shown in Section 3.2.4. Meanwhile the total interference, I_0, from all SUs to the PU is also shown in Figure 5.7. As expected, the total interference is higher for the power control game without pricing due to higher transmit powers. On the other hand, due to lack of LOS component, the total interference under Rayleigh fast-flat fading channels is higher than that for Rician fast-flat fading channels.

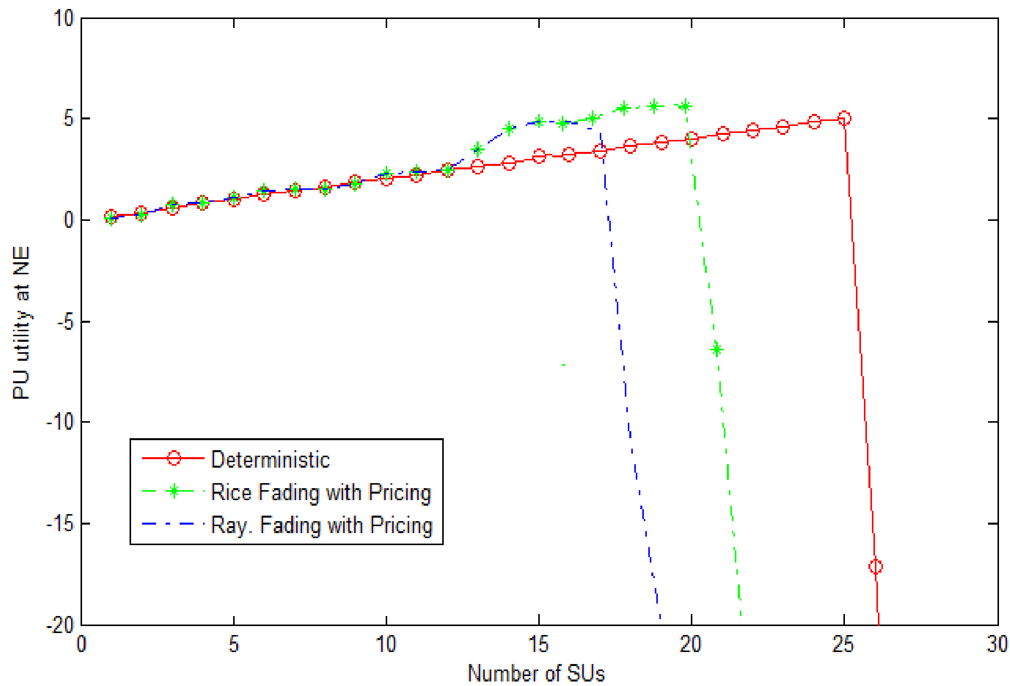

Figure 5.6: Primary user's utility at the NE for Rician fast fading with pricing

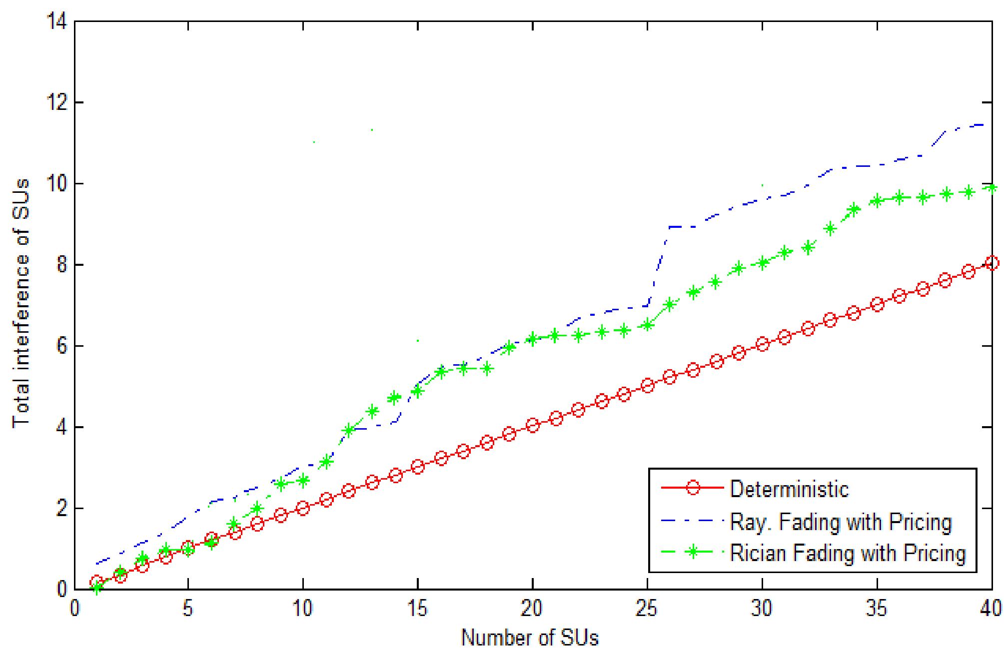

Figure 5.7: Total interference from all SUs for Rician fast fading with pricing

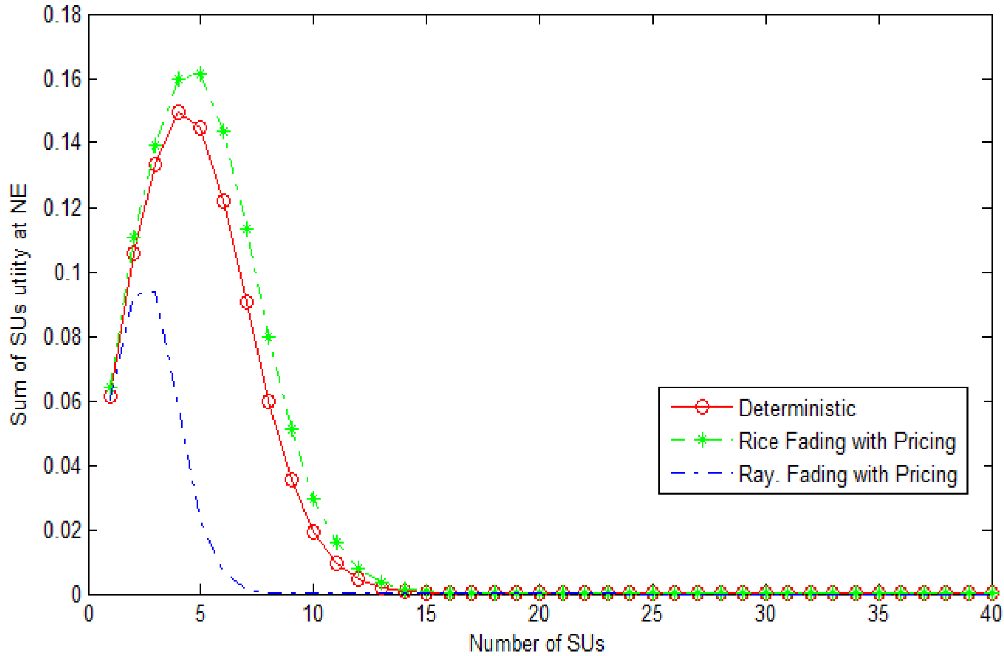

Figure 5.8: Sum of secondary users' utility at the NE for Rician fast fading with pricing

Next, Figure 5.9 shows that the aggregate utility achieved by all SUs decreases by increasing the number of SUs at the NE. These results show that the sum of all SUs' utility has a unique maximum when $N = 4$ for AWGN channel, when $N = 5$ for Rician fast-flat fading channels with pricing, and when $N = 3$ for Rayleigh fast-flat fading channels with pricing. In addition, Figure 5.10 also shows the number of SUs that the PU can afford as a function of the total number of SUs. This could be any number of SUs as long as $\bar{Q}_0 > I_0$, where $N = 25$ for AWGN channel, $N = 22$ for Rician fast-flat fading channels with pricing, and $N = 19$ for Rayleigh fast-flat fading channels with pricing. As expected, the total number of SUs that the PU can afford is lower in the case of Rayleigh fast-flat fading channels model. Meanwhile, Figure 5.10 plots the average utility of the SUs. Here as the number of SUs increases, each SU (as well as the PU) sees more interference due to the increased user counts. Thus each SU has to transmit at a higher power (than that with smaller number of SUs in the system) in order to achieve the same optimum SINR. This reduces the

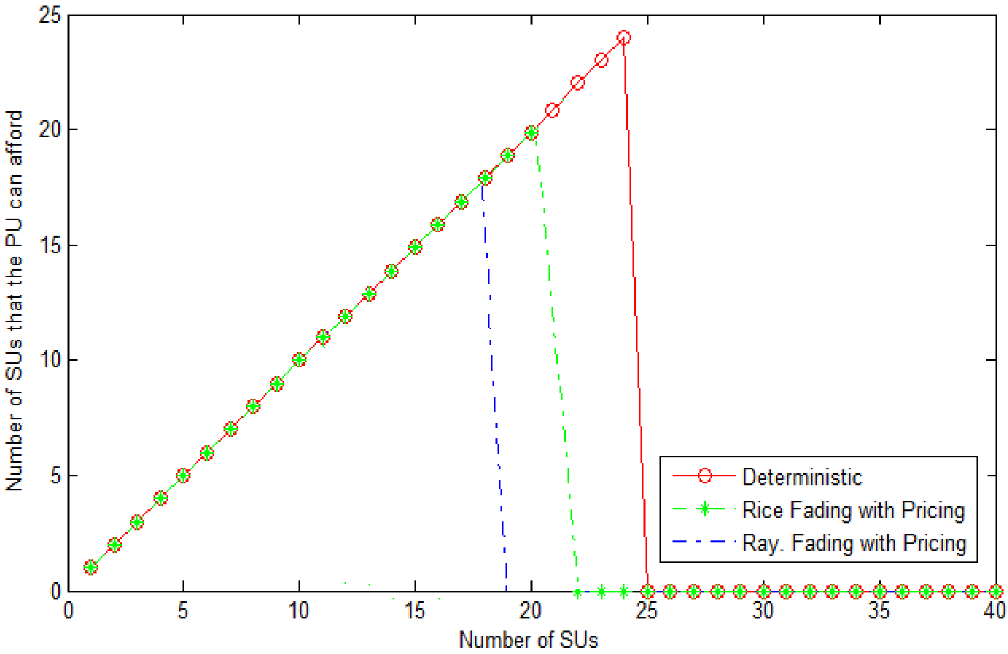

Figure 5.9: The maximum number of SUs supported for Rician fast fading with pricing

average utility, i.e., when $N < 4$ for AWGN channel, $N < 5$, and $N < 3$ for both Rician and Rayleigh fast-flat fading channels, respectively. Here the decrease in the average SU utility is dominated by the increase of the number of SUs, and hence the aggregate utility of all SUs still increases. Conversely the aggregate utility decreases due to the decay of the average SU utility.

Finally, the number of SUs in energy efficient mode is also plotted in Figure 5.11. Here one can see that all SUs will maximize their utility by achieving their optimum SINR, i.e., $\bar{\gamma}_i^*$, $\bar{\gamma}_i^{(Rice)*}$ and $\bar{\gamma}_i^{(Ra)*}$, when $0 < N \leq 4$ for AWGN channel, when $0 < N \leq 3$ for Rician fast-flat fading channels with pricing, and when $0 < N \leq 1$ for Rayleigh fast-flat fading channels with pricing. Otherwise the network cannot afford these SUs, i.e., no SU can achieve its optimum SINR, and they will all transmit at their maximum possible power level, which equals $\bar{P}_i = 20$ for AWGN channel and $P_i^{(max)}$ for both Rician and Rayleigh fast-flat fading channels. Overall, the total performance for the game with pricing is superior to that without pricing.

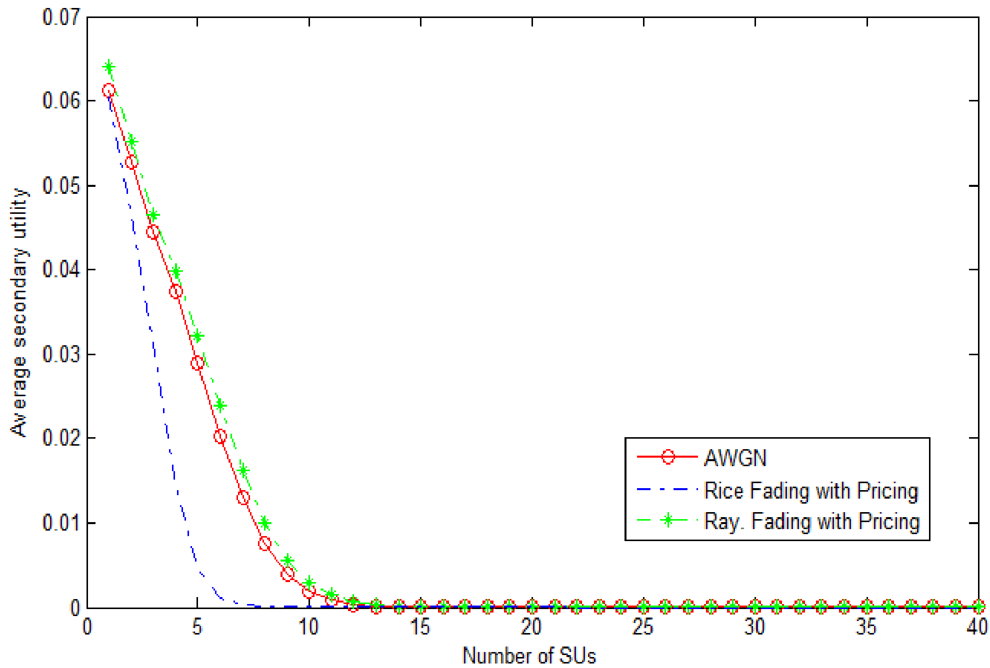

Figure 5.10: Average SU's utility at the NE for Rician fast fading with pricing

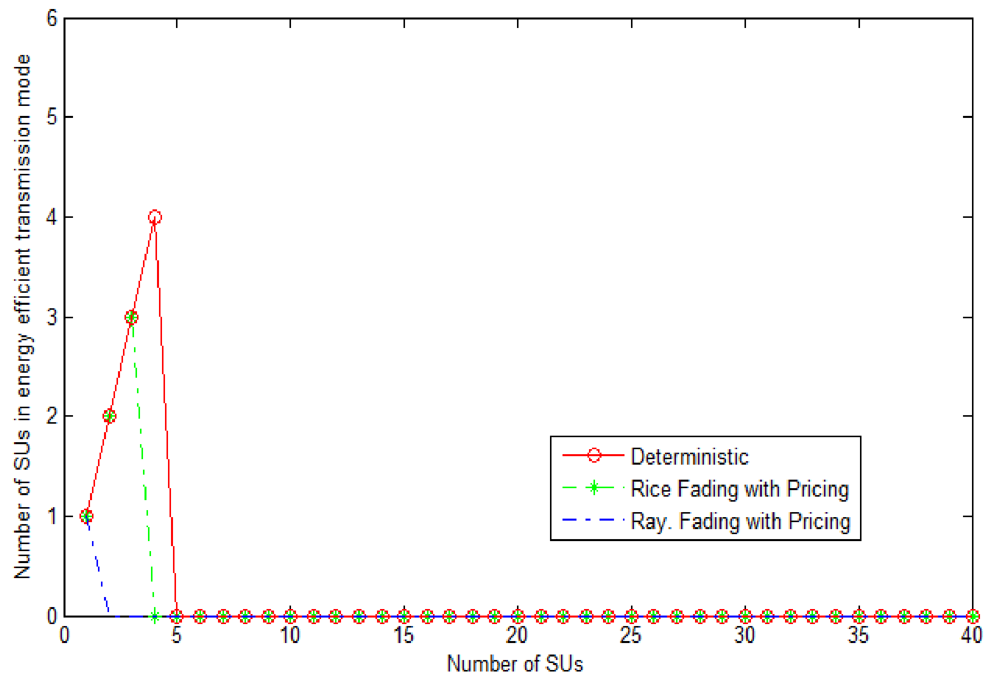

Figure 5.11: Number of SUs in energy-efficient mode for Rician fast fading with pricing

5.3 Conclusions

This chapter introduces a novel primary-secondary user power control solution with pricing. This formulation incorporates the primary users as active decision makers, and analyzes the power and utility performance of the scheme for both Rayleigh and Rician fast-flat fading channels with linear pricing function. In particular, detailed derivations are done to show that the modified realistic game can achieve a unique NE point. Simulations results also confirm that the proposed scheme yields good energy efficiency for SUs without compromising transmission quality for PUs. However, Rayleigh and Rician fast-flat fading channels are seen to have direct impact on the performance of the pricing game in terms of reduced numbers secondary users supported by the primary user due to higher interference and lower utility as compared to AWGN channel. Moreover, pricing helps shift the equilibrium point to lower power regimes (as compared to non-pricing games). However, utility values are still higher and SUs can achieve increased battery life with reduced power usages.

Chapter 6

Conclusions and Future Directions

This dissertation presents a comprehensive modeling of user behaviors in CR networks. In particular, a novel primary-secondary user power control framework is developed using an extended game-theoretic approach (Chapter 2). The formulation builds upon recent studies by incorporating primary users as active decision makers in the game. This framework is extended and used to analyze the power and utility performance of the game for both fast- and slow-flat fading Rayleigh and Rician channels (Chapters 3 and 4). Detailed analytical derivations are also performed for each game instance in order to prove the existence and uniqueness of the NE point. Finally, pricing functions are also incorporated into the game-theoretic formulation to help further improve the model and support larger numbers of users, i.e., for both Rayleigh and Rician fast-flat fading channels (Chapter 5). The overall conclusions of this effort are now presented along with some discussions on future work directions.

6.1 Conclusions

Foremost, the analytical formulations confirm that the proposed game-theoretic schemes can yield unique NE points for the various fast and slow flat-fading channel models. In addition, realistic simulation results also show that the proposed power-control strategies can yield realistic energy savings (efficiency) for SUs without unnecessarily compromising the transmission quality for the PU. However, the findings also indicate that Rayleigh and Rician flat-fading channel models (fast and slow) have a very direct impact on the performance of CR networks. Specifically, these channels yield notably lower performances versus the more basic AWGN channel model, i.e., in terms of fewer numbers of supported users (due to higher levels of interference) and lower throughput per-unit-power (utility). Hence the AWGN model is deemed to be overly optimistic and not very reflective of realistic transmission conditions. However, the introduction of pricing strategies into the game can yield sizeable improvements in overall bandwidth efficiency of the game-theoretic power control strategies.

6.2 Future Directions

Overall, this dissertation presents a strong set of contributions in the area of game-theoretic modeling of CR networks under realistic fast and slow fading channel conditions. As such, this foundation opens up many new avenues for future research work. Some of these are now detailed here. First, new efforts can look at incorporating the Nakagami fading channel model [47] into the game-theoretic formulation. In particular, this model closely matches empirical measurements for many real-world conditions, and hence can provide a valuable addition to the proposed framework. Next, rate control features can also be added, as this topic is becoming an important concern in increasingly dense cellular networks with surging data transfer demands.

Moreover, the impact of more advanced LMMSE receivers at the SUs can also be studied. It is envisioned that these detectors will improve overall capacity efficiency in CR networks and thereby allow more users to be supported. Finally, spatial diversity techniques can be considered for mitigating the effects of fading channel behaviors to further improve the overall performance.

References

[1] Z. Han, K. J. Liu, *Resource Allocation for Wireless NWs: Basic Techniques and Applications*, Cambridge Press, 2008.

[2] http://www.cmpe.boun.edu.tr/WiCo/doku.php?id=research

[3] M. Alayesh, N. Ghani, *et al*, "Performance of a Primary-Secondary User Power Control Game for Cognitive Radios under Rayleigh Fast Fading Channel", *IEEE High Capacity Optical Networks and Enabling Technologies (HONET) 2010*, Cairo, Egypt, December 2010.

[4] M. A. Alayesh, N. Ghani, "Impacts of Fast Flat Fading Channel on the Performance of a Primary-Secondary User Power Control Game for Cognitive Radios", *IEEE Globecom 2010 Workshop on Broadband Wireless Access (BWA)*, Miami, FL, December 2010.

[5] S. Haykin, "Cognitive Radio: Brain-Empowered Wireless Communications", *IEEE Journal on Selected Areas in Communications*, Vol. 23, No. 2, February 2005, pp. 201-220.

[6] J. Mitola, "Cognitive Radio: An Integrated Agent Architecture for Software Defined Radio", *Ph.D. dissertation*, Royal Institute of Technology (KTH), Stockholm, Sweden, 2000.

[7] S. Jayaweera, T. Li, "Dynamic Spectrum Leasing in Cognitive Radio Networks via Primary-Secondary User Power Control Games", *IEEE Transaction on Wireless Communications*, Vol. 8, No. 6, June 2009, pp. 3300-3310.

[8] Andrea Glodsmith, *Wireless Communications*, Cambridge Press, 2005.

[9] David Tse, Pramod Viswanath, *Fundamentals of Wireless Communication*, Cambridge University Press, 2005.

[10] M. K. Simon, M. S. Alouini, "Digital Communication Over Fading Channels: A Unified Approach to Performance Analysis", *John Wiley and Sons,* New York, 2000.

[11] D. Gesbert, M. Shafi, D. Shiu, P. J. Smith, A. Naguib, "From Theory to Practice: An Overview of MIMO Space-Time Coded Wireless Systems (Tutorial Paper)", *IEEE Journal on Selected Areas in Communications,* Vol. 21, No. 3, April 2003, pp. 281-302.

[12] http: *//en.wikipedia.org/wiki/Cognitive_radio*

[13] W. Lehr, J. Crowcroft, "Managing Shared Access to a Spectrum Commons", *Proc. 1st IEEE Symp. New Frontiers Dynamic Spectrum Access Networks*, Baltimore, MD, November 2005.

[14] Y. Benkler, "Overcoming Agoraphobia: Building the Commons of the Digitally Networked Environment", *Harvard Journal of Law Technology*, Vol. 11, No. 2, Winter 1998.

[15] Q. Zhao, B. M. Sadler, "A Survey of Dynamic Spectrum Access", *IEEE Signal Processing Magazine*, Vol. 24, No. 3, May 2007, pp. 79-89.

[16] R. Coase, "The Federal Communications Commission", *Journal of Law and Economics*, 1959, pp. 1-40.

[17] D. Hatfield, P. Weiser, "Property Rights in Spectrum: Taking the Next Step", *Proc. 1st IEEE Symposium on New Frontiers Dynamic Spectrum Access Networks*, Baltimore, MD, November 2005.

[18] L. Xu, R. Tonjes, T. Paila, W. Hansmann, M. Frank, M. Albrecht, "Driving to the Internet: Dynamic Radio for IP Services in Vehicular Environments", *Proc. 25th Annual IEEE Conference on Local Computer Networks*, Tampa, FL, November 2000.

[19] O. Ileri, D. Samardzija, and N. Mandayam, "Demand Responsive Pricing and Competitive Spectrum Allocation via a Spectrum Server", *Proc. 1st IEEE Symposium on New Frontiers Dynamic Spectrum Access Networks*, Baltimore, MD, November 2005.

[20] R. Etkin, A. Parekh, D. Tse, "Spectrum Sharing for Unlicensed Bands", *Proc. 1st IEEE Symposium on New Frontiers Dynamic Spectrum Access Networks*, Baltimore, MD, November 2005.

[21] C. Raman, R. Yates, N. Mandayam, "Scheduling Variable Rate Links via aSpectrum Server", *Proc. 1st IEEE Symposium on New Frontiers Dynamic Spectrum Access Networks*, Baltimore, MD, November 2005.

[22] J. Huang, R. Berry, M. Honig, "Spectrum Sharing with Distributed Interference Compensation", *Proc. 1st IEEE Symposium on New Frontiers Dynamic Spectrum Access Networks*, Baltimore, MD, November 2005.

[23] S. Chung, S. Kim, J. Lee, J. Cioffi, "A Game-Theoretic Approach to Power Allocation in Frequency-Selective Gaussian Interference Channels", *Proc. IEEE International Symposium on Information Theory*, Yokohama, Japan, June 2003.

[24] A. T. Hoang, Y. C. Liang, M. H. Islam, "Power Control and Channel

Allocation in Cognitive Radio Networks with Primary Users' Cooperation", *IEEE Transactions on Mobile Computing*, Vol. 9, No. 3, March 2010, pp. 348-360.

[25] V. Shah, N. B. Mandayam, D. J. Goodman, "Power Control for Wireless Data based on Utility and Pricing", *PIMRC'98*, Cambridge, MA, September 1998.

[26] D. J. Goodman, N. B. Mandayam, "Power Control for Wireless Data", *IEEE Personal Communications*, Vol. 7, No. 2, April 2000, pp. 48-54.

[27] C. U. Saraydar, N. B. Mandyam and D. J. Goodman, "Efficient Power Control Via Pricing in Wireless Data Networks", *IEEE Transactions on Communications*, Vol. 50, No. 2, February 2002, pp. 291-303.

[28] C. U. Saraydar, N. B. Mandayam, and D. J. Goodman, "Pricing and Power Control in a Multicell Wireless Data Network", *IEEE Journal on Selected Areas in Communications,* Vol. 19, No. 10, October 2001, pp. 1883-1892.

[29] F. Meshkati, H. V. Poor, S. C. Schwartz, N. B. Goodman, "An Energy-Efficient Approach to Power Control and Receiver Design in Wireless Data Networks", *IEEE Transactions on Communication*, Vol. 53, No. 11, February 2002, pp. 1885-1894.

[30] F. Meshkati, A. J. Goldsmith, H. V. Poor, S. C. Schwartz, "A Game-Theoretical Approach to Energy-Efficient Modulation in CDMA Networks with Delay QoS Constraints", *IEEE Transactions on Communication*, Vol. 25, No. 6, August 2007, pp. 1-14.

[31] P. Zhou, *et al*, "Joint Power and Rate Control in Cognitive Radio Networks: A Game-Theoretical Approach", *IEEE International Conference on Communications (ICC'08)*, Beijing, China, May 2008.

[32] A. B. MacKenzie and S. B. Wicker, "Game Theory and the Design of Self-Configuring, Adaptive Wireless Networks", *IEEE Communications Magazine*, Vol. 39, No. 11, November 2001, pp. 126-131.

[33] M. Xiao, N. Shroff, P. Chong, "Utility-Based Power Control in Cellular Wireless Systems", *IEEE INFOCOM 2001*, Anchorage, AK, April 2001.

[34] G. J. Foschini, Z. Miljanic, " A Simple Distributed Autonomous Power Control Algorithm and its Convergence", *IEEE Transactions on Vehicular Technology*, Vol. 42, No. 4, November 1993, pp. 641-646.

[35] J. Zander, "Distributed Cochannel Interference Control in Cellular Radio Systems", *IEEE Transactions on Vehicular Technology*, Vol. 41, No. 2, August 1992, pp. 305- 311.

[36] D. Mitra, "An Asynchronous Distributed Algorithm for Power Control in Cellular Radio Systems", *Proc. 4th WINLAB Workshop on 3rd Generation Wireless Information Networks*, Rutgors, NJ, October 1993.

[37] R. D. Yates, " Framework for Uplink Power Control in Cellular Radio Systems", *IEEE Journal on Selected Areas in Communications*, Vol. 13, No. 7, September 1995, pp. 1341-1347.

[38] C. Y, G. Yu, Z. Zhang, H. Chen, P. Qiu, "On Cognitive Radio Networks with Opportunistic Power Control Strategies in Fading Channels", *IEEE Transaction on Wireless Communications*, Vol. 7, No. 7, July 2008, pp. 2752-2761.

[39] M. H. Islam, Y. Liang, A. T. Hoang, "Joint Power Control and Beam Forming for Cognitive Radio Networks", *IEEE Transaction on Wireless Communications*, Vol. 7, No. 7, July 2008, pp. 2415-2419.

[40] Z. Ji, K. Liu, "Cognitive Radios for Dynamic Spectrum Access - Dynamic Spectrum Sharing: A Game Theoretical Overview", *IEEE Communications Magazine*, Vol. 45, No. 5, May 2007, pp. 88-94.

[41] J. O'Daniell, "Analysis and Design of Cognitive Radio Networks and Distributed Radio Resource Management Algorithms", *Ph.D. Dissertation*, Virginia Polytechnic Inistitute and State University, 2006.

[42] F. Meshkati, H.V. Poor, S.C. Schwartz, "Energy-Efficient Resource Allocation in Wireless Networks: An Overview of Game-Theoretic Approaches", *IEEE Signal Processing Magazine*, Vol. 24, No. 3, May 2007, pp. 58-68.

[43] W. Wang, Y. Cui, T. Peng, W. Wang, "Noncooperative Power Control Game with Exponential Pricing for Cognitive Radio Network", *Vehicular Technology Conference (VTC) 2007*, Dublin, Ireland, April 2007.

[44] W. Wang, *et al*, "Optimal Power Control Under Interference Temperature Constraints in Cognitive Radio Network", *IEEE Wireless Communications and Networking Conference (WCNC) 2007*, Hong Kong, China, March 2007.

[45] N. Gatsis, *et al*, "Utility-Based Power Control for Peer-to Peer Cognitive Radio Networks with Heterogeneous QoS Constraints", *IEEE International Conference on Acoustics, Speech and Signal Processing (ICASSP) 2008*, Las Vegas, NV, April 2008.

[46] J. G. Proakis, *Digital Communications*, McGraw Hill Press, New York, NY, 2001.

[47] M. Hayajneh, "Application of Game Theory to Power and Rate Control for Wireless Data", *Ph.D. Dissertation*, University of New Mexico, 2004.

[48] M. Alayesh, N. Ghani, "Game-Theoretic Approach for Primary-Secondary User Power Control under Fast Flat Fading Channels", *IEEE Communications Letters*, Vol. 15, No. 5, May 2011, pp. 491-493.

[49] M. Alayesh, N. Ghani, "Cognitive Radios Power Control Game under Rayleigh Slow Fading Channel", *International Conference on Communications and Information Technology (ICCIT) 2011*, Aqaba, Jordan, March 2011.

[50] M. Alayesh, N. Ghani, "Game Theoretic Power Control Under Rician Slow Flat Fading Channels in Cognitive Radio Networks", *IEEE International Conference on Computer Communication Networks (ICCCN) 2011*, Maui, Hawaii, August 2011.

[51] M. Alayesh, N. Ghani, Min Peng, "Power Control Game-Theoretic Approach in Cognitive Radios Networks under Rician Fast-Flat Fading Channel with Pricing", *International Conference on Wireless Communications, Networking and Mobile Computing (WiCOM) 2011*, Wuhan, China, September 2011.